THE PHYSICAL NATURE OF F PLASMID TRAI AND ITS EFFECT DURING CONJUGATIVE TRANSFER

By
Tegan K. Feehery

A dissertation submitted to Johns Hopkins University in conformity with the requirements for the degree of Doctor of Philosophy

Baltimore Maryland
October, 2014

THE PHYSICAL NATURE OF F PLASMID TRAI AND ITS EFFECT DURING CONJUGATIVE TRANSFER

Tegan K. Feehery

The Johns Hopkins University, 2014

Dr. Joel F. Schildbach, Advisor

ABSTRACT

F plasmid TraI (192 kD) is essential for DNA transfer during bacterial conjugation. TraI is composed of a relaxase domain, ssDNA binding domain, helicase domain, and C-terminal domain. Some TraI mutants, created by the Traxler lab, have a 31 AA insertion (i31) in different domains that exhibit higher mating efficiencies than wild-type (WT) TraI. We used a live cell SeqA-YFP fusion protein system to investigate the observed higher mating efficiency. DNA appeared earlier in the recipient in the i31 mutants compared to WT, and the change was not due to a difference in second strand synthesis. To investigate where the transfer process is altered, we employed a TraI fusion protein system to determine if altering the stability of a protein inserted within the i31 of the TraI mutants would alter mating efficiency.

Utilizing TraI-YFP cloned into the i31 sites, we created YFP point mutants with altered stability, G67A and I161A. Mating efficiency is reduced when YFP is inserted into TraI. However, when the YFP chromophore is destabilized (G67A), or a hydrophobic cluster is altered (161A) mating efficiency recovers to near i31 levels. These data indicate that altering the stability of the protein can affect transfer efficiency. These data also suggest that altered stability may play a role in producing the i31 phenotype. To investigate the stability and folding of the i31 mutants, a region

of TraI (309-858) containing various i31 insertion points were cloned and expressed. These fragments were analyzed by circular dichroism and chemical titration denaturation to determine the ΔG of unfolding for each fragment. There were no significant differences in the ΔG values, however subtle differences in the data are consistent with stability playing a role for the increased mating efficiency for i681. These data also indicate the increased mating efficiency seen for all the i31 mutants analyzed may have multiple different causes, the nature of which is dependent on the location of the insertion.

Joel Schildbach, Jie Xiao, Readers

ACKNOWLEDGMENTS

Getting through the past number of years of my thesis work has been tough, but there have been many friends and family who have lent their support generously. The first people who I'd like to thank are all the great friends I've made in graduate school. Specifically, I want to thank my friend Monica Berrondo, a once fellow graduate student who I met while doing Tae Kwon Do in the Johns Hopkins TKD club. I'd like to thank all my TKD and Kung Fu friends, as wells as all my friends inside and outside of graduate school.

I'd like to thank my family, for pushing me to be great at whatever I'm doing, and never telling me I couldn't do something. They have been incredibly supportive over the past years I've been in school. Included in my family is my cat Toki, who has had his fair share of harassment; at the end of a long and stressful day and all I want to do is cuddle with him and he wants nothing to do with me. Thanks for being the best and tolerating my affections and de-stressing all these years.

After many years of thanking my lab and collaborators in my acknowledgements on posters and presentations, I finally get to thank them on my dissertation. I'd like to thank all the past members, especially Lubos Dostal for helping me in my rotation, and Casey Hemmis for answering questions and helping me learn my way around lab. To the current members, Katie Cox and Beth Buenger, thanks for all the random non-science discussions that keep the lab entertaining and a great place to work. To my collaborators Jie Xiao and Jackson Buss, who helped me with all of my microscopy work and are responsible for a whole section of this

dissertation, thank you for putting up with me and all of my probably dumb questions and problems (especially in the beginning). Thanks to my committee members Jie Xiao and Trina Schroer, and to my mentor, Joel, thanks for helping me through all my problems, bad experiments, experiments that worked or didn't, and life in general for the past seven years. All the sarcasm aside, I truly appreciated being your student and all the guidance and advice.

Last but not least, to my partner Chris, I love you and truly appreciate you being with me for the entire graduate school journey. Your encouragement and support has gotten me through some tough patches, and I would not be the strong and independent person I am today without you.

To Chris

Table of Contents

List of Figures

List of Tables

INTRODUCTION

Antibiotics were first widely used during World War II, and their use in treating wounds and ulcers dramatically changed the outcomes for many gravely wounded soldiers (Waksman, 1947). Injuries that once would have proved fatal due to infection were now survivable. Use in hospitals skyrocketed, and they were seen as a cure-all for any infection. Over time however, infections that were once easily treated with standard antibiotics started to become resistant and they became much harder to successfully treat.

Evolution of antibiotic resistance genes in various microbes has become a huge problem in the field of medicine. Antibiotic resistance has become a prominent modern medical issue due to overuse of antibiotics since their discovery (Levy, 2002). Every year, more and more hospitals spend increasing amounts of money to treat hospital-acquired infections, which are often multi-drug resistant. This problem is only being compounded by over prescription of antibiotics and patients taking those antibiotics improperly, creating bacteria with drug resistances that can pass those resistances to pathogenic bacteria. The occurrence of multi-drug resistant bacteria in recent years has had a high medical and human cost (Centers for Disease Control, 2013).

The process that passes the resistance genes from one bacterial cell to another is known as horizontal gene transfer. Horizontal gene transfer occurs through multiple methods, one of which is the process of bacterial conjugation. In bacterial conjugation, a bacterial cell containing a mobile genetic element finds a cell without that mobile

genetic element, and begins transferring the mobile genetic element from one cell to the other. The donor cell passes a single strand of DNA through a pore complex into the recipient cell, and following second strand synthesis the recipient cell either incorporates the newly acquired DNA into its genome or maintains the element as a separate element (Willetts, 1972). DNA passed from a donor cell to a recipient cell can then be passed vertically to its progeny, potentially conferring to this cell line evolutionary advantages such as antibiotic resistance or the ability to utilize a new metabolite.

Bacterial conjugation is accomplished through a complex of proteins known as the relaxosome. The roles of many of these proteins is known, but there are still parts of the process that we known little about. It is important to analyze these proteins, as they may give insight into how to halt this process on a molecular level and develop new strategies to treat infections. One of these relaxosome proteins, TraI, is responsible for many steps in the process of conjugation. We know parts of its structure and its functions, but how it is regulated or how it interacts with other components is still being investigated. Gaining a more complete understanding of TraI is crucial to fully describing bacterial conjugation and its role in the process. In this introduction the components of the relaxosome, their structures and functions, are described to give a deeper understanding of the importance of TraI in bacterial conjugation.

The Relaxosome

A mobile genetic element, F plasmid, is a 100 kb long single copy plasmid found in Escherichia *coli* (*E. coli*). F plasmid contains within it most of the genes necessary for transfer in a region known as the tra operon (Zechner *et al.,* 2000). This region contains the *tra* and *trb* gene clusters, which encode a series of genes required for conjugation. F plasmid also has an origin of replication (*oriV*) and an origin of transfer (*oriT*). The *oriT* is the position where a group of proteins known as the relaxosome bind and nick the DNA in preparation for transfer of a single strand of DNA (known as the T strand) from cell to cell (Willetts, 1972).

The relaxosome is a protein complex composed of Integration Host Factor (IHF), TraY, TraM and TraI, all encoded by F plasmid except for IHF. IHF is encoded by the host genome. TraY and IHF are necessary for creating the correct architecture required for TraI to nick and unwind F plasmid. These proteins bind within a region of the F plasmid known as the *oriT.* The *oriT* region contains protein binding sites as well as structural elements necessary for the binding and nicking of the DNA by TraI (Figure 1.1). Organizationally, the *nic* site is located on the bottom DNA strand and the structural elements and protein binding sites are all located 5' to *nic* (Di Laurenzio *et al*., 1992, Frost *et al*., 1994, Tsai et al., 1990).

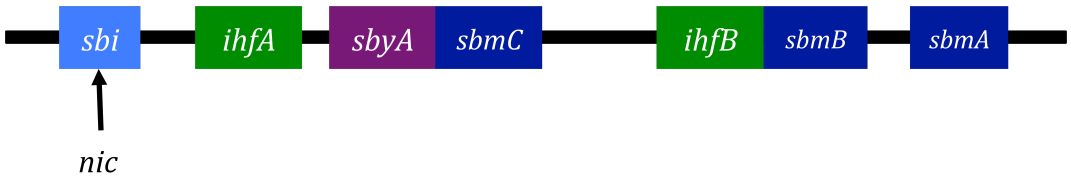

Figure 1.1. Adapted from Williams and Schildbach, 2007, the organization of the *oriT* region of F plasmid. In light blue is the *sbi* site where TraI binds *oriT*. In green are the IHF binding sites, and in dark blue are the *sbm* binding sites, which are bound by TraM. The *sbyA* site in purple is bound by TraY. The binding of the *oriT* region by TraY and IHF bends the DNA and gives TraI access to the single stranded *nic* site, which TraI binds to and nicks to begin the transfer of F plasmid from donor to recipient.

Integration Host Factor

Detailing the components of the relaxosome, IHF is a small heterodimer consisting of two 10 kDa subunits that are closely related to HU, a nonspecific DNA binding protein. HU proteins and members of that family of proteins have been found in many prokaryotes (Oberto and Rouviere-Yaniv, 1996). IHF binds at the *oriT* site *ihfA* and creates a 160˚ bend in the DNA, reversing the direction of the helix axis by binding at the minor groove of DNA (Williams and Schildbach, 2007, Rice *et al*., 1996). As seen in the crystal structure of IHF (Figure 1.2), the dimer bends the DNA by over 160 degrees, reversing the direction of the helix axis. It is able to bend the DNA so drastically due to a proline residue that interrupts the base stacking by intercalating into the DNA. IHF also binds at the lower affinity *ihfB* site, but it is not necessary for nicking of F plasmid (Fu *et al*., 1991). IHF identifies its binding site by indirect readout, which is recognition of a sequence dependent alteration in the conformation of DNA. In the IHF binding site, there is a six base run of adenine that narrows the minor groove, which IHF is able to identify. The binding of IHF creates two large kinks in the DNA, bending it around IHF (Rice *et al.,* 1996). This bending of DNA is necessary for TraI to bind to the *oriT* (Csitkovits *et al.*, 2004).

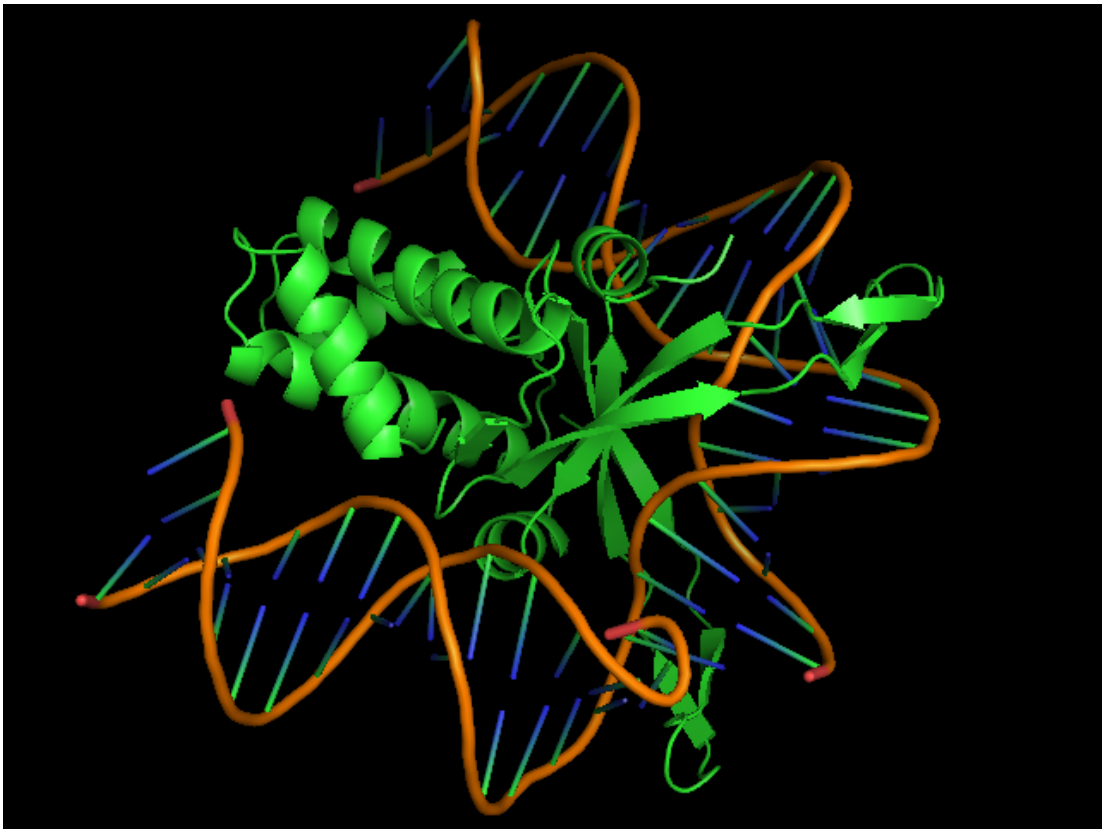

Figure 1.2. Crystal structure of integration host factor (IHF) in green from *E. coli* bound to DNA. IHF depicted as its backbone cartoon structure, and DNA as its cartoon structure (backbone in orange). The DNA is wrapped around the protein, bending it by over 160 degrees by interrupting base stacking by an intercalating proline (not pictured). Structure generated in PyMOL from PDB entry 1IHF, deposited by Rice *et al*., 1996.

TraY

Also participating in the relaxosome, TraY is a site specific double stranded DNA binding protein (Karl *et al*., 2001, Luo *et al*., 1994). There is no crystal structure of TraY, but it is monomeric and has been classified in the ribbon-helix-helix motif (RHH) family of proteins. It contains tandem repeats of this motif, which is unusual (Schildbach *et al.,* 1998). TraY binds at *sybA* located 5' of the nic site and further bends the DNA, allowing TraI to access its binding site *sbi* and nick the DNA at the *nic* site (Nelson et al., 1995, Williams and Schildbach, 2007). The binding site of TraY, *sbyA*, consists of three subsites, two of which are bound cooperatively. These two sites contain imperfect inverted GA(G/T)A repeats, while the third site is direct repeat (Lum *et al*., 2002). Inserting sequence between its binding site *sbyA* and the binding site of IHF, *ihfA*, drastically reduces plasmid mobilization (Williams and Schildbach, 2007). In addition to binding the *oriT* region to promote the nicking reaction, TraY also plays a role in regulating gene expression of the transfer region (Silverman and Scholl, 1996). After TraY and IHF have created the correct DNA architecture for TraI, it can bind to the *oriT* DNA and carry out its function in the relaxosome complex.

TraM

While not required for the cleavage of *oriT* and not involved in creating the architectural elements TraI requires to carry out its role in conjugation, TraM is required for conjugation. TraM is thought to interact with TraD to bring the relaxosome complex into proximity with the transfer machinery. It does this by

binding at the *sbmA, B, and C* sites in the *oriT* (Achtman *et al.,* 1971, Lu *et al.*, 2008). TraM may also interact with TraI to enhance the activity of TraI and the nicking reaction (Ragonese *et al*., 2007). TraM is a small tetrameric DNA binding protein. It recognizes its high affinity binding site, *sbmA*, as a dimer of tetramers. The crystal structure from plasmid pED208, an F-like plasmid, was recently solved and gave insight into the role of TraM in the relaxosome complex (Figure 1.3) (Wong *et al*., 2011). TraM contains an N-terminal ribbon-helix-helix (RHH) motif that binds DNA in a staggered arrangement that allows for DNA binding without any direct contact between the tetramers. The tetramers of TraM target the sequence motif of GANTC 12 bp apart within *sbmA*. Each tetramer targets a pair of these sequence motifs by coordinated kinking and unwinding of the DNA to align the motifs on the same side of the helix. This allows for the C-terminal tetramerization domain of TraM to remain free, and the tetramerization domain can interact with TraD. TraD is the pore coupling protein, and the interaction between the tetramerization domain and TraD drives recruitment of the relaxosome to the pore complex (Wong *et al.,* 2011).

Figure 1.3. The crystal structure of the asymmetric unit of TraM bound to ssDNA. Each monomer of the tetramer is colored separately. The N terminal domain of TraM (closest to the ssDNA strand) interacts with the ssDNA, while the C-terminal tetramerization domain remains free of DNA contacts to interact with TraD. Structure created in PyMOL from PDB entry 3ON0 from Wong *et al*., 2011.

TraI

The protein central to the relaxosome, TraI is a multiple domain protein that carries out different functions during conjugation. TraI is a 1756 amino acid long 192 kD single-chain protein, possessing four distinct domains. TraI has an N-terminal relaxase (nickase) domain encoded in the first 300 amino acids, a single-stranded DNA binding domain extending from residue 300 to 822, a helicase domain encompassing residues 980 to 1500, and a 200 amino acid C-terminal domain (Figure 1.4)(Traxler and Minkley Jr, 1988, Wright *et al.*, 2012, Dostal and Schildbach, 2010). The relaxase domain recognizes the *nic* site and cuts a single strand of F plasmid. The recognition of the *oriT* and the *nic* site by TraI is highly sequence specific for an 11 bp region of *oriT*, and a single base substitution in that region can reduce the affinity of TraI for a ssDNA oligonucleotide containing the *oriT* sequence by as much as 8000-fold (Stern and Schildbach, 2001). Substitutions between bases 140' and 141' in the *oriT* sequence (numbering as defined by the Frost lab) reduce affinity by at least 5000-fold (Stern and Schildbach, 2001).

A.

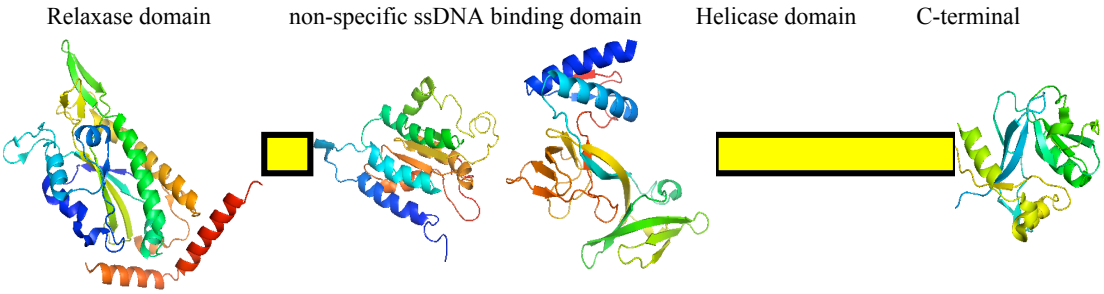

B.

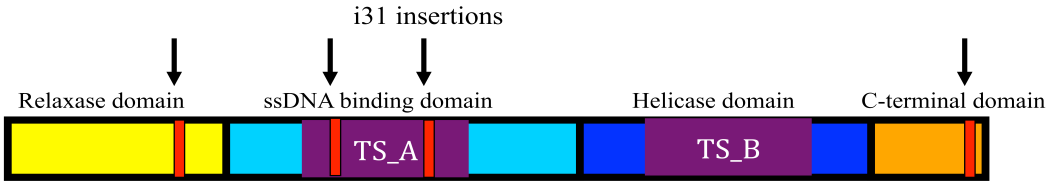

Figure 1.4. **A**, TraI consists of four domains (from left), a relaxase domain; non-specific single stranded DNA binding domain, a helicase domain, and a C-terminal domain. Parts of the structure of TraI have been solved as seen above, but sections of TraI (depicted by yellow boxes) are lacking specific structural data. Each domain carries out a different function during the mating process, with the relaxase domain binding to the *oriT* of F plasmid and nicking the DNA at the *nic* site. The helicase domain acts to unwind the DNA for transfer of a single strand to the recipient cell. The C-terminal domain is thought to be involved in interactions with the pore complex. **B**, a schematic representation of TraI, including the four domains, the locations of the two translocation (TS) sequences, and the positions of the i31 mutations within TraI.

TraI Nicking Reaction

The nicking reaction is a key step in conjugation, and the details of the reaction are key to understanding the importance of TraI. Once TraY and IHF have assembled on their binding sites at the *oriT*, TraI binds at the *sbi* site and locates the *nic* site. TraI nicks the DNA via a Mg^{+2} dependent nucleophilic attack at a tyrosyl hydroxyl oxygen on a DNA phosphate at *nic*. The attack at the oxygen leads to a covalent tyrosinyl-DNA bond between the DNA and Tyr16 of TraI that is isoenergetic and reversible (Street *et al.*, 2003). The 5' end of the F plasmid DNA is bound to TraI in a long-lived intermediate (Byrd and Matson, 1997). TraI, bound to DNA, is transferred from donor to recipient through a type IV secretion system pore. Once transferred through the pore, the nicking reaction is reversed and the DNA is recircularized. Once the plasmid DNA has been recircularized, second strand synthesis occurs, and the cell receiving the plasmid now contains a double-stranded copy of the plasmid (Dostal and Schildbach, 2011, Lang *et al.*, 2010).

TraI Relaxase Domain

The activity of each domain is important to the overall function of TraI in conjugation. The relaxase domain of TraI contains a His-hydrophobe-His (HUH) motif in its active site. These histidine residues in the active site are part of a three histidine cluster that bind a divalent cation (as stated above) that is required for the cleavage of *oriT*. Substitutions for the histidine residues were found to alter the binding of the metal ion, indicating their role in the binding site (Larkin *et al*., 2007).

TraI can utilize various metals to coordinate the *nic* reaction, and is able to use Mg^{2+} and Mn^{2+} at millimolar and micromolar concentrations respectively (Datta *et al*., 2003). This metal binding motif aids in the binding and nicking of ssDNA by positioning the DNA and increasing the positive charge on the phosphorus of the DNA backbone to enhance the nucleophilic attack by the other active site residue crucial to the reaction, Tyr16 (Larkin *et al*., 2005, Dostal *et al.,* 2011). Tyr16 is required for the *nic* reaction, as the nucleophilic reaction covalently links the hydroxyl oxygen of Tyr16 to the 5′ end of the DNA (Dostal *et al.,* 2011).

Non specific ssDNA Binding Domain

The ssDNA binding domain is located between residues 300 and 822. The ssDNA binding domain region resembles RecD, but does not possess any ATPase activity (Wright *et al.,* 2012). The ssDNA binding domain competes with the relaxase domain for DNA binding, meaning when one domain is occupied it prevents the other from binding (Dostal and Schildbach, 2010). The ssDNA binding domain displays sequence specificity and binds ssDNA with high affinity. The negative cooperativity between domains is believed to be part of the regulation of the timing of transfer of F plasmid (Dostal and Schildbach, 2010).

Helicase Domain and Translocation Sequences

Once the DNA is cut and bound to the relaxase domain, the helicase domain functions to unwind the DNA in a 5′ to 3′ manner (Lang *et al.*, 2010, Dostal and Schildbach, 2011). TraI contains within the single stranded DNA binding domain and

the helicase domain two regions, called translocation sequences (TS) that function as pore recognition sequences. In the conjugative model system plasmid R1, interaction between a domain of TraD (T4CP) and TraI have been demonstrated to be necessary for initiation of transfer through the pore (Mihajlovic *et al*., 2009, Sut *et al.*, 2009). The translocation sequences TSA (amino acids 530-816) and TSB (1255-1564) in plasmid R1 target the relaxosome complex to the secretion pore (Lang *et al.*, 2010, Redzej *et al.*, 2013). TraI from plasmid R1 and TraI from F plasmid are highly homologous, and although the translocation sequences for F plasmid TraI have not been investigated, due to the sequence homology the translocation signals are most likely in the same regions.

C-terminal Domain

The C-terminal domain is comprised of the last 200 amino acids of TraI. The C-terminal domain may be necessary for interaction with TraM. TraM, as previously described, is part of the relaxosome and interacts with TraD to bring the relaxosome to the transfer machinery and may also interact with TraI through its C-terminal domain (Lu *et al*., 2008, Ragonese *et al*., 2007). Part of the structure of the C-terminal domain has been solved, which will be detailed in the next section (Guogas *et al*., 2009).

Structure of TraI

The overall structure of TraI has been difficult to determine, as sections of the protein are disordered and x-ray crystallography or nuclear magnetic resolution

spectroscopy (NMR) of the entire protein are not possible. The structures of sections of TraI have been solved, including the relaxase domain, part of the single stranded DNA binding domain, and part of the C-terminal domain, but the full structure is still unsolved. Having already detailed the activities of the domains of TraI, the structure is no less important to understanding the full role of TraI.

The structure of the relaxase domain gave insight into the structure of the active site of the relaxase, and helped to identify the active site residues and the mechanism by which TraI cleaves the *oriT* (Figure 1.5)(Larkin *et al.,* 2007). Since the structure of the relaxase was solved, other sections of TraI have been crystallized or analyzed by NMR to obtain structural data. The solution of the NMR structure of residues 381-569 provided insight into the domain organization of this region. The structure closely resembles a RecD domain, although there is no ATPase activity present in this domain (Figure 1.6)(Wright *et al.,* 2012). The structure of part of the C-terminal domain has been solved, giving insight into its role in conjugation (Figure 1.8)(Guogas *et al*., 2009). Most recently, the structure of R1 TraI from 575 to 786 was solved, which includes the Translocation A (TSA) sequence (Figure 1.7). Like the structure of the N-terminal section of the ssDNA binding domain (Figure 1.6), this domain also resembles RecD (Redzej *et al*., 2013).

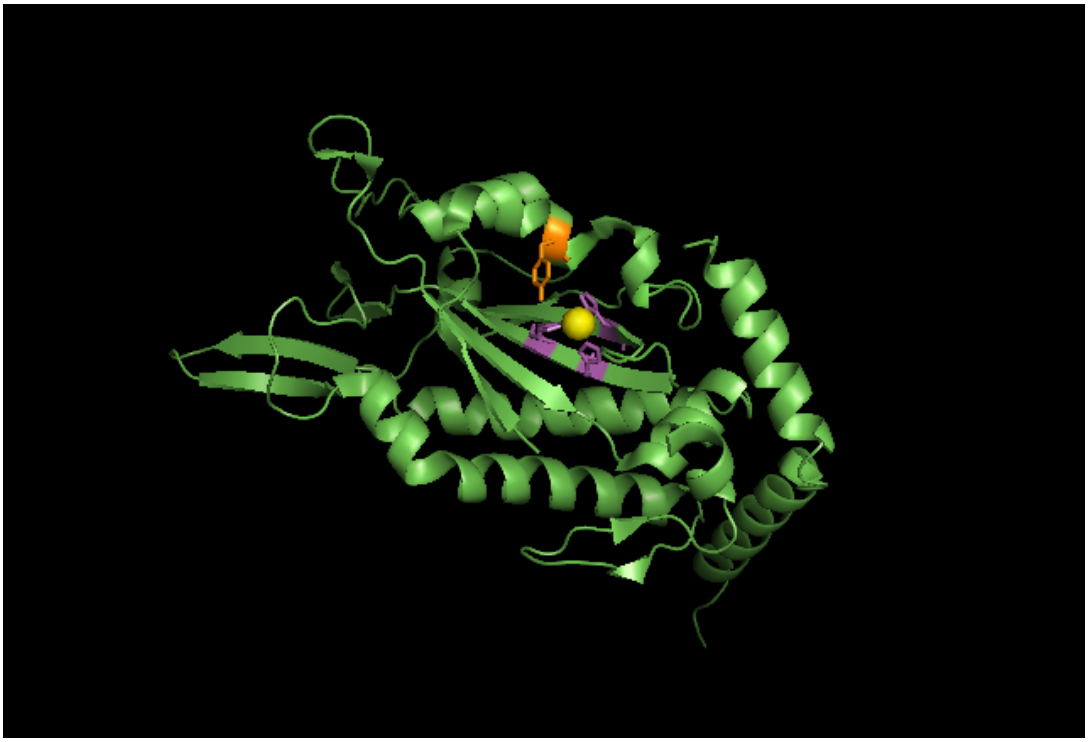

Figure 1.5. The relaxase domain of TraI, generated in PyMOL from PDB entry 1P4D from Datta *et al*., 2003. The relaxase uses a metal ion (in yellow), coordinated by the His-hydrophobe-His (HUH) cluster (in magenta) in the active site to position the nic site DNA for Tyr16 (in orange), which performs a nucleophilic attack at a tyrosyl hydroxyl oxygen on a DNA phosphate, and cleaves the ssDNA.

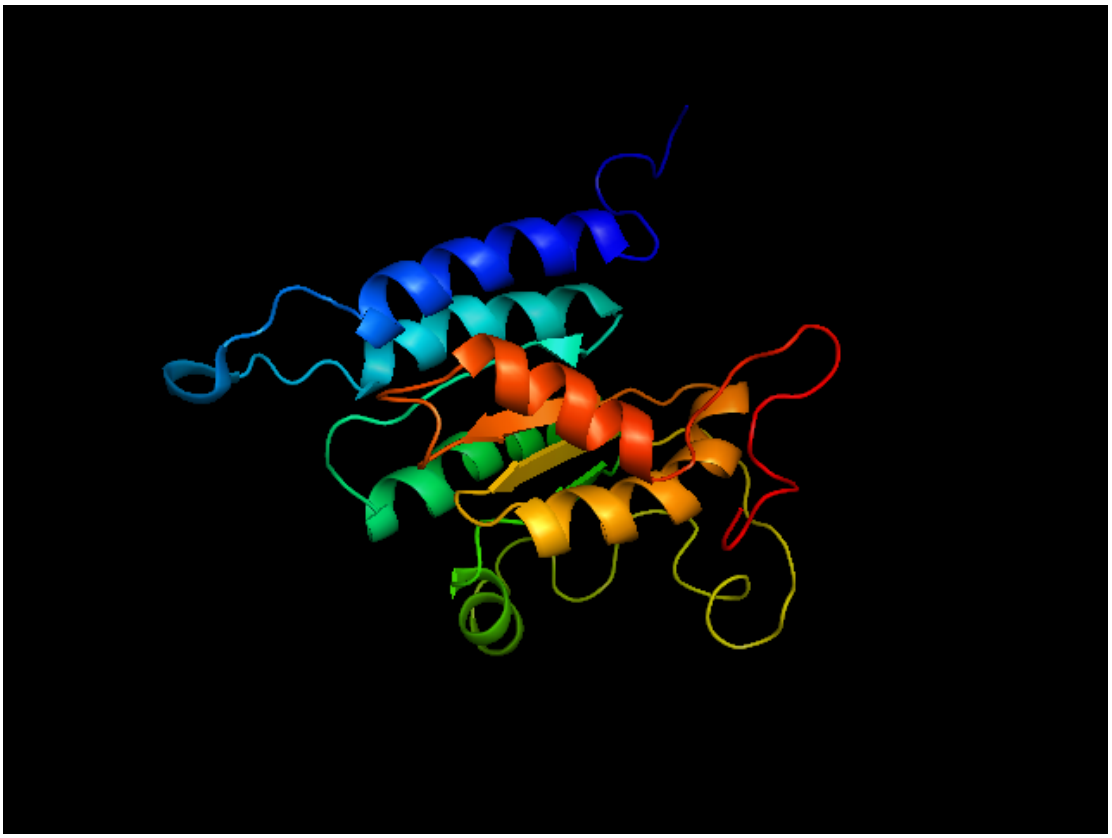

Figure 1.6. TraI 381-569, part of the ssDNA-binding domain, similar to RecD, from PDB entry 2L8B. Image generated in PyMOL from Wright *et al.,* 2012, the single stranded DNA binding domain is thought to compete for DNA binding with the relaxase domain and prevent TraI from nicking. The negative cooperativity between the ssDNA binding domain and the relaxase domain is thought to be a major regulator of F plasmid transfer.

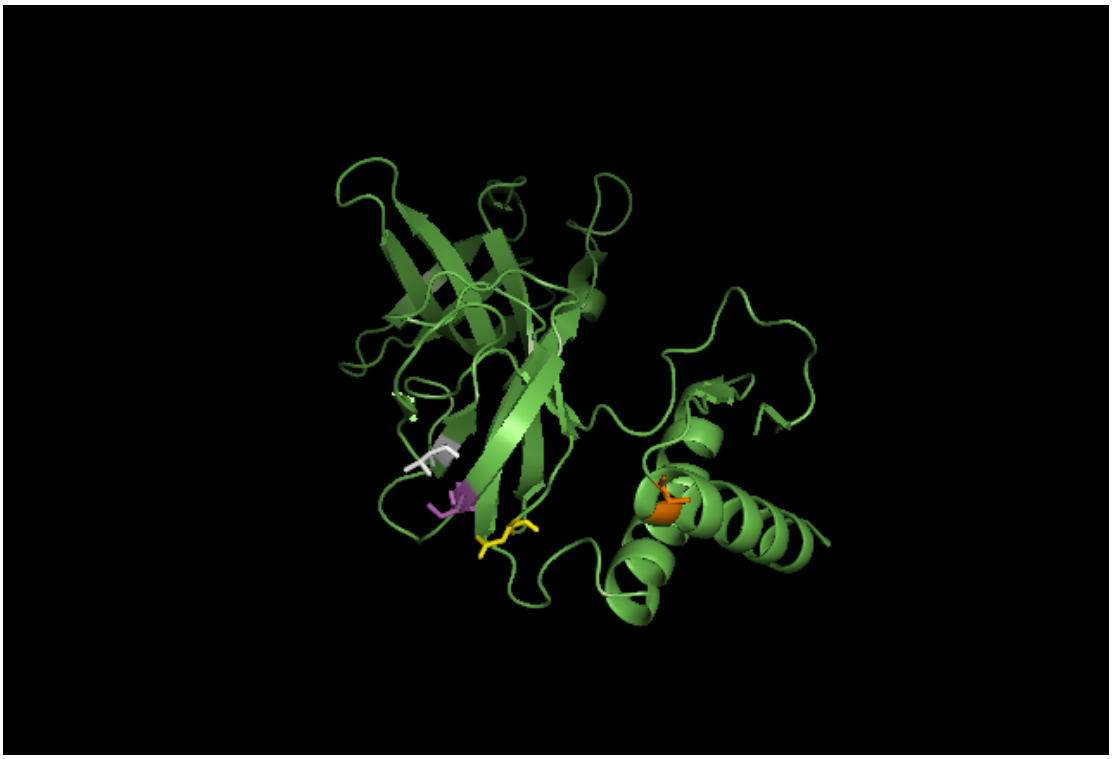

Figure 1.7. The TSA region of TraI, generated from PDB entry 4L0J in PyMOL from Redzej *et al.,* 2013, displayed as a cartoon structure. The TSA region contains specific residues, A593 (orange), D714 (yellow), S739 (magenta), and T746 (white), which are thought to make specific contacts with the pore coupling protein, TraD. These residues, shown as a stick models, define an interaction surface in the TSA of the protein.

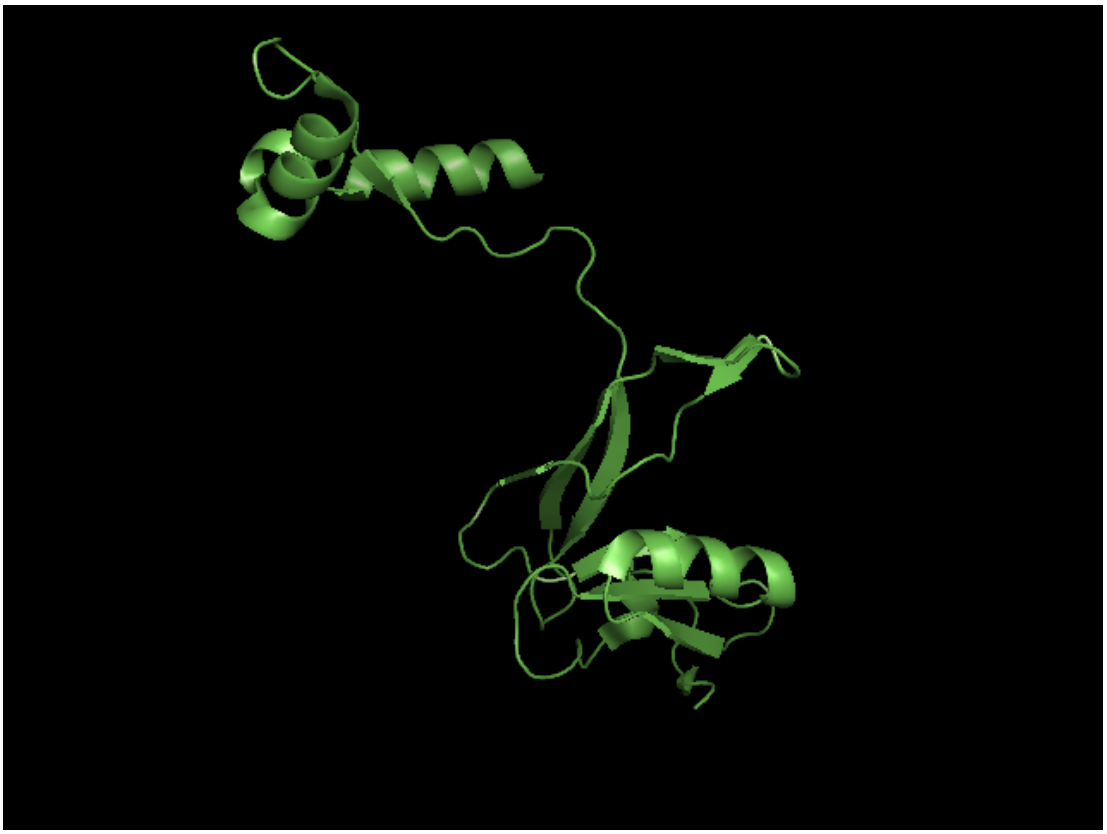

Figure 1.8. The C-terminal domain of TraI generated in PyMOL, shown in green, PDB entry 3FLD, from Guogas *et al*., 2009. The C-terminal domain of TraI is thought to play a role in recruitment of the relaxosome to the pore complex through interactions of the C terminal domain and pore complex proteins.

The amino acid sequence of the TSA of R1 TraI is nearly identical to F TraI, with only a two-residue difference between the two in the region of 575 to 786. The structure of this domain is therefore similar to the domain in F TraI. The structure of this domain aided in identifying residues within the TSA that are crucial for translocation. The TSA comprises the region of amino acids 530 – 816. The second translocation sequence, the TSB, is located closer to the C-terminus of the protein, in between residues 1255 and 1564. Only one of these translocation sequences is required for transfer of the protein (Lang *et al.*, 2011).

Using the structure and previous research, Redzej *et al.,* were able to determine that residues 593, 714, 736, and 739 play an important role in the transport of R1 TraI from donor to recipient (Redzej *et al.,* 2013). These residues, which are identical in F TraI, may also play an important role in F TraI and these recent structures give increasing insight into the function of TraI. Although a full structure has not been solved, an envelope structure of the protein has been developed using small angle x-ray scattering (SAXS), indicating an elongated conformation in solution (Cheng *et al.*, 2011). Recent work on calculating the solution structure of TraI by modeling simulations have generally agreed with the envelope structure of TraI determined by Cheng *et al.,* 2011. These structures generally predict that TraI folds into a compact molecule despite the unstructured regions (Clark *et al.*, 2014).

The TraI protein from F plasmid belongs to a large family of TraI and TraI-like relaxase proteins from mobilizable plasmids across incompatibility groups. The relaxases from the various groups share functionality (nicking ssDNA), but are highly divergent in general sequence and organization. In the IncF group, the relaxases

generally consist of the N-terminal relaxase domain, a C-terminal helicase domain, and a C-terminal domain involved in plasmid transfer (Garcillan-Barcia et al., 2009). In other groups, the proteins can look quite different and be of varying sizes, but they all carry out the same function; nicking ssDNA for transport and transfer from cell to cell.

TraI Unfolding

During the mating process, TraI is transported along with DNA from one cell to another (Dostal *et al.,* 2011, Willetts, 1972). It is widely accepted that TraI will pass through the conjugative pore on its way to the recipient, but the pore structure has a main ring structure with a cap that has a 20 Å opening to the pore exit (Fronzes *et al*., 2009). While there is likely some rearrangement of the pore structure to increase the diameter of the pore to allow exit of substrate from the pore into the recipient cell, even with mechanical force the folded structure of TraI would probably not transit the pore successfully. Moreover, TraI undergoes some degree of unfolding to transit the pore structure into the recipient cell. Many further studies on other protein translocation systems have investigated the forces necessary for protein translocation, and unfolding of protein substrate. For example, Eilers and Schatz discovered that mitochondrial pre-proteins that are folded before transport into the mitochondria must unfold for transport through the membrane (Eilers and Schatz, 1986). The mechanical principles behind protein unfolding are universal across all systems. Although most work on protein unfolding during transport has been

conducted in eukaryotic systems, there is ample precedent for protein unfolding being necessary for transport across a membrane in prokaryotes.

Having described the relaxosome in detail, another important part of the transfer machinery is the pore. The relaxosome and its components function to transport ssDNA from one cell to another, and to get from one cell to another a pore is required. Understanding the pore and its structure is crucial to fully understanding the transport process. In the next section, the type of pore that is used by F and F like plasmids is described.

Type IV Secretion Systems

As large as TraI is, it is able to pass through a type IV secretion system pore (T4SS) along with the T strand DNA it is covalently bound to (Juhas *et al.,* 2008). Both Gram negative and Gram positive bacteria use type IV secretion systems for the transfer of mobile genetic elements. Type IV secretion systems are versatile systems capable of transporting substrates of various types and size, including known relaxases MobA and VirD2 (Vergunst *et al.,* 2005, Ninio and Roy, 2007). There are at least six known secretion systems used by Gram negative bacteria to secrete a variety of factors into the environment and other cells (Alvarez-Martinez and Christie, 2009). The various types of secretion systems can be further broken down into sub-categories. The F plasmid uses the T4SS IVA to transport plasmid DNA and protein during bacterial conjugation. This system resembles the T4SS in *Agrobacterium tumefaciens,* the VirB/D4 pore system. The VirB/D4 is one of the most well studied T4SS, and many parallels between the F plasmid T4SS and the VirB/D4 systems can

be drawn to illuminate F plasmid and TraI transfer during conjugation (Christie *et al.,* 2005). Other type IVA systems include those in RP4 (IncP), R388 (IncW), and pKM101 (IncN) as well as F plasmid (IncF) (Juhas *et al.,* 2008, Christie *et al.,* 2005).

Only recently has the structure of a type IV pore been solved. The structure of the type IV pore from the plasmid pKM101 was solved at 15 Å by cryo-EM, and recently refined to 8.5 Å (Fronzes *et al*., 2009, Rivera-Calzada *et al.*, 2013). A higher resolution structure of the outer membrane portion of the pore complex was solved by crystallography at a resolution of 2.6 Å (Chandran *et al.*, 2009). These structures have given insight into the structure and organization of the pore complex (Figures 1.9 and 1.10). The genes encoding the proteins that comprise the pore complex are usually located in a single operon or group of operons, and are highly related within the T4SS IVA systems. The VirB/D4 transfer system is composed of 12 proteins, VirB1-VirB11 and VirD4. The F plasmid encodes eight T4SS subunits homologous to subunits in the VirB/D4 complex, as well as subunits only found in the T4SS used by F plasmid (Lawley *et al*., 2003, Christie *et al.,* 2005).

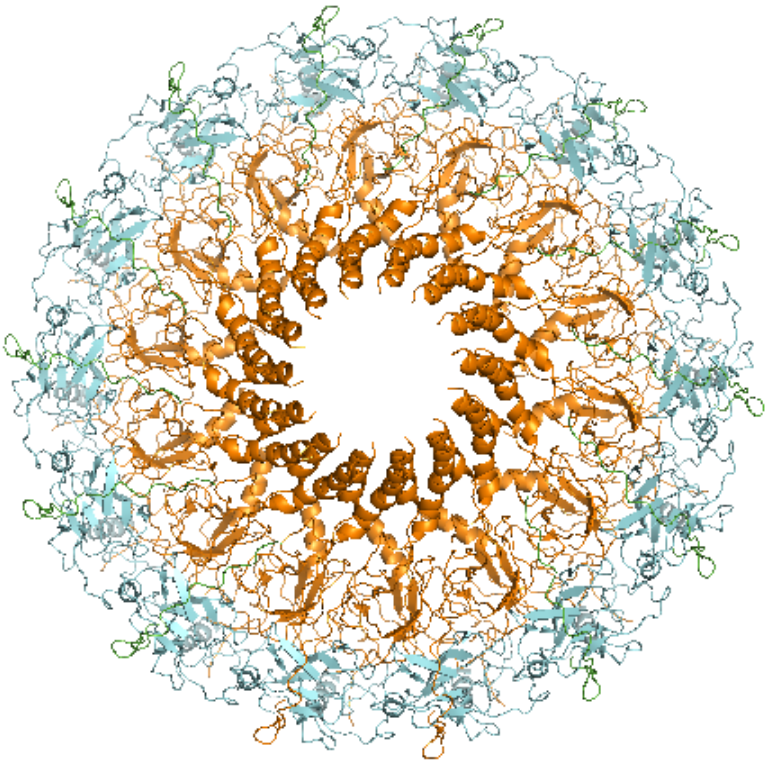

Figure 1.9. The structure of the O-layer of the pore complex from pKM101, as seen from the top down, generated in PyMOL from PDB entry 3ZBI, deposited by Rivera-Calzada *et al.,* 2013. In green is TraN, in orange is TraF, and in blue is TraO. These proteins (14 copies of each) form a ring structure with a cap that has a 10 Å constriction. TraF forms the interior of the outer layer of the pore, while TraO forms the outer sheath of the pore. TraF acts as a signal transmitter through the entire pore, interacting with the ATPases and propagating conformational changes by ATP hydrolysis throughout the structure (Jackubowski *et al.,* 2009).

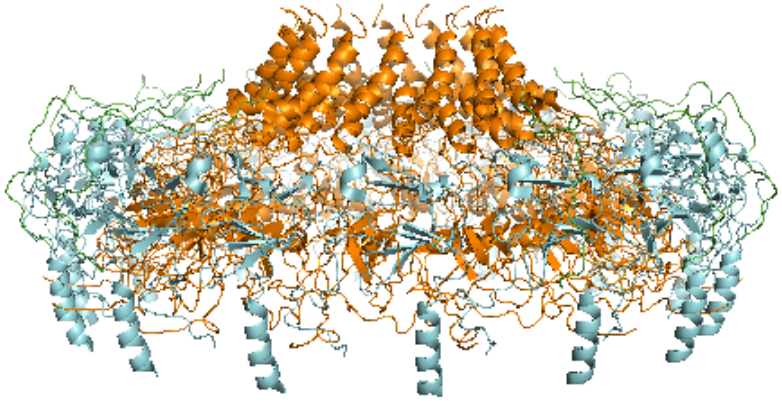

Figure 1.10. A side view of the structure of the O-layer of the pore complex from pKM101, as seen from the top down, generated in Pymol from PDB entry 3ZBI, deposited by Rivera-Calzada *et al.,* 2013. In green is TraN, in orange is TraF, and in blue is TraO. Here we can more clearly see how TraF extends from the cap structure at the top down into the interior surface of the pore. TraO forms the exterior of the I layer.

Type IV secretion system complexes span both the inner and outer membranes. In the structures reported in Fronzes *et al*., 2009 and Chandran *et al.*, 2009, the core complex is a 1.07 megadalton structure comprising VirB7, VirB9, and VirB10 (in pKM101, these are TraN, TraO, and TraF respectively). The whole core complex measures approximately 185 Å from top to bottom and from side to side. The core complex is comprised of 14 copies of each protein, with the structure divided into an inner (I) layer inserted into the inner membrane, and an outer (O) layer inserted into the outer membrane of the bacteria (Figure 1.10). The I layer is composed of the N-terminal domains of TraO and TraF. The O layer consists of TraN and the C-terminal domains of TraO and TraF, creating a main ring structure with a cap that has a 20 Å opening and a 10 Å constriction (Fronzes *et al*., 2009). The diameter of the constriction varies, as the crystallography structure reports a constriction of 20 Å, indicating the structure of the core complex is flexible. The diameter of dsDNA is ~20 Å, and although only ssDNA is being transported, the diameter of ssDNA in addition to protein as they are transferred through the pore is more than likely larger than 10 Å. There is probably some movement within the cap region of the pore to widen its diameter and allow the passage of substrate from one cell to another, but unfolding of the protein substrate is also possibly required (Chandran *et al.,* 2009, Mandelkern *et al.,* 1981).

The cap of the pore is comprised of TraN only, created by a hydrophobic ring of 2-helix bundles. TraO and TraF surround the inner TraN ring. The inner membrane channel is likely formed by three proteins; VirB3, VirB6, and VirB8 (Cascales and Christie, 2004). Three ATPases power secretion through the pore complex, VirB4,

VirB11, and VirD4. These ATPases, acting in concert with one another, form a complex on the cytoplasmic face of the pore and provides the energy for the translocation of substrate through the pore (Waksman and Fronzes, 2010). The F plasmid encodes most of the core T4SS components, including genes for pilus and pore formation (Lawley *et al.,* 2003). Before these recent structures the exact details of the T4SS pore were not well understood. The general structure of a pore used in a conjugative process is now known, giving us insight into what F plasmid DNA and TraI might pass through on its way into the recipient. The various T4SS used by different species of bacteria all provide similar functionality (Tseng *et al.,* 2009). In addition to the pore structure, the pilus is an important part of the transfer machinery involved in identifying potential mating targets. In the next section the F pilus is described to give a deeper understanding of the mating machinery.

F Pilus

As part of the pore structure and the translocation machinery, conjugative plasmids encode proteins that form a pilus structure on the cell surface. In *E. coli*, a donor cell (F^+) will extend a pilus to recognize a recipient cell (F^-). Once an F^- cell is identified by the pilus, the F^+ cell initiates mating pair formation (Mpf) and mating pair stabilization (Mps). It is not entirely clear how the pilus identifies an F^- recipient, but it is thought to be either an interaction between lipopolysaccharides or a negative charge on the cell surface (Frost *et al*., 1994, Hazes and Frost, 2008). After Mps and the identification of the F^- recipient by the F^+ donor, an unknown signal is transmitted

to the donor to begin the process of transferring the F plasmid DNA to the recipient through the T4SS-like pore (Frost *et al*., 1994).

The F pilus is composed solely of the F plasmid encoded pilin protein. F plasmid pili can be up to 20 μm long, and have an outside diameter from 85Å to 95 Å and a central lumen of approximately 2-3 nm (Lawn, 1966). The F pilus is classified as a thick flexible pili, involved in both Mpf and Mps (Bradley, 1980). The F pilus is made up entirely of pilin, encoded by the *traA* gene (Frost *et al*., 1984). Pilin is a small 70 residue protein that is largely α-helical in structure. Before it is incorporated into the pilus structure, the *traA* product is processed to mature pilin. A 51 amino acid signal sequence must be removed, and the amino acid terminus of the remaining protein is acetylated (Frost *et al*., 1984). The *traA* product is processed by TraQ, which cleaves the 51 amino acid signal sequence, and TraX, which performs the acetylation of the amino terminus (Maneewannakul *et al.,* 1993). Finally, plasmid incompatibility groups are important for understanding plasmid inheritance.

Plasmid Incompatibility Groups

Using the pili, a F^+ cell identifies an F^- cell to transfer the plasmid. Both Gram negative and Gram positive bacteria contain plasmids. Plasmids can be transferred from one cell to another of the same species and across species. However, the transferred plasmid is not always retained and is often not kept by the cell; the plasmid is not stability inherited. This can be due to the presence of another plasmid already in the cell. The plasmid that is already present is unable to stably coexist with the new plasmid, and it destabilizes the inheritance of the second plasmid. This

phenomenon of lack of stable inheritance is known as plasmid incompatibility, which occurs when the plasmids present in a cell contain the same origin of replication and are competing for replication factors (Novick, 1987). Plasmids have been divided and categorized into various incompatibility groups, with F and F-like plasmids being grouped into the IncF group. These plasmids are generally repressed for transfer by the FinOP system, with mating events occurring about once for every thousand cells (Boyd and Hartl, 1997). The structure and function of TraI, the relaxosome components, the pore structure, and details on bacterial conjugation have been presented to give a full understanding of the mating process.

Altering the proteins involved in the relaxosome and the transfer of F plasmid can alter the mating process. For example, knocking out the ATPase activity of TraI eliminates the transfer of DNA (Dostal *et al.,* 2011). There are TraI mutants that can increase or decrease mating efficiency, depending on where the mutation occurs. These strains are known as the i31 collection.

i31 *E. coli* strains

How F plasmid is regulated for transfer is only partially understood, and the role TraI plays in this regulation is not completely defined. There is a cost to bacteria for maintaining a plasmid, as there is a limited amount of energy available for replication. There is a cost to expressing a gene, and while gene replication only accounts for 2% of the energy used by a cell, gene translation (protein synthesis) takes up 75% of a cell's energy (Harold, 1986). If a cell suddenly has an increase in the number of genes, say from a plasmid, the energy cost increases. This puts

pressure on the cell, and creates a cost to the plasmid that can lead to destabilization of the inheritance of the plasmid, despite potential benefits the plasmid might have conveyed. Many conjugative plasmids carry a system that inhibits their horizontal transfer (*fin*) due to plasmid costs to the host cell. The *fin* system self-represses the conjugative transfer of that plasmid. When a conjugative plasmid's *fin* system is removed, the plasmid becomes more costly to the cell, and although a fin^- plasmid spreads more quickly, the plasmid is subsequently replaced by fin^+ plasmids (Haft *et al.,* 2009).

To maintain and transfer only a single copy of F plasmid, the transfer process is highly regulated. TraI itself has negative feedback mechanisms and recognition motifs. There is negative cooperativity between the relaxase domain and the single stranded DNA binding domain, and within the ssDNA binding domain and the helicase domain are two pore-signaling translocation sequences (Zechner *et al.,* 2010, and Dostal and Schildbach, 2010). However, it is not known exactly how these mechanisms act on DNA transfer. To better understand the DNA transfer in the conjugative process, we set out to use novel methods to probe TraI mutants. The TraI mutants that were used primarily in this study were TraI i31 mutants previously created by the Traxler lab and published in Haft *et al.*, 2006.

In that study, they used a transposon mutagenesis screen (lambdaTn*lacZ*/in system) to create in-frame small 31 amino acid scars (Manoil *et al.*, 1997, Manoil *et al.*, 2000). The i31 insertion includes a unique cloning site, a BamHI site that can be used for cloning DNA encoding small peptides or proteins into TraI. They found that insertions in certain regions of the protein were not only tolerated, but that the mutant

TraI proteins facilitated transfer with a mating efficiency increased over that of wild-type (WT) TraI on the same vector (Haft *et al*., 2006). They postulated that the increase in mating efficiency could be due to the insertions releasing the protein from some sort of negative regulation of transfer (Haft et al., 2006). However, the mechanism by which the release from negative regulation was achieved was not determined. Here we aim to use a SeqA-YFP reporter system to better understand the relationship between DNA transfer and the TraI mutants. This system utilizes a fluorescent reporter, SeqA, in the recipient cell to assay DNA transfer during bacterial mating.

SeqA

The protein SeqA is an integral part of bacterial chromosomal replication timing. The indication of a replication timing mechanism was first published by Russell and Zinder in 1987, when they discovered that cells that lack a dam adenine methylase could not be efficiently transformed by methylated *oriC* containing plasmids. However, when these cells were transformed by unmethylated plasmids containing an *oriC*, transformation efficiency was restored. This indicated that the methylation status of DNA was important for *oriC* initiation (Russell and Zinder, 1987). Further investigation by various researchers into the components of the replication timing mechanism eventually led to the discovery of the protein SeqA. SeqA forms part of the timing mechanism that prevents reinitiation of the *oriC* (Lu *et al.,* 1994). DNA binding by SeqA sequesters the *oriC* for approximately one third of

the replication process. Along with other control mechanisms, this prevents the premature re-initiation of the *oriC* (Lu *et al.,* 1994, Campbell and Kleckner, 1990).

SeqA binds at both methylated and hemimethylated GATC sites within DNA. It preferentially binds hemimethylated DNA, with a K_D in the nm range (Brendler and Austin, 1999). A dimer of SeqA binds the *oriC* to prevent reinitiation after it is initiated by DnaA (Skarstad and Boye, 1994). Binding of SeqA to DNA is cooperative, with a Hill Coefficient of 4.7 (Skarstad *et al*., 2000). SeqA requires multiple GATC sites spaced 5 - 34 bases apart to bind and form an oligomer that will sequester the site. The *E. coli oriC* has such an arrangement of GATC sites, (Figure 1.11) and no other site on the chromosome has such an arrangement (Oka *et al*., 1980). The *oriC* is about 245 base pairs in length with both DnaA targeting sequences and GATC sites targeted by SeqA (Oka *et al*, 1980, Asada *et al*., 1982).

SeqA is 181 amino acids long and has two domains, an N-terminal oligomerization domain, and a C-terminal DNA binding domain (Figure 1.12). The first 50 residues comprise the oligomerization domain, and residues 51-181 comprise the DNA binding domain (Guarne *et al.,* 2002). The oligomerization domain (residues 1 - 33) folds into two α-helices and one β-sheet. Residues 34 - 63 form a flexible linker between the oligomerization domain and DNA binding domain, and is responsible for the ability to bind GATC sequences up to 34 base pairs apart (Guarne *et al*., 2005, Brendler and Austin, 1999). Residues 64 - 181 fold into a small three-strand antiparallel beta sheet, and seven alpha helices (Figure 1.12) (Guarne *et al.*, 2002).

Arrangement of GATC sites within the *oriC* of *E. coli*

Figure 1.11. The *oriC* of *E. coli*, about 245 bases long, has a distinct arrangement of GATC sites (yellow ovals) that SeqA bind to sequester the oriC to prevent reinitiation. The GATC sites in the cluster are located within 34 bp of each other, as SeqA cannot bind and form an aggregate if they are farther apart. We found that F plasmid has a similar arrangement of GATC sites that would allow for SeqA binding and aggregate formation. Schematic of the *oriC* adapted from Hupert-Kocurek K and Kaguni JM (2011).

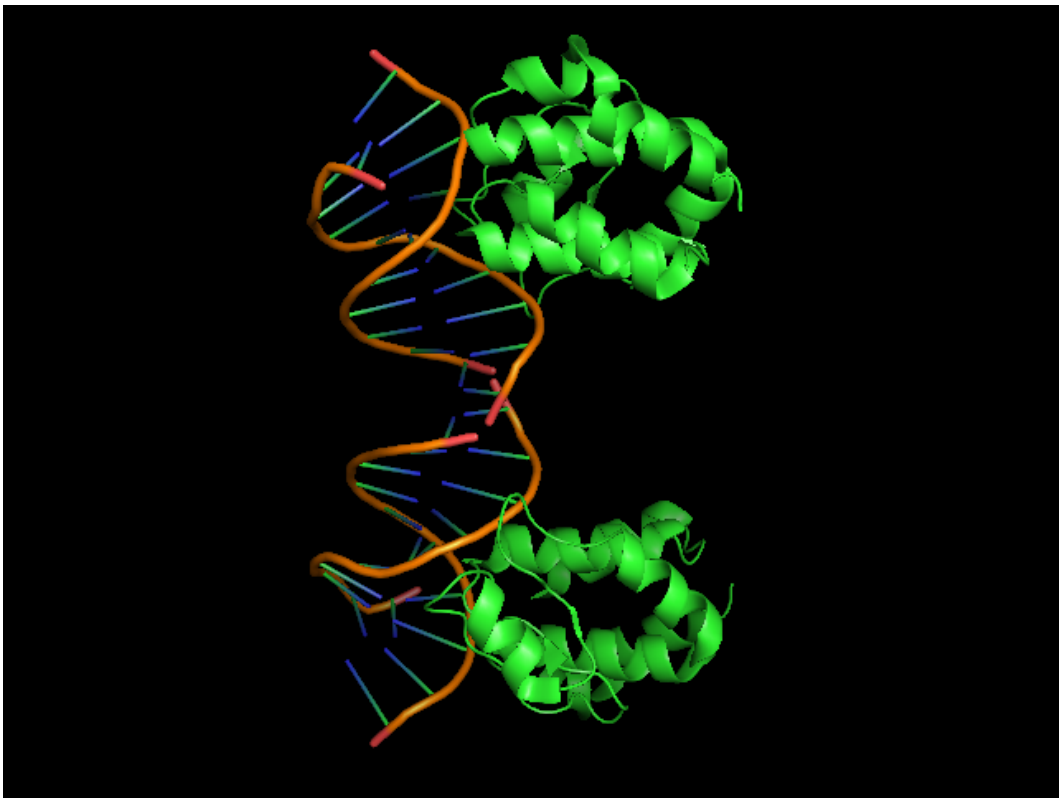

Figure 1.12. Adapted from the PDB entry 1IU3, The DNA binding domain of SeqA, residues 71 – 181, in complex with hemimethylated DNA. In green, represented in cartoon format, are two DNA binding domains from two SeqA molecules bound to DNA (cartoon format). In order to form an aggregate, GATC sites on the DNA need to be situated close together for the N-terminal dimerization domains of SeqA to bind. A flexible linker connects the DNA binding domain and dimerization domains, and GATC sites can be up to 34 bases apart and SeqA will still form an aggregate filament.

SeqA binds DNA as a dimer, and oligomerization occurs by multimerization of the dimers. This creates a left-handed helical filament with each dimer turned 90 degrees to the previous one (Guarne *et al*., 2005). The SeqA filaments can form large aggregates that sequester the DNA it is bound to due to the cooperativity of binding, and requires at least 6 GATC sites in close proximity to stabilize the aggregate (Han *et al*., 2003). This is important for sequestering the *oriC* during replication, as this aggregate physically blocks DnaA from reinitializing the *oriC*. Without the dimerization domain, SeqA binding would not be able to block DnaA. SeqA was recently used as a reporter in a new type of mating assay that utilizes the protein in live cell fluorescent microscopy (Babic *et al*., 2008).

Traditional Mating Assays

Fluorescence microscopy is a powerful tool for studying single molecule interactions, sub-cellular structures, and many other cellular processes. Recently, it has been used to create an assay for tracking DNA transfer in mating bacterial cells (Babic *et al.,* 2008). There are many advantages of a microscopy-based assay over traditional plate based assays. Bacterial mating assays have traditionally been plate based, analyzing the frequency of transfer of a reportable marker, most often antibiotic resistance genes. These assays are reliable indicators of plasmid transfer and establishment, but they are an assay of the end product of the conjugative process. They do not indicate whether a plasmid can be transferred but not established in a cell, and they only show the presence of a bacterial colony that has acquired a new marker. A real time assay that can track DNA transfer would enable a better understanding of

the conjugative process. Such a system was described in Babic *et al*., 2008, where they created a SeqA-YFP fusion protein under native promoter control. This allowed them to directly visualize DNA transfer in real time in a high frequency of recombination (Hfr) *E. coli* strain (Babic *et al.,* 2008).

In their work, they described the development of the SeqA-YFP system and what they were able to use the system to investigate. They were specifically interested in the role of the F pilus during conjugation, the fate of the transferred DNA, and the pattern of inheritance of donor DNA present in the initial transconjugate cell. Using their system, Babic and colleagues were able to visualize and quantify DNA as it was transferred from one cell to another, and to watch the acquisition of stable genomic information through recombination. This system operates in the recipient cell, where they created a SeqA-YFP fusion protein to allow for visualization of transferred DNA. When DNA is transferred, SeqA-YFP binds to the DNA after second strand synthesis, and forms a fluorescent focus that can easily be detected (Babic *et al.,* 2008).

SeqA not only binds to the *oriC*, but also binds at other hemi-methylated GATC sites and plays a role in gene expression (Guarne *et al*., 2005). This suggests that the SeqA-YFP system developed by Babic *et al*., 2008 could be used to track not just Hfr transfer, but F plasmid transfer as well. Analysis of F plasmid (NC_002483.1) reveals portions of F plasmid contain the required number of GATC sites within the proximity needed to form an aggregate of SeqA. Thus, it may be possible to apply this system to visualizing F plasmid transfer. In addition to probing TraI function and regulation with a live cell microscopy system, the TraI i31 mutants can be used to probe aspects of TraI utilizing the i31 insertion itself.

Dihydrofolate Reductase

It is not known to what degree the stability of TraI plays a role in bacterial conjugation. If TraI must partially or completely unfold to facilitate transfer through the conjugative pore, altering the stability of certain regions might affect the efficiency of transfer. There is no structural data on the full-length protein, and not much known about the elements of the protein that would lend themselves to the structure and stability of the protein. Therefore we decided to take advantage of TraI's tolerance for inserted proteins to help address this question.

A previous graduate student in the lab, Marijke Koppenol, had created a TraI-YFP construct, with YFP inserted in the i31 at amino acid position 593. As previously stated, the i31 sequence contains a unique BamHI site that allows for constructs to be cloned into that site. The insertion of YFP does lower mating efficiency but it does not eliminate it completely. This led us to the idea of inserting another small protein, dihydrofolate reductase (DHFR) into TraI. Dihydrofolate reductase is a 22 kDa protein that is highly conserved across many mammalian species, and also found in prokaryotes (Smith *et al.,* 1979). DHFR is a crucial enzyme, as it has a central role in DNA precursor synthesis. The first structure of DHFR was solved over thirty years ago, and many structures of DHFR from various species have subsequently been solved. It has a core beta sheet structure, usually consisting of an eight stranded beta sheet surrounded by four alpha helices (Figure 1.13). The protein possesses two subdomains separated by the active site, and substrate and cofactor bind at a deep hydrophobic cleft between domains. DHFR catalyzes the reduction of dihydrofolate

to tetrahydrofolate, utilizing NADPH as a cofactor for the reaction (Schnell *et al.*, 2004). The active site consists of conserved proline and tryptophan residues, the tryptophan being involved in substrate binding (Filman *et al.*, 1982, Bolin *et al.*, 1982).

When bound to its ligand, DHFR is resistant to mechanical unfolding and the thermodynamic stability of the protein is also altered (Ainavarapu *et al.,* 2005, Wallace and Matthews, 2002). The mechanical stability of DHFR without bound ligands is quite low, around 27 pN. When bound to MTX however, the mechanical stability increases to 82 pN, nearly tripling the force required to unfold the protein (Ainavarapu *et al.,* 2005). DHFR fusion proteins have also previously been used to study protein translocation across other membranes, such as the mitochondrial membrane (Eilers and Schatz, 1986). There have been numerous studies that suggest mitochondrial import motors function as a Brownian ratchet or are capable of mechanical work to import protein, and that mechanical unfolding is an essential step in protein translocation (Okamoto *et al*., 1998, Huang *et al.*, 1999). These studies utilized DHFR and MTX to probe the translocation of protein to the mitochondria. When DHFR is bound to its natural substrates, the chemical stability of the protein is also altered; the midpoint of a urea titration shifts from 1.4 M to 2.8 M (Wallace and Matthews, 2002). DHFR exhibits increased stability when bound to its ligands, and this makes it an ideal candidate for studying protein stability and a good candidate for insertion into TraI.

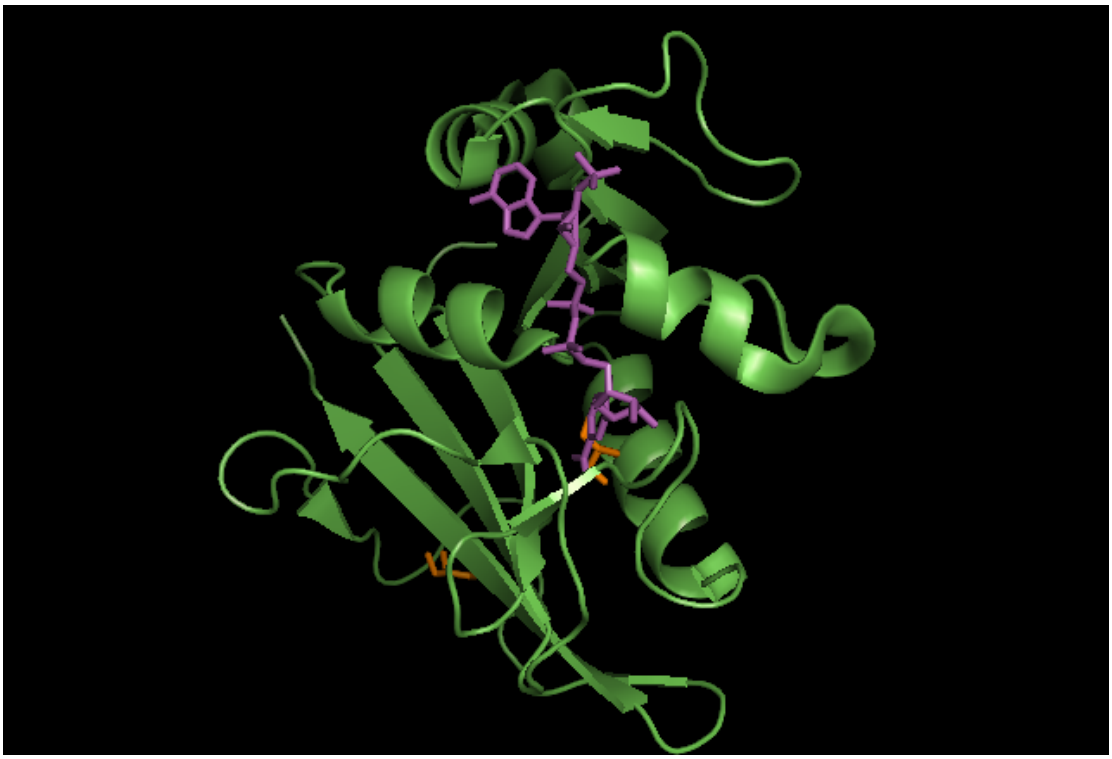

Figure 1.13. Murine DHFR (in green), in complex with 2.4-diamino-6-(-2'-hydroxybenz[b,f]azepin-5-yl) methyl pteridine (in pink), an inhibitor of DHFR like MTX. The structure was generated in PyMOL from the PDB entry 3D84, submitted to the PDB by Cody *et al*., 2008.

Dihydrofolate reductase has previously been used to study transport of proteins across membranes, and in those studies, murine DHFR was used. Dihydrofolate reductase from *E. coli* has a dissociation constant for the binding of methotrexate to DHFR of 9.5 nM and the affinity of MTX for DHFR is about 1000 fold that of folate (Rajagopalan *et al.*, 2002). In the presence of MTX, murine DHFR (mDHFR) fused to a mitochondrial presequence was blocked from entering the mitochondria (Eilers and Schatz, 1986, Esaki *et al.,* 1999, Gehde *et al.,* 2008). Since murine DHFR has previously been used to study protein translocation, it will be used for the study of protein stability with TraI. Use of a non-bacterial DHFR will also preclude the cell from potentially dying immediately upon introduction of MTX to the cell.

Yellow Fluorescent Protein

Yellow fluorescent protein is a protein often used as a reporter for fluorescence microscopy or as a report of protein expression. In the SeqA-YFP system, it has been fused to SeqA to report on DNA transfer (Babic *et al*., 2008). In addition to its use as a reporter, YFP has other qualities that make it amenable to other uses. Yellow fluorescent protein (YFP) is a derivative of green fluorescent protein, originally isolated from *Aequorea victoria* (Figure 1.14)(Shimomura *et al.,* 1962). Green fluorescent protein (GFP) is 238 amino acids long and 26.9 kDa (Prendergast and Mann, 1978). GFP has a major excitation peak at 395 nm, and a minor excitation peak at 475 nm. Its emission peak occurs at 509 nm, in the lower part of the green portion of the visible spectrum, which gives the protein its name and

distinctive characteristic (Johnson *et al.,* 1962). Green fluorescent protein has been used as a reporter for many years, and over those years modified forms of the protein have been developed. GFP itself does not mature efficiently at 37˚C, or any other temperatures above those naturally experienced by *A. victoria*.

Different versions of GFP were subsequently developed for further study of the protein and expanded laboratory use. The first major improvement was a single point mutant, S65T, which improved the spectral characteristics of the protein, the fluorescence intensity, and the photostability (Tsien *et al.,* 1995). Another mutant, the F64L point mutant, increased folding efficiency at 37˚C and was dubbed enhanced GFP (eGFP) (Heim *et al.,* 1995). Adding to these changes created spectral variants of GFP, one of those being Yellow Fluorescent Protein (YFP). YFP has an excitation peak at 514 nm, and an emission peak at 527 nm. The mutations M153T, V163A, and S175G around the chromophore are what cause the excitation and emission peak shifts. Along with the S65T mutation, one of the improved versions of YFP, mVenus also contains the F64L mutation, which accelerates the formation of the chromophore at 37˚C (Cormack *et al.,* 1996).

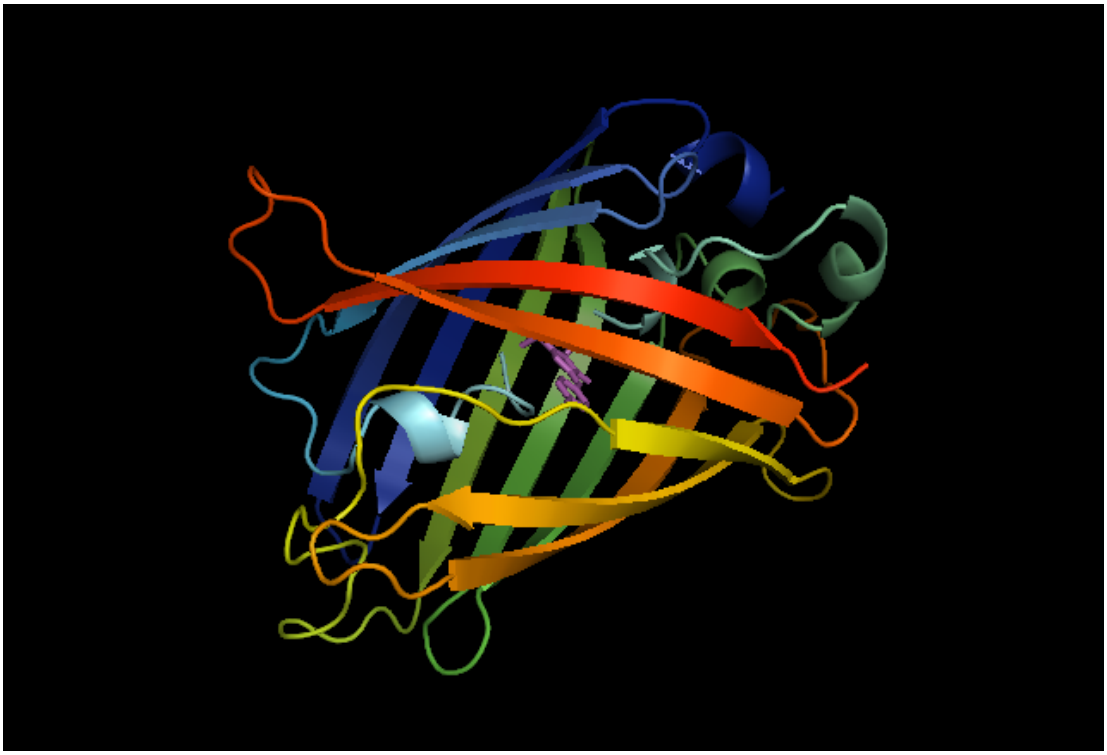

Figure 1.14. Crystal structure of YFP generated in PyMOL from PDB entry 1YFP, submitted to the PDB by Watcher *et al.,* 1998. The protein chain is colored as a rainbow from the N-terminus to the C-terminus, and the chromophore is colored in pink.

The stability of GFP and its derivatives have only recently been investigated. Once the chromophore of the molecule is formed, it is very stable and remains intact during protein unfolding. The reverse of the original folding reaction is not possible. However, if the chromophore is destabilized, folding of the protein becomes reversible. When one residue of the chromophore of GFP is mutated, G67A, the folding of the protein becomes largely reversible (Kutrowska *et al.*, 2007). In addition to chemical stability, the mechanical stability of eYFP has been measured. It has two distinct unfolding peaks, one with a mean unfolding force of 69 +/- 23 pN, and the other with a mean unfolding force of 122 +/- 23 pN (Jimenez *et al.,* 2006). YFP is not easily unfolded under native conditions, since the protein's chromophore is highly resistant to unfolding. Since YFP is generally stable, that characteristic can be leveraged for investigating the stability of TraI.

In addition to the G67A mutation, GFP was found to have two hydrophobic clusters on opposite sides of the protein. Melting of cycle-3 GFP and two of its mutants, I14A and I161A, reveal the protein most likely denatures in a three-stage process. The I161A mutant in particular destabilizes one of the hydrophobic clusters and creates a less stable unfolding intermediate (Melnik *et al*., 2011). Both of these stability mutations could be utilized for studying protein stability in TraI using the i31 as the insertion point. In addition to using DHFR, YFP can be used to investigate the role of protein stability in the mating process.

Circular Dichroism

We can use various protein insertions and mutants to analyze the function and regulation of TraI, but those methods are indirect as we are manipulating proteins within TraI. To get a more complete understanding of TraI, we can measure the stability of the protein itself. Circular dichroism (CD) has been a method used by structural biologists since the 1960s to examine protein structure and stability. Circular dichroism is the measurement of the unequal absorption of left-handed and right-handed circularly polarized light. Circular dichroism in the near UV spectrum is used to investigate the secondary structure of proteins since amino acids will give different signals depending on their optical transitions. The result of this difference in optical transitions is different characteristic spectra for the different structural elements. The α-helix has signal minima at 222 nm and 208 nm, and a maximum at 193 nm, while β-helices produce a spectrum with a minimum at 218 nm and a maximum at 195 nm (Holzwarth G, Doty P., 1965, Greenfield and Fasman, 1969). Proteins with disordered regions and random coil structures have low ellipticity above 210 and a signal minimum near 195 nm (Venyaminov *et al.,* 1993). These marked differences in signal can give a picture of the secondary structure of the protein, and these wavelengths can be used to monitor protein stability and unfolding.

Objectives of the Thesis

TraI is a complex, multidomain protein responsible for carrying out the nicking and unwinding of F plasmid during a mating event. While some of its structure has been determined, the regulation between the domains and the negative

cooperativity between the ssDNA binding domain and the relaxase domain is not well understood. We currently do not have a full understanding of this negative cooperativity and what can cause F plasmid transfer to become derepressed (as we see in some mutants of TraI). The Traxler group created the collection of i31 TraI mutants using transposon mutagenesis, which left behind 31 amino acids in TraI wherever the transposon had inserted (Haft *et al*., 2006). Some of these mutants had a mating efficiency well above that of WT TraI. They postulated that these 31 amino acid insertions were releasing TraI from some type of negative regulation, but no explanation of how that occurred was identified.

Our lab examined some of the i31 mutants in more detail and discovered that they have reduced affinity for ssDNA and a reduction in the apparent negative cooperativity compared to WT TraI (Dostal and Schildbach, 2010). These results confirmed that negative cooperativity was an important factor in controlling mating and changing the frequency of mating events, but what exactly the i31 was causing to create the change in negative cooperativity was still unknown. The i31 sequence is apparently relatively unstructured, and some of the i31s in the mutants are inserted into structured regions. We asked why the insertion of an unstructured peptide increases mating efficiency and releases TraI from negative cooperativity. To answer this question, we employed a new technique for analyzing mating events, a live cell microscopy system that allows for visualization of DNA transfer in real time.

Much of the research investigating transfer of mobile genetic elements has been done via assays that utilize transfer of a reportable marker from donor to recipient. This is a reliable method for determining if a plasmid transfers and

establishes itself in the recipient. This method however, has its drawbacks, as it is a measure of the end result of the transfer process. A newer method, which utilizes a fluorescent marker in the recipient cell, the SeqA-YFP system, has been developed which can be used for monitoring mating in a much narrower time window (Babic *et al*., 2008). Using this system, we obtained data that correlated with the previously published mating assay data, and indicated the i31 mutants not only had a higher mating efficiency, but transferred DNA appears more quickly in the recipient as well.

After obtaining these data, we utilized unfolding studies and probed protein stability with proteins inserted into TraI to determine if the unstructured character of the i31 was changing the stability of TraI. We postulated this was the cause of the changes seen in the i31 mutants, but we did not see any gross changes in protein stability. Inserting proteins into TraI reduces mating efficiency, but when the inserted protein is destabilized, mating efficiency recovers. These data indicate TraI stability may play a role in conjugation. Although our direct stability measurements of TraI did not show any major changes, we did see small but consistent changes in stability of one of the i31 mutants. These data indicate stability may be playing a role in the phenotype of the i31 mutants, but at a local structural level and not a global one. Our data also indicate there is no global explanation of the i31 phenotype. In this work, we will demonstrate that the altered mating efficiency in the i31 mutants correlates with dsDNA appearing earlier in recipients when mated in the live cell SeqA-YFP system, and the possible causes of this phenotype.

CHAPTER 2

MATERIALS AND METHODS

Bacterial Strains and Plasmids

Escherichia coli recipient strain BA24 was kindly provided by the Radman lab. *Escherichia coli* strains XK1502, XK1502 i369, i593, i681, and i1753 containing F plasmid with the *traI* gene substituted by tetracycline resistance cassette (XK1502/FΔTraI) were kindly provided by Prof. Beth Traxler (University of Washington, USA). All strains and plasmids are listed in tables 2.1, 2.2, and 2.3.

Live Cell Fluorescence Microscopy Assay

Mating and microscopy procedures were carried out according to a protocol adapted from the methods of Babic *et al*, 2008. Donor strains were grown in LB media containing ampicillin (100 μg/ml) to an OD_{600} of .6, and the recipient strain BA24 was grown to an OD_{600} of 0.9 in minimal media (M9 salts) supplemented with 0.4% succinate, 0.1% CAA, 30 μg/ml thiamine, 3 mM $MgSO_4$, 20 μg/ml uracil, and 50 μg/ml of streptomycin. Donor strains all use the XK1502 (F^- Δ*lacU169 nalA*) parent strain to carry various TraI mutants on plasmids (Haft *et al*., 2006). Once the recipient and donor strains reached the proper OD_{600}, 1 ml of each was washed twice in minimal media (M9-) and resuspended in 1 ml of M9-. For real time mating under the microscope, cells were mixed in a 1:1 ratio, and plated on an agarose slab (1.5% agarose in M9-) in a temperature controlled live cell micro-observation chamber (Bioptechs) and transferred to the microscope for time lapse observation.

Time-lapse microscopy was performed using an inverted microscope (IX-81, Olympus) with a 100X oil-immersion objective (Olympus). The sample was held at 37˚C using cover slide and objective heaters (Bioptechs) and imaged with a 525 nm longpass filter (Chroma) and an emission filter (ET540x30m, Chroma). Fluorescent illumination was provided by the 514 nm line of an Innova Ion I-308 laser (Coherent) with an illumination power density of 1kW/cm^2. Excitation light was filtered through a 514 nm laser line filter (Semrock). Images were taken through a cooled EM-CCD (Andor Ixon DU888), using an imaging algorithm built into Metamorph (Molecular Devices) imaging software. Using the algorithm, up to 10 cell clusters were imaged automatically every 3 minutes. Image analysis was performed using imageJ (NIH).

Interrupted Mating Assay

Cells were grown as previously described for the live cell microscopy mating assay. Prior to imaging on the microscope, cells were mixed in a 1:1 ratio and mated for a set time period. Mating was halted with vigorous vortexing and addition of 0.01% sodium dodecyl sulfate (SDS). Cells were then plated on an agarose slab and imaged at 25˚C.

Protein Purification

Overnight cultures for TraI were inoculated from single colonies into LB containing 30 mg/mL kanamycin (LB-kan, Sigma). One liter of LB supplemented with 30 μg/ml kanamycin was inoculated with 1 mL of overnight culture and grown at 37˚C to an OD_{600} of 0.6. Protein expression was induced with Isopropyl β-D-1-

thiogalactopyranoside (IPTG) (1 mM final concentration) (Thermo Scientific) and the culture was grown overnight at 20 ˚C. Cells were harvested, pelleted (15000 rpm, 30 min, 4 ˚C) (Thermo Fisher), and stored at -80˚C. Cells were thawed at 4˚C and resuspended in buffer A (50 mM Tris pH 7.5, 50 mM NaCl, 1 mM EDTA) with protease inhibitor (Sigma). Cells were lysed by sonication, and the resulting product was spun down at 4˚C for 15 minutes at 15,000 rpm. Ammonium sulfate (30% v/v, MP Biomedicals) was added to the resulting supernatant, and spun down again for 1 hour (4˚C, 15,000 rpm). The resulting pellet was resuspended in buffer A, and passed through a 0.45 micron filter (Millipore) prior to application of the sample to a 5 mL Heparin column (GE Life Sciences) equilibrated in buffer A.

The sample was fractionated using a gradient from 50 mM NaCl to 1 M NaCl using an AKTA Prime Plus (GE Life Sciences) and elution was monitored by A_{280}. Fractions containing protein were pooled and 3 M ammonium sulfate was added to a final concentration of 1 M. The sample was then applied to a 5 mL Phenyl column (GE Life Sciences) and fractionated using a gradient from 1 M ammonium sulfate to 0 M. Fractions containing protein were assessed by SDS-gel electrophoresis and Coomassie staining, and the fractions were estimated to be more than 95% pure. The fractions were pooled and dialyzed overnight into buffer containing 100 mM NaCl, 20 mM $NaPO_4$ (pH 7.5), and 0.1 mM EDTA. The protein sample was concentrated using a Centricon (Amicon) concentrator to approximately 50-100 µg/mL. Protein samples were subsequently used in nicking assay experiments.

TraI Fragment Purification

The TraI 309-858 fragments were purified as described above through fractionation using the heparin column. Fractions from the heparin column containing protein were pooled and dialyzed for 2 hours in buffer A, and then applied to a 5 mL Q column (GE Life Sciences) and a gradient from 50 mM NaCl to 1 M NaCl was run over the column. For the i593 and wild type + i31 fragments, an additional phenyl column (as described above) was run after the Q column to improve purity. The protein samples were dialyzed overnight into buffer containing 20 mM $NaPO_4$ pH 7.4, 0.1 mM EDTA, and 100 mM NaCl. Protein samples were concentrated as above and the concentration of each sample was determined by guanidine denaturation. Protein was diluted into 7.5 M guanidine HCl and 25 mM $NaPO_4$ pH 6.5, and the absorbance of the protein at 280 nm was determined. The absorbance measurement was used to determine concentration by the Beer-Lambert equation (Edlehoch, 1967). Circular dichroism (CD) experiments were performed with the protein samples.

Nicking Assay

Purified full length TraI and TraI i31 mutants were diluted to 1 μM stock for use in all nicking assays. The protein was diluted to 100 nM final concentration in each assay. The protein, oligo (Cy5 oriT, 20 nM, IDT) and buffer (20 mM $MgCl_2$, 100 mM NaCl, 40 mM Tris pH 7.5) were mixed to a total volume of 18 μL and incubated at 37˚C for a set amount of time. The reaction was halted with the addition of 2 μL proteinase K (20 mg/mL, to final concentration of 2 mg/mL). To the reaction mix, 21 μL formamide was added and incubated at 95 ˚C for 5 minutes. The reaction

mix was run on a 16 % polyacrylamide 8 M urea gel, 20 V per cm, with each well containing 20 μL of reaction mix. Gels was run for one hour and fifteen minutes, then imaged on a Typhoon 9410 Variable Mode Imager (GE Healthcare) using excitation at 648 nm and emission at 668 nm.

Circular Dichroism

Circular dichroism experiments were carried out similarly to methods used in Street *et al*., 2003. Unfolding and refolding experiments were conducted using urea as denaturant. Thermal denaturation of the TraI 309-858 fragment was found to be irreversible. An Aviv model 420 Circular Dichroism spectrometer was used for all CD measurements. After running an initial wavelength scan of 2 μM wild-type TraI 309-858, it was determined the structure was primarily α-helical and all subsequent unfolding experiments could be measured at 222 nm. For wavelength experiments, protein was diluted in buffer (20 mM $NaPO_4$ pH 7.4, 0.1 mM EDTA, and 100 mM NaCl) to either 5 μM or 10 μM and scanned from 350 nm to 195 nm with scans every 1 nm and measured for an averaging time of 5 seconds. For denaturation experiments, 2 μM solutions of wild-type TraI 309-858 (or i31 mutants) were made in both 0 M urea and 8.0 M urea. The change in ellipticity was monitored in a cuvette at 25˚C by removing a set amount of solution from the cuvette and adding in the appropriate amount of titrant by an automated titrator (Aviv). Solutions were allowed to stir together for 6 minutes and the ellipticity at 222 nm was averaged for 30 seconds. Initial experimentation with the wild type 309-858 fragment over a wide range of urea concentrations indicated TraI 309-858 was fully unfolded at a urea concentration

of 3M. The range of urea concentrations to test was optimized to 0 to 4.5M, with 0.2M steps. Urea denaturation was found to be reversible and the data fit into a two state transition model between native and denatured states. The data was fit with a non-linear least squares fit (Kaleidagraph, Synergy Software) to determine the ΔG (Eq 1).

Eq. 1

$$Y_{obs} = \frac{Y_{D_1H_2O} + \beta_D\,[x] + (Y_{N_1H_2O} + \beta_N\,[x])e^{-(\Delta G^{\circ}_{H_2O} + m[x])/RT}}{1 + e^{-(\Delta G^{\circ}_{H_2O} + m[x])/RT}}$$

Mating Assays

XK1502 FΔTraI with p99i-TraI (and various TraI mutants created from p99i-TraI) was used as the donor strain. GM124 (streptomycin resistant) was used as the recipient in all plate based mating assays. Both donor and recipient were grown overnight in LB plus appropriate antibiotics. The overnight culture was diluted 1:1000 into fresh LB and grown to an OD_{600} of 0.45. Donor and recipient cells were mixed in a 1:10 ratio (donor to recipient) with 100 µL of donor being mixed with 900 µL of recipient. The donor/recipient mix was incubated for 1 hour at 37˚C and vortexed vigorously for 30 seconds to break apart mating pairs. The sample was chilled on ice for 10 minutes and a serial dilution series of the sample was made and plated onto LB-agar. Transconjugates were selected for on LB-agar plates containing 25 µg/mL tetracycline and 50 µg/mL streptomycin (LB-tet/strep) while donors were selected for on LB-agar plates with 25 µg/mL tetracycline and 100 µg/mL ampicillin

(LB-tet/amp). Efficiency of the mating was calculated as the number of transconjugates per donor.

Mating Assays with Methotrexate

Mating assays were carried out as described above, with additional steps to add in methotrexate (MTX). MTX was made in a 50 mM stock solution, filter sterilized, and appropriate amounts were added to each mating assay. Prior to mixing the donor and recipient, both donor and recipient cells were spun down to remove the media. Media containing 50 μM MTX was added to the cells, the cells were resuspended in the MTX containing media, and incubated at room temperature for 15 minutes prior to mixing donor and recipient. Cells were mixed in a 1:10 ratio, mated for 60 minutes, and spun down after mating to remove any remaining MTX from the reaction before plating. Cells were mated in either no MTX (0 nM) or 50 μM MTX.

DNA Transformation

50 μL of cells was mixed with 1.5 μL of plasmid DNA and incubated on ice for 30 minutes. Cells were heat shocked at 42˚C for 45 seconds and allowed to recover on ice for 10 minutes. LB (950 μL) was added to the tubes and cells were incubated for outgrowth for an hour in a 37˚C shaker incubator (New Brunswick Scientific). The cells (50 μL - 250 μL) were plated on LB-agar containing the appropriate antibiotic and incubated at 37˚C overnight. Single colonies were picked and miniprepped for confirmation of clones by DNA sequencing (Genewiz).

TraI-DHFR Construction

Using TraI cloned into the p99 plasmid (p99i), mDHFR (pCMV-sport6 *mdhfr*) was inserted at various permissive sites (369, 593, 681, 1753, which refer to the amino acid position) within TraI. These positions on TraI have previously had a BamHI site (in frame) cloned into TraI via the i31 insertion library. The DHFR gene used in this cloning is *mdhfr* cloned into pCMV-sport6 (American Type Culture Collection). The gene was PCR amplified from pCMV-sport6 (Table 2.2). The gene plus engineered BamHI sites were cloned into pNEB193, allowing for easy manipulation. Using this construct, the mDHFR gene was cut with BamHI, ligated with p99i variants and transformed into XK1502 cells. The p99i-mDHFR fusion protein plasmids were purified and successful insertion of mDHFR was confirmed by sequencing and expression test. Any successful transfer can only be due to the p99i-mDHFR plasmid that has been transformed into the strain. These strains can be used to determine the mating efficiency of the TraI-mDHFR fusion proteins with and without MTX.

TraI-YFP Construction

DNA was prepped and purified by phenol/chlorform (Invitrogen) and ethanol precipitation due to the large size of the plasmids used for cloning (over 10 kb). Restriction enzymes were obtained from New England Biolabs. DNA fragments for cloning were amplified with Taq polymerase (New England Biolabs). Plasmid pZH007 containing mVenus (Zhao Lab), and i31 TraI mutants were prepped and purified, and mVenus was PCR amplified from pZH007 (see table for primers,

primers purchased from Integrated DNA Technologies). The PCR product was confirmed by DNA agarose gel electrophoresis (Biorad). Both the mVenus PCR product and p99i-TraI 593 were digested with BamHI for 2 hours at 37˚C. The plasmid and PCR product were precipitated with phenol/chlorform to purify the cut DNA. PCR product and plasmid were ligated together with T4 DNA ligase (New England Biolabs) for one hour at room temperature. Ligation reactions were transformed into chemically competent XL-1 Blue *E. coli*. Colonies were selected for on LB-agar plates containing ampicillin (100 μg/mL). Single colonies were grown out in LB-amp, and DNA was prepped and purified by phenol/cholorform precipitation and sent for sequencing to confirm the correct insertion of the mVenus PCR product. This cloning strategy was used for all subsequent cloning of mVenus into TraI.

TraI Fragment Cloning

Plasmid DNA and PCR product were prepped as described above. The fragments were PCR amplified from p99i-TraI with added NdeI and XhoI sites (Table 2.2). PCR product for TraI 309-858 and pET24a was digested with NdeI and XhoI for 2 hours at 37˚C (New England Biolabs). The pET24a plasmid was incubated with Calf Intestinal Phosphotase (CIP) (New England Biolabs) for 1 hour at 37˚C before phenol/chloroform extraction to remove the CIP. The PCR product and plasmid were ligated together and transformed as above, and colonies were screened for the insert via sequencing and expression test.

Quikchange Mutagenesis

Quikchange mutagenesis was performed according to the Quikchange mutagenesis protocol by Stratagene. Template plasmid DNA was combined with mutagenesis primers, dNTPs (Fermentas), ddH_2O, Pfu Turbo buffer and Pfu Turbo DNA polymerase (Agilent). After PCR amplification of the plasmid, the sample was incubated with DpnI (New England Biolabs) for 1 hour at 37˚C to remove the template. Additional Dpn I was added to the sample and incubated for another hour at 37˚C. Dpn I was inactivated at 80˚C for 20 minutes prior to transformation. Mutant plasmids were generated from p99i-TraI and substitutions were analyzed and confirmed via DNA sequencing (Genewiz).

Protein Expression Test

To confirm correct cloning of plasmid constructs, expression tests were conducted. Overnight cultures for each construct were inoculated from single colonies into LB containing appropriate antibiotics. One 5 mL of culture with appropriate antibiotics was inoculated with 50 µL of overnight culture and grown at 37˚C to an OD_{600} of 0.6. Protein expression was induced with Isopropyl β-D-1-thiogalactopyranoside (IPTG) (1 mM final concentration) (Thermo Scientific) and incubated at 37˚C for three hours. From each culture, 40 µL of cells was pelleted by centrifugation, resuspended in loading buffer, and assessed by SDS-gel electrophoresis and Coomassie staining.

Plasmid	Description	Reference/ Source
p99I	pTrc99A with wild-type traI cloned into the MCS	Traxler Lab, Haft *et al*., 2006
p99I-i369	pTrc99A with i369 mutant traI cloned into the MCS	Traxler Lab, Haft *et al*., 2006
p99I-i593	pTrc99A with i593 mutant traI cloned into the MCS	Traxler Lab, Haft *et al*., 2006
p99I-i681	pTrc99A with i681 mutant traI cloned into the MCS	Traxler Lab, Haft *et al*., 2006
p99I-i1753	pTrc99A with i1753 mutant traI cloned into the MCS	Traxler Lab, Haft *et al*., 2006
pZH007	Vector containing mVenus	Xiao Lab
pET24a	Kan^r cloning vector	Schildbach Lab
TraI WT + i31 309-858	pD441-SR with WT 309-858 + i31	DNA 2.0
pCMV-Sport6 *mdhfr*	pCMV-Sport6 with *mdhfr* cDNA	ATCC

Table 2.1 The p99i plasmids used in this study, and plasmids obtained from other sources. All p99i plasmids contain TraI with a 31 amino acid transposon mutagenesis insert.

pZH007	Vector containing mVenus	Xiao Lab
p99I-i369-YFP	pTrc99A with i369 mutant traI with mVenus inserted at the i31 into TraI	This study
p99I-i593-YFP	pTrc99A with i593 mutant traI with mVenus inserted at the i31 into TraI	This study
p99I-i681- YFP	pTrc99A with i681 mutant traI with mVenus inserted into TraI at the i31	This study
P99i-369-DHFR	pTrc99A with i369 mutant traI with *mdhfr* inserted into TraI at the i31	This study
P99i-681-DHFR	pTrc99A with i681 mutant traI with *mdhfr* inserted into TraI at the i31	This study
pET24a TraI 309-858	pET24a with TraI 309-858 cloned into the MCS	This study
pET24a TraI - i369 309-858	pET24a with TraI i369 309-858 cloned into the MCS	This study
pET24a TraI – i593 309-858	pET24a with TraI i593 309-858 cloned into the MCS	This study
pET24a TraI – i681 309-858	pET24a with TraI i681 309-858 cloned into the MCS	This study
p99I-i593-YFP G67A, I161A, or I47A	pTrc99A with i593 mutant traI with mVenus inserted at the i31 with one of the following mutations: G67A, I161A, or I47A	This study
p99I-i593-YFP G67A, I161A, or I47A	pTrc99A with i681 mutant traI with mVenus inserted into traI at the i31 with one of the following mutations: G67A, I161A, or I47A	This study
p99i TraI A593V, S739N, or D672N	pTrc99A with wild type TraI with one of the following mutations: A593V, S739N, or D672N	This study

Table 2.2. All plasmids created in this study.

E. coli strains		
XK1502	F^- Δ*lacU169 nalA*	Traxler Lab Haft *et al*., 2006
BA24	*seqA-yfp mutS- dam-*	Radman Lab, Babic *et al*., 2008
XL-1 Blue	*endA1 supE44 thi-1 recA1 gyrA96 hsdR17 relA1 lac[F¢ proAB* lac^q*ZΔM15 Tn10(*Tet^r*)]*	Stratagene
BL21 DE3	*F- ompT hsdSB (*$r^-_B m^-_B$*) gal dcm met (DE3)*	Novagen
DH5 α	*end*A1 *lac*ZΔM15 *rec*A1 F-	Invitrogen
GM124	F-, *lacZ118*(Oc), *rpsL275*(strR), *dam-4*	CGSC
HFR3000	Hfr(PO1), *supQ80*?, *λ*, *e14*, *relA1*, *spoT1*, *thiE1*	CGSC
KL19	Hfr(PO67)	CGSC

Table 2.3. All strains used in this study.

Mutation or PCR product	Primer
mVenus	FWD 5' CGC GGA TCC A GGA AGC AAG GGC GAG GAG CTG 3' REV 5' CGT GGA TCC CCG TAC AGC TCG TCC ATG CCG 3'
mDHFR	FWD 5' GCA GTA GGA TCC A GGA GTT CGA CCA TTG AAC TGC 3' REV 5' GCA GTA GGA TCC GTC TTT CTT CTC GTA GAC 3'
309-858 TraI Fragment	FWD 5' GCA GCA CAT ATG GCT TCA CAG GAC GGG C 3' REV 5' GCA GCA CTC GAG TAA GGA CTT CTG ATG ACT GAT AGC CG 3'
I161A	FWD 5' CAA GCA GAA GAA CGG CGC CAA GGC CAA CTT CAA G 3' REV 5' CTT GAA GTT GGC CTT GGC GCC GTT CTT CTG CTT G 3'
G67A	FWD 5' ACC CTG GGC TAC GCC CTG CAG TGC TGC TT 3' REV 5' AAG CAC TGC AGG GCG TAG CCC AGG GT 3'
I47A	FWD 5' CCC TGA AGC TGG CCT GCA CCA CCG G 3' REV 5' CCG GTG GTG CAG GCC AGC TTC AGG G 3'
K998A	FWD 5' TGC CGG TGT GGG TGC GAC CAC ACA GTT T 3' REV 5' AAC TGT GTG GTC GCA CCC ACA CCG GCA 3'
A593V	FWD 5' GCC AGC GTG AAA GTC GGA GAA GAG AGC 3' REV 5' GCT CTC TTC TCC GAC TTT CAC GCT GGC 3'
S739N	FWD 5' CGC CTG CAG GTG GCA AAC GTC AGT GAA GAT GC 3' REV 5' GCA TCT TCA CTG ACG TTT GCC ACC TGC AGG CG 3'
D672N	FWD 5' GAC CGC TAT GTT ATC AAC CGG GTG ACG GCG 3' REV 5' CGC CGT CAC CCG GTT GAT AAC ATA GCG GTC 3'

Table 2.4 All primers used in this study for cloning. Primers were used for cloning PCR products from plasmids and for Quikchange mutagenesis.

CHAPTER 3

FLUORESCENCE MICROSCOPY USING SEQA-YFP TO TRACK TRANSFER OF F PLASMID

Objectives of this Chapter

A plate based mating assay is a measure of the end product of a mating event. We want to be able to track mating as it occurs, and be able to assay the process of F plasmid transfer as it happens. There are steps of the mating process that we may be missing with plate-based assays. Vital information about the process such as changes in DNA transfer, plasmid establishment, and plasmid integration may be overlooked. Using the live cell SeqA-YFP assay, we will be able to track DNA transfer, and possibly detect differences in the DNA transfer process, plasmid establishment, and other steps in the mating process. We may also be able to determine properties of TraI that were previously unknown and could not determine using a plate based assay, such as if helicase activity is required for DNA transfer or plasmid establishment. We know bacterial mating can occur rapidly, but the system can observe DNA transfer in near real time (Babic *et al.*, 2008).

Results

Using Hfr Strains to Test the System

The first set of experiments with Hfr strains was undertaken to ensure the SeqA-YFP system would work in our hands. Microscopy mating assays with various Hfr strains were conducted to ensure the system was operational. The recipient strain,

BA24, graciously provided by the Radman Lab, contains the SeqA-YFP fusion protein. This fusion protein is on the native bacterial chromosome, under control of the native promoter. It is expressed as native SeqA would be expressed in the cell. This strain is *dam*$^-$, as it needs to lack Dam methylase to create a fluorescent focus upon transfer of single-stranded methylated plasmid DNA. When a single strand of methylated DNA is transferred to the *dam*$^-$ recipient, second strand synthesis creates a hemimethylated plasmid that SeqA-YFP will bind to and create an aggregate.

One of the donor strains used in Babic *et al.*, 2008, was Hfr3000, and it was the first strain that we tested with BA24 to see if the system would work (Figure 3.1). Focus formation is measured by the reduction of background fluorescence in a recipient cell and the visualization of a punctate, circular structure (the focus) within the cell. Foci formation was confirmed to be consistent with results from Babic *et al*., 2008. A *dam*$^-$ donor strain strain, GM695, was used as a negative control to confirm that foci formation will not occur when both donor and recipient are *dam*$^-$. We did not see foci formation with both a *dam*$^-$ donor and recipient (Figure 3.2). As a positive control, we used the strain GM1655 *dam*$^+$. This strain contains the SeqA-YFP fusion protein, and has its native Dam methylase. It forms foci without mating, indicating SeqA-YFP functions in its native role without disruption due to the fusion of YFP. We also mated BA24 with other Hfr strains with the *oriC* present at different locations within the genome to determine if *oriC* location was important to transfer timing. We determined location of the *oriC* did not change how quickly SeqA-YFP reported the DNA transfer event (Figure 3.3).

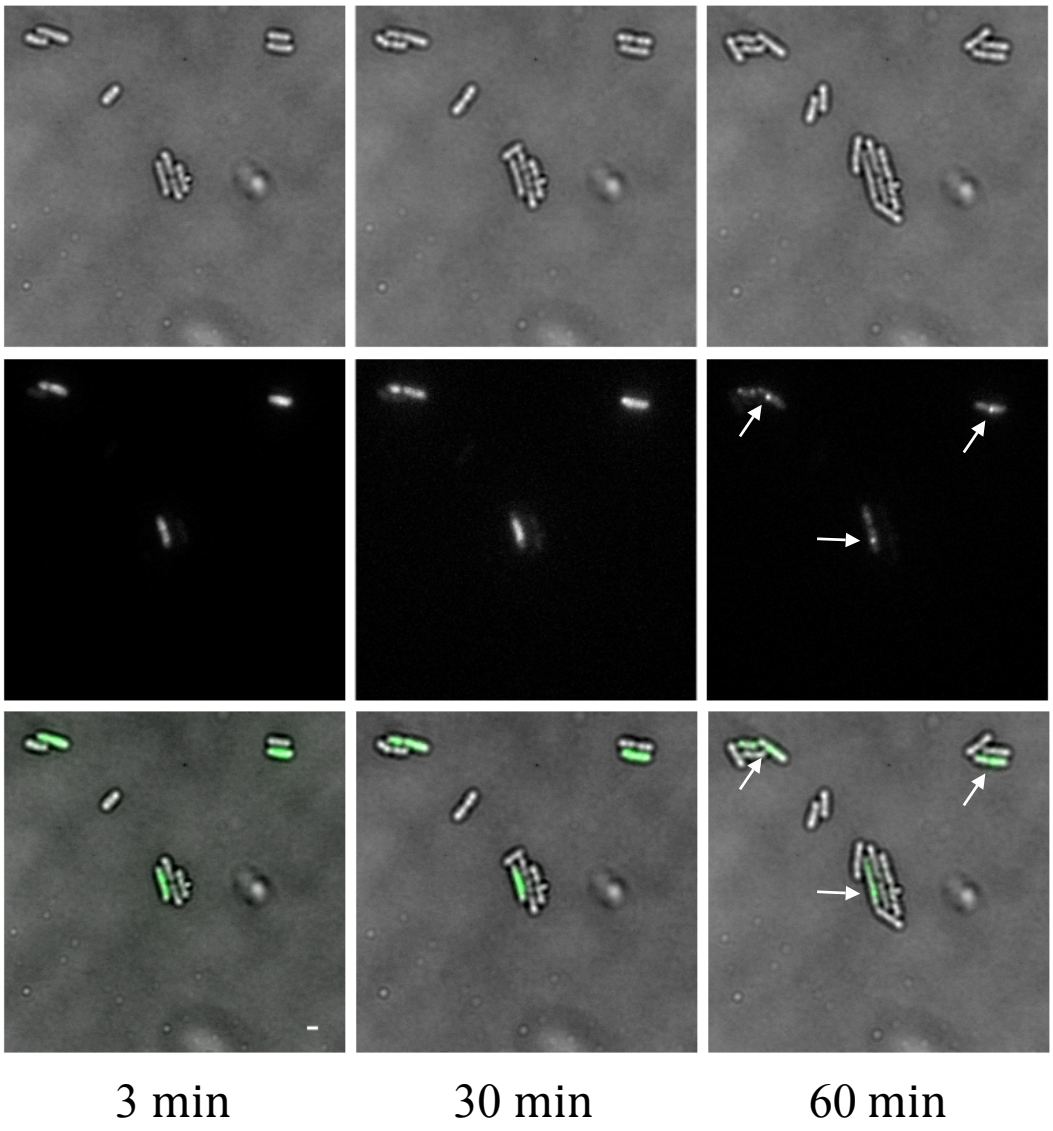

Figure 3.1. Microscopy mating assay with the recipient BA24 and donor Hfr3000. Cells are imaged at 3, 30, and 60 minutes after mixing and plating on an agarose slab. The development of a focus over time within the recipient cell can be seen. Top row, bright field, middle row fluorescence image, and bottom row, fluorescence overlay.

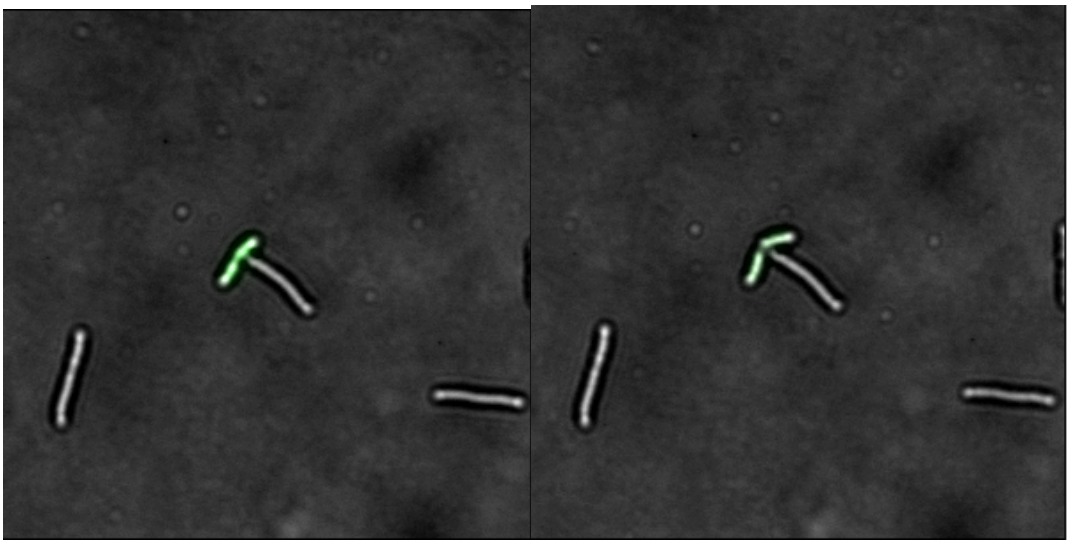

25 min 46 min

Figure 3.2. The *dam*$^{-}$ donor GM695 did not cause foci formation since the transferred DNA was not methylated and SeqA does not bind to non-methylated DNA.

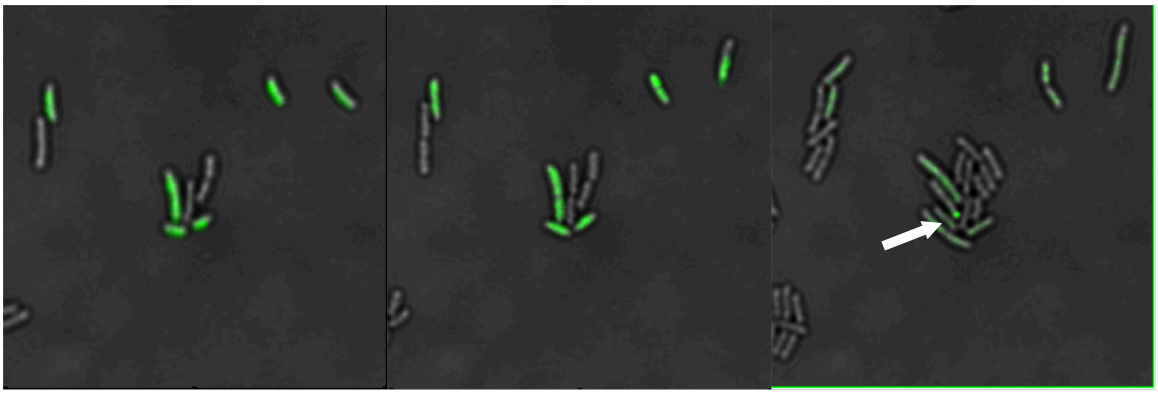

30 min 48 min 90 min

Figure 3.3. An additional Hfr strain, KL19, was used to show different Hfr strains with the oriC positioned at different minutes in the genome still showed foci formation.

The SeqA-YFP System Can Be Used To Track F Plasmid Transfer

Once the Hfr strains had been used to test and confirm the system was operational, we next tested F plasmid containing donor strains. We had analyzed the F plasmid sequence in Genbank to determine if using the system with F was possible since it does not contain an *oriC*, but since F plasmid does not contain an array of GATCs similar to the *oriC* it was unknown if the system would function. The first F plasmid strain tested was XK1502 FΔTraI p99i (Figure 3.4). XK1502 FΔTraI is host to an F plasmid that has a TraI deletion and carries tetracycline resistance in its place, creating a transferrable selectable marker for traditional plate based assays. The p99i plasmid is pTrc99a with *traI* cloned into it. With the XK1502 FΔTraI p99i strain, we determined that it is possible to track focus formation using F plasmid strains. We saw foci formation in this F plasmid strain, and confirmed the system works to track F plasmid (Figure 3.4).

Once we had determined the assay was possible with F plasmid strains, we next set out to test the TraI i31 mutants with the system. Upon running the assay with p99i TraI i681, we noted that the time it took for a focus to form in this strain (44.5 ± 14.5 minutes) was less than the time required for p99i TraI WT (125.4 ± 32.4 minutes). Intrigued by this difference, we determined that the average time to focus formation in p99i TraI i681 was significantly shorter than in the WT strain (Figure 3.5). We continued testing the rest of the i31 mutants in our collection, i369, i593, and i1753. The time to focus formation for all the i31 mutants tested was shorter than that of WT (Figure 3.5). The average time for a focus to form in i681 in this assay is 44.5 ± 14.5 minutes (n = 3), whereas the average time in WT is 125.4 ± 32.4 minutes

(n = 3). The time it took for a focus to form with the strain containing WT TraI was much longer than the time it took for the i31 mutant. These data correlate with the mating assay data collected in Haft *et al*., 2006. That mating assay data shows increased mating efficiencies over WT for the i31 mutants tested in the microscopy mating assay. The average foci formation times for i369, i593, and i1753 are 67.0 ± 19.9, 45.7 ± 22.4, and 57.5 ± 23.7 minutes respectively (n = 3) (Table 3.1).

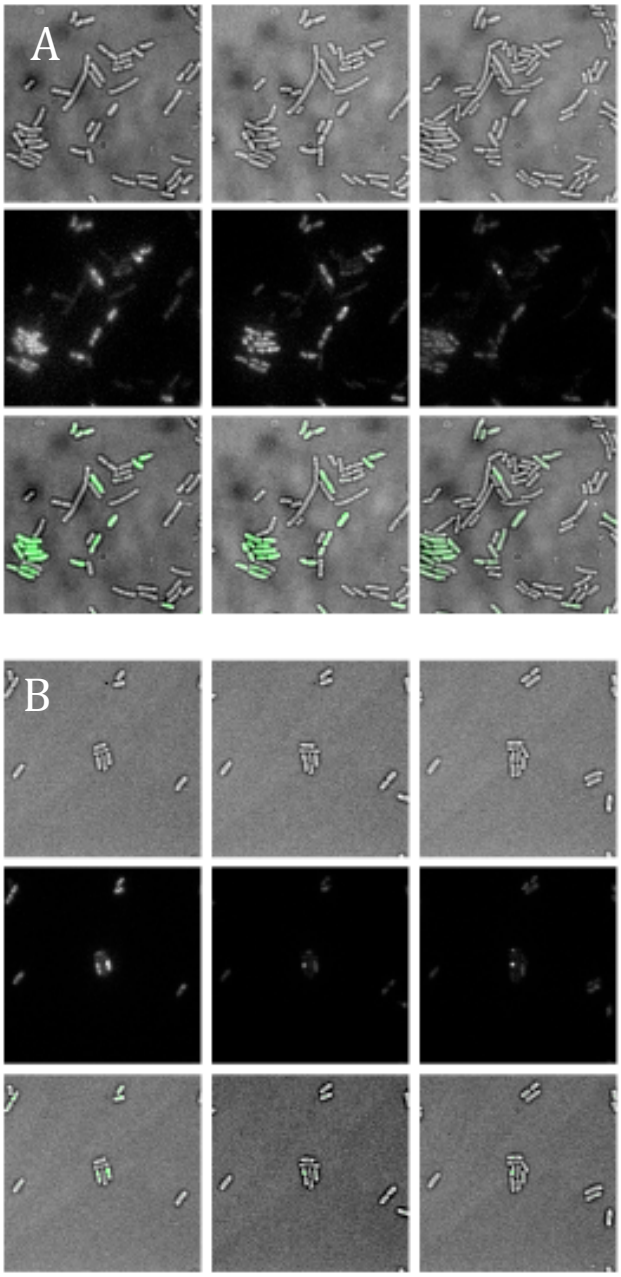

Figure 3.4. Microscopy mating assay with the recipient BA24 and donors (A) XK1502 p99i WT TraI and (B) XK1502 i681 TraI. Cells are imaged at 3, 30, and 60 minutes after mixing and plating on an agarose slab. The development of a focus over time within the recipient cell can be seen. For A and B, Top row, bright field, middle row fluorescence image, bottom row, fluorescence overlay.

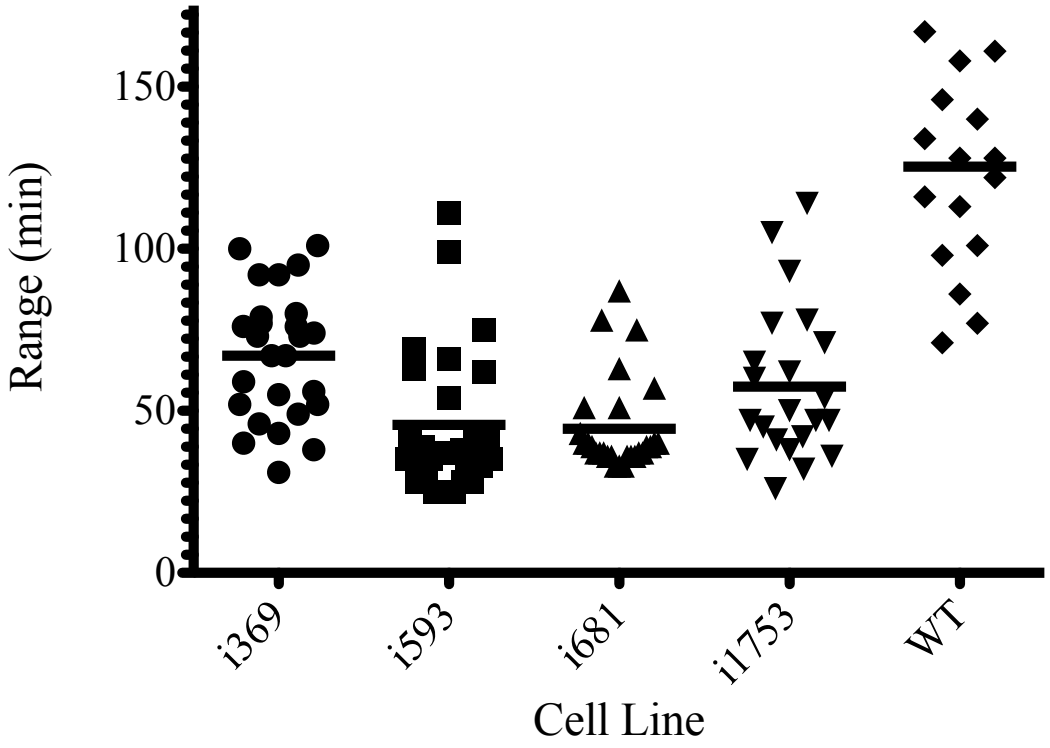

Figure 3.5. TraI variants with an i31 transposon insertion at various points in the protein sequence have altered rates of transfer compared to wild type as visualized by the fluorescence microscopy assay. For each cell line, data from at least three independent experiments were combined.

TraI Variant	Average Focus Formation Time (min)
i369	67.0 ± 19.7
i593	45.7 ± 22.4
i681	44.5 ± 14.5
i1753	57.5 ± 23.7
WT	125.4 ± 32.4

Table 3.1. The average foci formation times for all the i31 mutants and WT. Values for each variant represent the combination of at least three independent experiments. Standard deviation of the focus formation time is shown.

Interrupted Mating Assay Shows No Change in Second Strand Synthesis

We next wanted to test if the differences seen in the live cell mating assay were caused by changes once the DNA had entered the recipient cell. It is possible that the rate of second strand synthesis is changed in the i31 mutants. The assay was modified to identify foci that had formed within a defined period of mating prior to imaging. If a change in second strand synthesis had occurred, similar numbers of foci would be present at different time points. The cells were mated for a set amount of time (either 5, 10, or 15 minutes), and subsequently interrupted by vigorous shaking and addition of 0.01% SDS. The interrupted cells were then imaged for 60 minutes and foci were counted. The percent of cells that contain a focus in the i31 strains is markedly different versus WT (Figure 3.6). At the 15 minute mating time point, WT has 0.39% of cells with a focus, while the i31 strains have 0.72% and above. The i369 strain has 0.79%, i593 has 1.39%, i681 has 1.4%, and i1753 has 0.72% of cells with a focus at the 15 minute time point. These numbers seem small, but the average mating efficiency in the i31 strains is 10^{-1} to 10^{-2}, meaning there is on average 1 mating event for every 100 to 1000 recipient cells (which is 0.01-0.1 %). These data do not indicate a change in second strand synthesis since the percentage of cells with foci are different for each cell line after 15 minutes of mating.

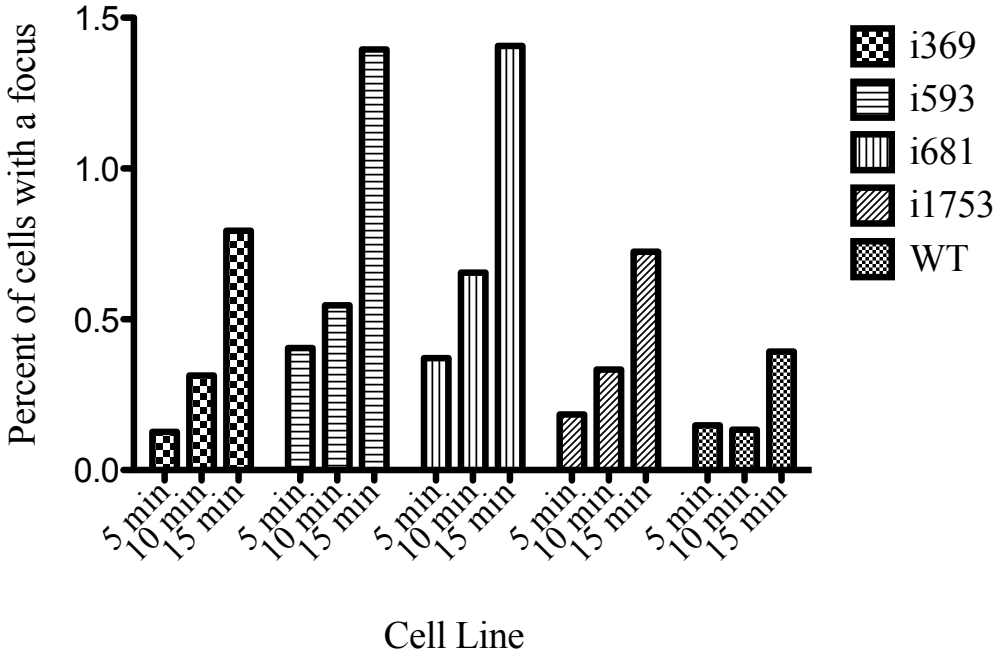

Figure 3.6. Results of the interrupted mating assay, the percentage of cells with a focus over time for TraI i31 mutants. Values (expressed as a percentage of all cells) for each cell line represent data from at least three independent experiments combined.

Determining if TraI Helicase Activity is Required for DNA Transfer

To test if mating was possible without helicase activity, we testing mating efficiency using a TraI K998A mutation. This mutation disrupts the helicase domain, and it does not form colonies in a traditional mating assay. It has no mating activity in the plate based assay, and we wanted to determine if any DNA was transferred and if the defect in mating was in plasmid establishment or DNA transfer. The SeqA-YFP system visualizes DNA transfer and allows us to track the entire process, not just the end result. The system can allow us to distinguish between DNA transfer and plasmid establishment. No foci formed in the recipient when using this strain as a donor. Cells were tracked for over three hours, well past the window when foci would normally appear. This indicates that TraI will not transfer DNA without helicase activity.

Using a Low Mating Efficiency Strain TraI i593 YFP

To determine if foci formation in a strain with a mating efficiency close to or lower than WT in a plate based assay has similar results in the microscopy assay, we ran TraI i593-YFP in the microscopy mating assay. WT TraI has a low mating efficiency, around 10^{-3} to 10^{-4}, which is similar to i593-YFP. We wanted to use the i593-YFP strain as a comparison for WT, to determine if the measured foci formation time in a strain with a mating efficiency close to or lower than WT TraI has foci formation times similar to or lower than WT. Although TraI i593-YFP is also fluorescent, we did not anticipate this signal would interfere with data collection since the fluorescence signal for foci is incredibly high. TraI i593-YFP was run with the normal microscopy mating assay recipient BA24 and we encountered some

unexpected results. This was meant as a control for the microscopy mating assay data set and did not anticipate the mating events would be difficult to image, even with two fluorescent signals. We did see what we thought were foci initially, but they are not actually foci (Figure 3.7). Foci that appear after a mating event are almost completely circular in appearance. The structures that appeared were not circular and had somewhat irregular shapes, and there were more than one in a single cell, which does not occur with foci formed after mating events. The shape of the structures also changed over time, which does not occur with mating event foci. These aggregate structures are not foci formed in the recipient, rather they are structures formed in the donor cells. The donor cells have a higher fluorescence signal than the recipient cells, and thus we were able to distinguish between donor and recipient. The mistaken identity occurred due to both donor and recipient possessing YFP signals. These structures do not occur in all cells, they occur in a small percentage of cells, around 5-10%.

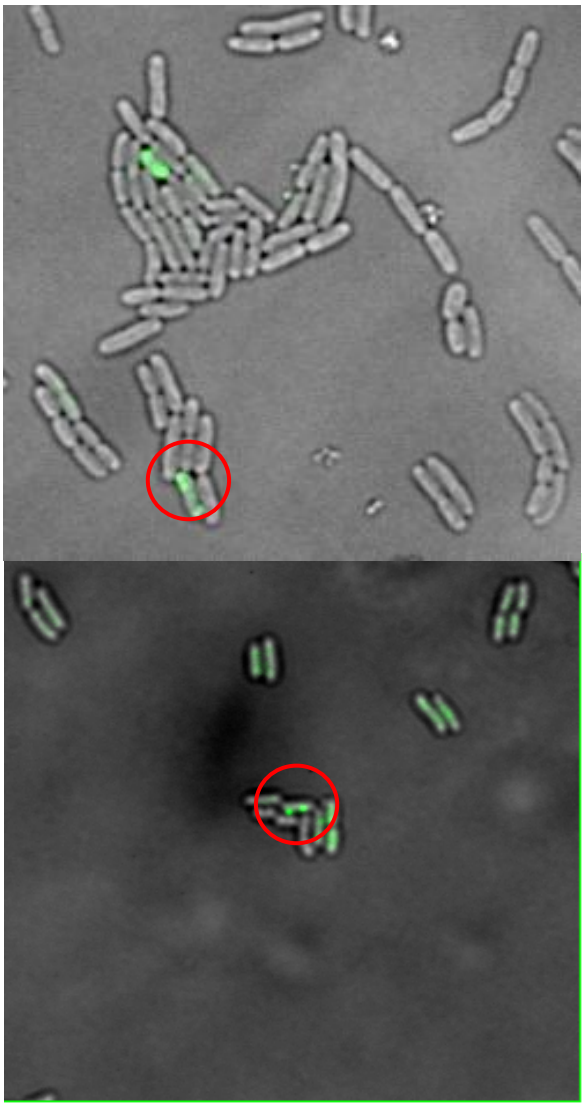

Figure 3.7. When mated, XK1502 TraI i593-YFP (top image) forms aggregates as seen in the red circle that appear similar to a focus formed by DNA transfer. However, the shape is not perfectly circular, as in an example Hfr3000 (bottom image). Foci formed by mating in BA24 are circular and punctate, while the i593-YFP aggregates are oval with irregular edges.

After determining the structures seen are not foci, the donor cell line was analyzed on the microscope by itself, with no mating (no BA24). The aggregate structures form without a recipient strain present. To determine if the structures we are seeing are aggregates due to the insertion of YFP into TraI or if the aggregation is due to TraI interacting with F plasmid, p99i TraI i593-YFP was transformed into XK1502 F^-. Without F, there is no F plasmid or *oriT* for TraI to aggregate onto. We also imaged i593-YFP I161A to determine if altering the folding stability of YFP alters the formation of the aggregate. After imaging each cell line separately, we found that the aggregate forms with F plasmid present (forms for both i593-YFP and i593-YFP I161A) but does not form in an F^- cell line. The i593-YFP cell line is not useful for creating a foci formation comparison for WT and instead we discovered aggregate formation in donor cells that is F plasmid dependent.

Discussion

Using the SeqA-YFP System With Hfr Strains

Upon receiving the strains from the Radman Lab, we needed to ensure the assay would work for us, and would work as described in Babic *et al*., 2008. We chose to use the same donor strain as they did, Hfr3000. Further controls with GM695 and other Hfr strains were run to confirm the experimental system worked as published. Despite somewhat different conditions, the system was operational and could be used for further experimentation. These results meant we could go ahead with using the system with F plasmid and potentially tracking F plasmid transfer.

Changes in DNA Transfer are Present in the TraI i31 Mutants

Once we knew the system worked, we tested the system with the F plasmid strain XK1502 FΔTraI p99i TraI. We were able to observe F plasmid transfer, which was surprising since F plasmid does not contain an *oriC* (Figure 3.4). After determining the average foci formation time for the WT strain, we decided to use a TraI mutant strain in the assay, XK1502 p99i i681. This strain has a known higher mating efficiency in the same strain background. Testing this strain in the assay, we discovered a difference in foci formation time. The time took to form foci in this strain was markedly reduced from WT TraI.

We decided to run the rest of the i31 strains that we had in the assay, i369, i593, and i1753, and found these were also different from WT. All of these mutants have a known higher mating efficiency than WT TraI. In conjunction with the mating assay data, this indicated a change in the mating machinery previously unidentified. We saw DNA appear in the recipient at earlier times in the TraI mutants than in WT. The change in DNA transfer indicated a change in the mating process, which appeared to occur more quickly in the i31 mutants. This result was unexpected, although the data correlate with the published mating efficiency data for these strains in Haft *et al.*, 2006. We did not anticipate being able to so markedly see a difference in the time it took to form foci. All of the i31 mutants have a faster foci formation time than WT, but there are differences in the average time to foci formation between the i31 mutants. The i593 and i681 mutants have the shortest average time to foci formation, while the i369 and i1753 mutants take longer to form foci than i593 and i681, although still faster than WT TraI.

These data show there are possibly different effects that the i31 has at different sites. The i31 mutations are in different domains of the protein, and the ones that are in the same domain are on different secondary structure elements of that domain. The i369 site is in a predicted unstructured region of TraI, while i593 and i681 are in the TSA region of TraI. The i593 mutation is at the end of an α-helix, while the i681 mutation is in a β-sheet, and the i1753 mutation is at the C-terminus of the protein. The differences in where the i31 is situated and the structural elements it is disrupting could be causing the apparent differences in foci formation time.

Mating in cells proceeds on a rapid time scale and only takes minutes at most to complete. Plate based mating assays usually mate cells for 20 to 60 minutes to capture as much mating activity as possible, but could be run for as little as five minutes and still give a good measure of mating efficiency. In the microscopy mating assay however, few mating events occur for 10-20 minutes after the cells are mixed due to the set up of the experiment. Most mating activity is captured after that initial period, and the microscopy mating assay proved to be able to measure foci formation in short time frame, although some foci did form before we could begin tracking mating pairs.

Due to foci forming before the mating pairs were being tracked and to determine the change in the mating process, the first step was to modify the mating assay to measure foci formation during set mating times. This would determine if the change in the mating efficiency and DNA transfer time was due to a change in the donor or recipient. To determine if the change was due to changes in second strand synthesis in the recipient, the interrupted mating assay was developed (described in

the methods section). This assay would allow us to determine the percentage of cells that contain a focus after mating for a set amount of time.

After running the interrupted mating assay, we did not find any indications that there was a defect in second strand synthesis (Figure 3.6). The percentage of cells that contain a focus in the i31 strains over time versus wild type is different. We did not observe any changes that indicate a change in the recipient is responsible for the observed change in DNA transfer.

The K998A TraI Mutant Shows No DNA Transfer

It was possible the DNA was being transferred, but not established in the recipient cell due to the ATPase defect in the K998A mutant. Our microscopy data indicate this is not the case, and in fact no DNA is transferred in an ATPase TraI mutant. TraI requires a functional ATPase to transfer DNA, as seen in our data. We also wanted to know if we could visualize foci formation in a TraI strain with a mating efficiency much lower than WT. We know that we do not see mating in an ATPase mutant, but we do see mating at a much lower efficiency in the TraI-YFP fusion proteins that have been created for other assays. These strains have a mating efficiency in the range of 10^{-4} to 10^{-5}, which is lower than WT TraI, and much lower than the i31 strains. The TraI-YFP fusion proteins were originally constructed for use in microscopy, but were not used for that purpose since the protein is expressed from a plasmid and expressed in a high copy number. This creates a high background signal and transfer of a single TraI-YFP from donor to recipient could not be

visualized. However, with the SeqA-YFP recipient line, we would not need that function of the donor line.

The i593-YFP Cell Line Was Not a Good Control

Using the i593 TraI-YFP fusion protein, we mated them with BA24 (SeqA-YFP) and tracked mating cell clusters (Figure 3.7). Determining mating cell clusters was difficult since both donor and recipient are fluorescent at the same wavelength. However, one cell line has higher signal intensity than the other, thus mating cell clusters could be determined. Once clusters were identified, they were tracked over time. We did not observe any foci formation, instead we observed aggregate like structures in the donor cells (Figure 3.7). These structures are not circular foci like those formed in recipient cells in other mating assays on the microscope, these structures were more irregularly shaped and the observed structure would vary. The occurrence of these structures was in approximately 5-10% of the observed cells. We hypothesized these structures were TraI-YFP aggregating on F plasmid.

To determine if these structures were TraI-YFP aggregating to F plasmid, we transformed the plasmid into an F^- strain. We imaged the cells alone without recipient in the F^- strain, and we also imaged i593-YFP and i593-YFP I161A with no recipient. We determined the cells do not form these structures without F plasmid present, meaning the cells are likely aggregating on F plasmid (Figure 3.7). The structures are present in the cells without mating, (i593-YFP alone) confirming that the structures are in the donor cell and not caused by DNA transfer to the recipient. Destabilizing TraI-YFP (the I161A mutant) does not cause the structures to disappear.

These data are interesting in that they show structures forming in the donor cells that were previously not seen. However, the purpose of using this cell line was to determine foci formation time for a strain with a mating efficiency lower than WT, and in this regard these data do not give any useful information. It is also possible the cells with the aggregate structure were not healthy cells and producing these structures as a result of being sick or dying. A method of staining for dead and dying cells could be used to determine if the cells with aggregates were indeed dead. However, these aggregates are not observed when F plasmid is not present, so they are more likely due to an interaction between TraI-YFP and F plasmid.

Overall Conclusions of the Chapter

Our data indicated a change in the mating process in the donor, and not in second strand synthesis. Since we did not see a change in second strand synthesis, we wanted to know what else could possibly be the cause of the change in DNA transfer seen in the i31 mutants. We proposed the model of altered protein stability of the TraI i31 mutants could be the cause behind these data. We also wanted to know if ATPase activity was required for DNA transfer. We used an ATPase mutant, TraI K998A to test if knocking out ATPase activity knocks out DNA transfer. We knew knocking out the ATPase activity of TraI knocks out mating in a plate-based assay. It was not known if the mating defect was due to lack of DNA transfer or lack of plasmid establishment, and we were able to confirm a lack of DNA transfer.

CHAPTER 4

INVESTIGATING THE STABILITY OF TRAI

Objectives of the Chapter

The work presented herein investigates possible explanations for the altered DNA transfer rate observed in the microscopy work on the TraI i31 mutants. One of the possible explanations of the higher efficiency in DNA transfer could result from increased instability of the i31 TraI mutants. This line of investigation was probed through multiple methods. We utilized protein fusion constructs and direct measurements of protein stability to analyze if altered stability of the TraI mutants could be part of the cause behind the change in the i31's mating efficiency. As reviewed in the introduction, TraI will tolerate the insertion of small proteins and cell lines with TraI fusion proteins can transfer DNA.

One of the crucial functions of TraI in bacterial conjugation is the nicking of the plasmid during the mating process. TraI is highly specific for the *nic* site, and will not nick effectively if the sequence is not specific for F plasmid TraI (Stern and Schildbach, 2001. It may be possible the *nic* activity of the i31 mutants has been altered and be part of the cause of the altered DNA transfer and increase in mating efficiency. We examined the nicking activity of TraI, to determine if the activity was altered in the i31 mutants.

We also investigated an alternative model, examining if altering the TSA of TraI could partially explain the changes in mating efficiency. The recent structure of the TSA, solved in Redzej *et al*., 2013, indicated that the TSA of R1 TraI is located

within an independent folding unit and a structural domain. The TSA of R1 TraI and F TraI are almost entirely identical, with two amino acid changes between the two domains in the solved structure. In their study, various residues within the TSA were mutated, altering protein translocation frequency (Redzej *et al.,* 2013). Previous work had also identified that insertion of 31 amino acids (i31) in the TSA without the presence of the TSB eliminated protein transfer (Lang *et al.*, 2010, Haft *et al*., 2006). Their work indicated only one TS was required for transfer (Lang *et al*., 2010).

Cloning DHFR into TraI Did Not Cause Changes in Mating Efficiency

Two constructs were successfully engineered, TraI i369-DHFR and TraI i681-DHFR. The clones were confirmed by sequencing and expression test to confirm expression of full-length protein and absence of truncation products. Using these two clones, we proceeded to test the effects of MTX on TraI-DHFR. MTX acts to stabilize DHFR and acts to inhibit the unfolding of DHFR (Ainavarapu *et al*., 2005). Mating assays using control strains in the presence of varying concentrations of MTX were run to determine the upper limit of toxicity that could be tolerated in a mating assay. It was determined that cells with WT TraI could tolerate 50 μM of MTX without any significant change to mating efficiency caused by the introduction of the drug to the mating assay. Higher concentrations caused cytotoxicity and reduced mating efficiency in control strains (WT and i31s without DHFR inserted).

Since concentrations of MTX over 50 μM caused cytotoxicity, the mating assay protocol was also optimized for length of use of the drug during mating. Cells were mixed with MTX for varying amounts of time prior to mating to determine if

drug exposure time would affect mating efficiency. We determined 15 minutes of exposure combined with 60 minutes of mating would not alter the mating efficiency due to drug exposure. This is the length of mating assays without drug, keeping both types of mating assays standard to each other. Both i369-DHFR and i681-DHFR were mated with the recipient strain GM124. Addition of DHFR to TraI did not change the mating efficiency of the construct (figure 4.1). The results of the mating assays indicated no change in mating efficiency of the TraI-DHFR constructs when MTX was added to the mating assay (Figure 4.1). Since there was no statistically significant change in mating efficiency with or without MTX (Table 4.1), we decided to shift to another approach to determine if altering protein stability could cause changes in mating efficiency.

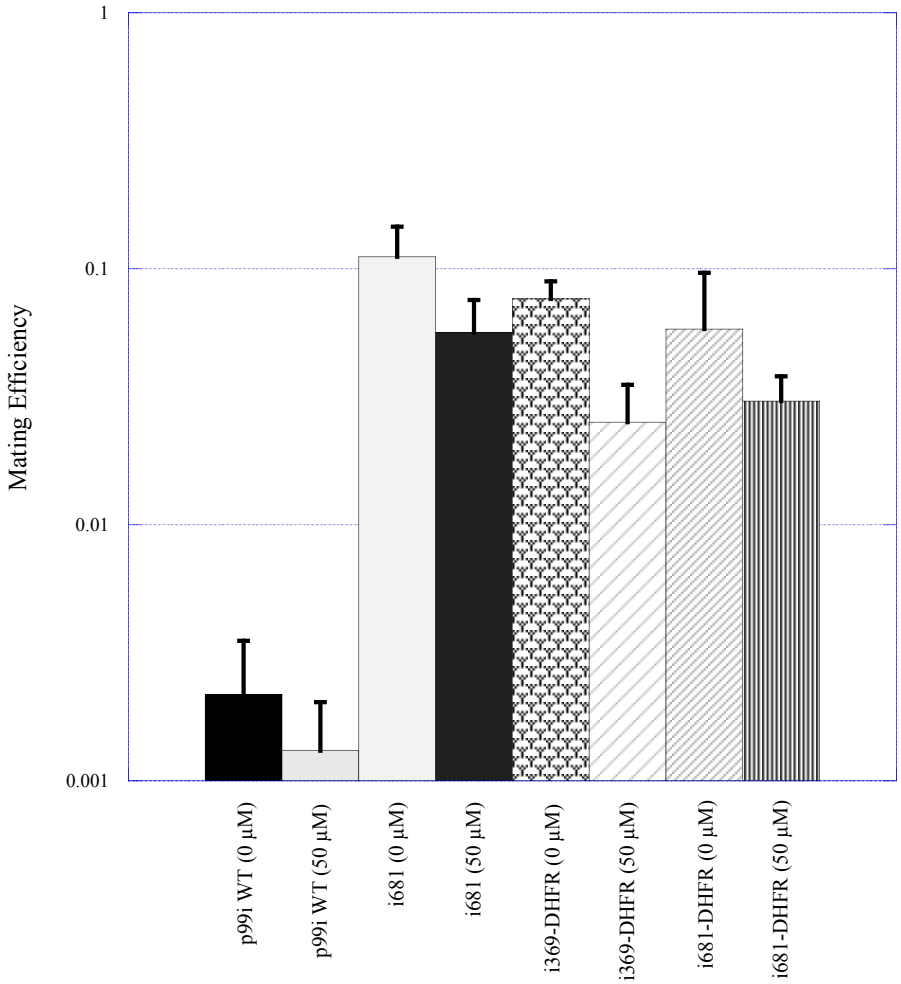

Figure 4.1. The mating efficiency of TraI-DHFR mutants with and without 50 µM methotrexate (MTX). No statistically significant difference in mating efficiency with or without drug was measured. For each cell line, data from at least three independent experiments were combined. Standard deviations are shown.

	p99i WT	TraI i681	TraI-369 DHFR	TraI-681 DHFR
0 μM MTX	$2.17 \bullet 10^{-3} \pm 1.34 \bullet 10^{-3}$	0.11 ± 0.034	0.078 ± 0.013	0.058 ± 0.039
50 μM MTX	$1.3 \bullet 10^{-3} \pm 7.16 \bullet 10^{-4}$	0.056 ± 0.019	0.025 ± 0.01	$0.03 \pm 7.6 \bullet 10^{-3}$

Table 4.1. Mating efficiency of TraI-DHFR with and without MTX. Values are reported as the average of at least three independent experiments with standard deviation reported.

TraI-DHFR Discussion

The addition of MTX to mating assays with DHFR inserted into TraI did not create any noticeable changes in the mating efficiency of those strains. Even after protocol optimization, we did not see any changes in mating efficiency. Insertion of a 22 kDa protein into TraI did not alter mating efficiency, and previous evidence suggested mating efficiency was lowered when a protein was inserted into TraI. In other systems that use DHFR to probe protein transfer across membranes, transport without MTX is not affected; only when drug is added to the system is there a change in protein transport (Eilers and Schatz, 1986).

We decided to shift the approach and look for alternative strategies for probing protein stability, as the TraI-DHFR work did not show any change in mating efficiency upon addition of MTX. We wanted to investigate if a similar approach could be undertaken with a different protein. YFP is a stable protein, and we wanted to examine if adding YFP to TraI and altering the stability of YFP by base substitutions could produce changes to the mating efficiency of these constructs.

Mutating YFP Inserted into TraI Causes a Change in Mating Efficiency

We identified point mutations that would most likely cause a change in the stability of the protein. The first mutation selected was G67A, a chromophore mutation that destabilizes the chromophore and causes the protein to be able to reversibly fold (Kutrowska *et al.*, 2007). The second mutation selected was I161A, a mutation that destabilizes a hydrophobic region of the protein, indicated in that role by Melnik *et al*., 2011. These two mutations, along with a control, I47A, were created

in both i593 and i681 YFP. Creating these mutations at two different sites was critical to understanding if altering the stability in one site created a different mating phenotype than the other site of TraI.

The resulting strains were mated in plate based mating assays with the recipient strain GM124. The resulting mating efficiencies are shown in Table 4.2. In both sites, the point mutants G67A and I161A altered the stability of the protein and mating efficiency recovered relative to TraI-YFP (Figures 4.2 and 4.3). The mating efficiency of TraI-YFP prior to mutation was on the order of 10^{-5} to 10^{-4}. With both mutations, the mating efficiency recovered into the range of 10^{-3} to 10^{-2}. These are statistically significant rises, indicating that significantly reducing the stability of YFP improved the mating efficiency. The mating efficiency of I47A did not change relative to TraI-YFP, indicating changing a random single residue (isoleucine in particular) alone will not alter mating efficiency. There was no previously published evidence to specify the residue was involved in altering stability. The residue is solvent exposed and at the end of a β-sheet, similar to I161, but does not alter mating efficiency when mutated. The point mutation needs to be targeted to altering the stability of the protein to produce an effect on mating. The mating efficiency changes seen at the i681 site are the same changes seen at the i593 site. This indicates that the changes wrought by the i31 insertion are not due to where the i31 is in the protein, and due rather to altering the stability of the protein.

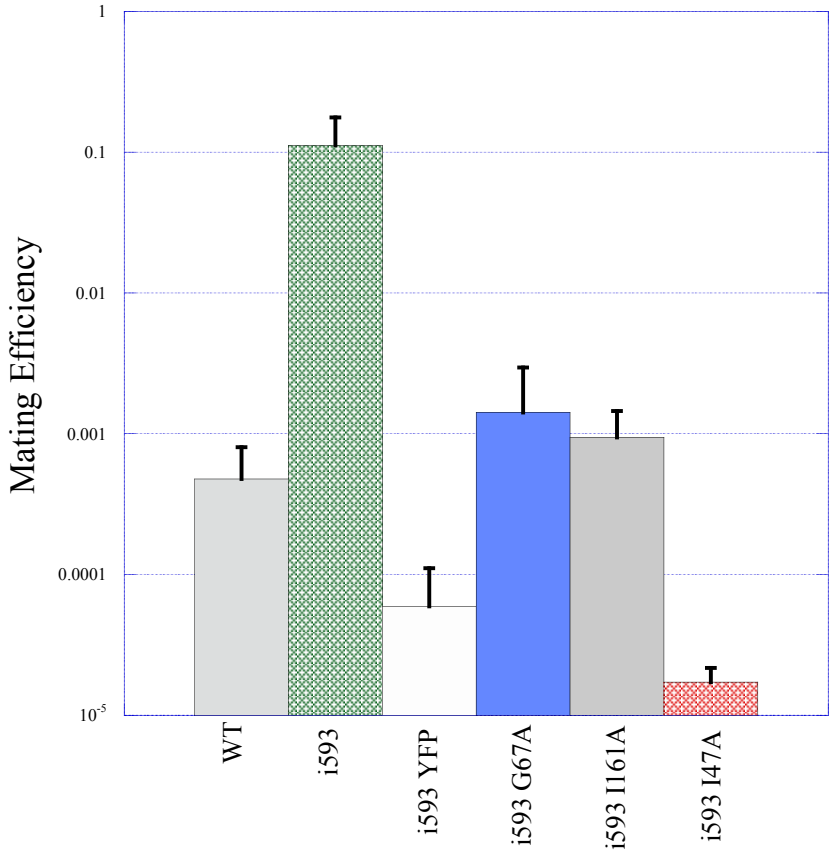

Figure 4.2. Mating assay data for i593-YFP point mutants. Mating efficiencies (transconjugates per donor cell) of the YFP point mutants in the i593 site were compared to WT TraI from plasmid p99i. Values for each cell line represent the combination of at least three independent experiments. Standard deviations are shown.

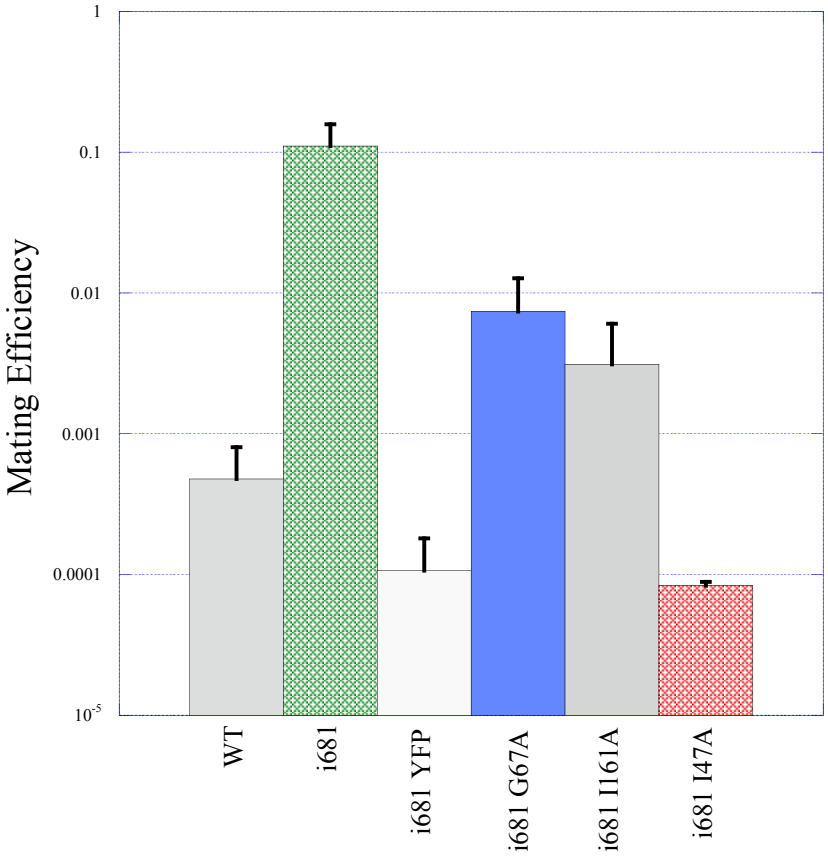

Figure 4.3. Mating assay data for i681-YFP point mutants. Mating efficiencies (transconjugates per donor cell) of the YFP point mutants in the i681 site were compared to WT TraI from plasmid p99i. Values for each cell line represent the combination of at least three independent experiments. Standard deviations are shown.

Strain	Mating Efficiency
p99i WT	$4.0 \bullet 10^{-4} \pm 3.2 \bullet 10^{-4}$
i593	0.12 ± 0.066
i593-YFP	$5.4 \bullet 10^{-5} \pm 5.1 \bullet 10^{-5}$
i593-YFP G67A	$1.3 \bullet 10^{-3} \pm 1.1 \bullet 10^{-3}$
i593-YFP I161A	$9.3 \bullet 10^{-4} \pm 2.7 \bullet 10^{-4}$
I593-YFP I47A	$1.72 \bullet 10^{-5} \pm 4.51 \bullet 10^{-6}$
i681	0.11 ± 0.047
i681-YFP	$1.1 \bullet 10^{-4} \pm 7.45 \bullet 10^{-5}$
i681-YFP G67A	$7.3 \bullet 10^{-3} \pm 5.34 \bullet 10^{-3}$
i681-YFP I161A	$3.1 \bullet 10^{-3} \pm 2.9 \bullet 10^{-3}$
i681-YFP I47A	$8.37 \bullet 10^{-5} \pm 5.12 \bullet 10^{-6}$

Table 4.2. Mating efficiency (transconjugates per donor) of the TraI-YFP point mutants. Values are reported as the average of at least three independent experiments with standard deviation reported.

TraI-YFP Discussion

In this work, we focused on probing the stability of TraI via an inserted protein. Although the TraI-DHFR work did not demonstrate a change in mating when MTX was added, we were able to prove that altering stability of the inserted protein can alter the mating efficiency of the strain with TraI-YFP. This is significant, as this indicates that altering stability may be part of the cause of the altered phenotype of the i31 mutants. The data at both i593 and i681 showed the same pattern of mating efficiency recovery with the G67A and I161A mutations. Altering the stability of YFP did indeed cause a recovery in mating efficiency. However, this is changing the stability of an inserted protein, not of TraI itself. While an important tool, inserting proteins into TraI and altering them is not the same as altering TraI itself. This data indicates a possible cause for the i31 phenotype, but does not fully explain it. Using this data as a support for the model of altered stability causing the i31 phenotype, the next logical step was to measure the stability of the TraI i31 mutants directly. Determining stability of the protein without an inserted protein could possibly provide more insight into the cause of the mating assay and DNA transfer rate differences in the i31 mutants.

TraI Mutant Nicking Activity is Not Changed

To determine if the nicking activity of the TraI i31 mutants was altered, we performed a nicking activity assay on full-length WT TraI and i31 mutants (see Methods). No changes in nicking activity of the i31 mutants versus wild type were observed (Figure 4.4). Analysis of the gels to determine the percent of oligo cut

showed that the proteins all have nicking activity (Figures 4.5 and 4.6). However there was wide variability seen in the percentages between different gels. These data also indicate that the mutants are active *in vitro*, and nicking activity is not adversely affected by the mutation. These data lead us to the conclusion that nicking activity is not affected by the i31 mutation and not part of the reason behind the changes seen in the i31 mutants.

Interactions of TraI and TraD in the Nicking Assay

The nicking assay was originally intended not only to show the i31 mutants have *in vitro* activity, but also to also quantitate the nicking reaction and determine if the nicking activity of the i31 mutants was significantly higher than that of WT. We did not see any major changes in nicking activity (Figure 4.4). We decided to investigate if adding TraD to TraI in the nicking reaction would enhance nicking more in the i31 mutants versus WT. When TraD is added to TraI, it nicks supercoiled *oriT* DNA and converts it to open circular plasmid more than without (Lang *et al*., 2011). Since we know in this assay TraD stimulates the activity of TraI, we wanted to know if this would be the case in the nicking assay, where we use short fluorescently tagged oligo to measure nicking activity. We used TraD C-terminal domain (CTD) as full length TraD contains a membrane insertion domain and cannot be purified with that domain.

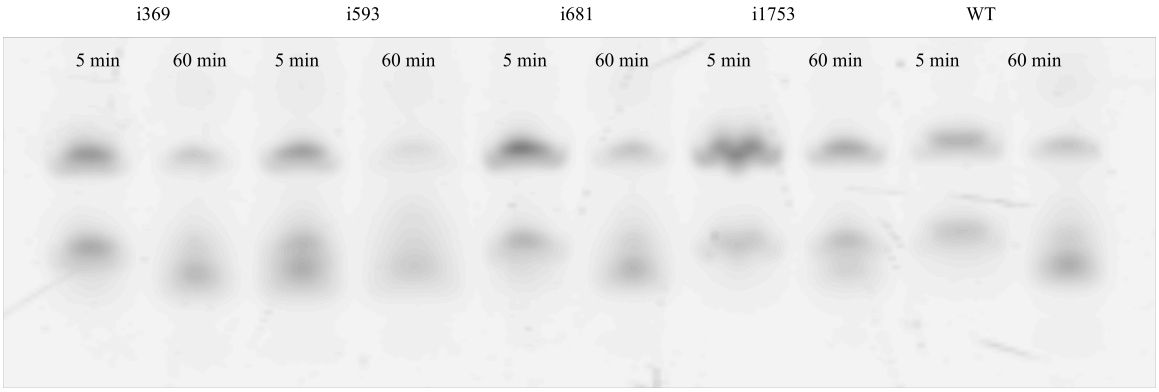

Figure 4.4. Results of a time course nicking assay with WT TraI and the i31 mutants. Reactions were run for either 5 or 60 minutes, and halted with addition of Proteinase K. Upper band (uncut Cy5 oligo) and lower band (nicked Cy5 oligo) show no major differences between the constructs at the 5-minute or 60-minute time point. No obvious defects in nicking activity in the i31 mutants can be seen.

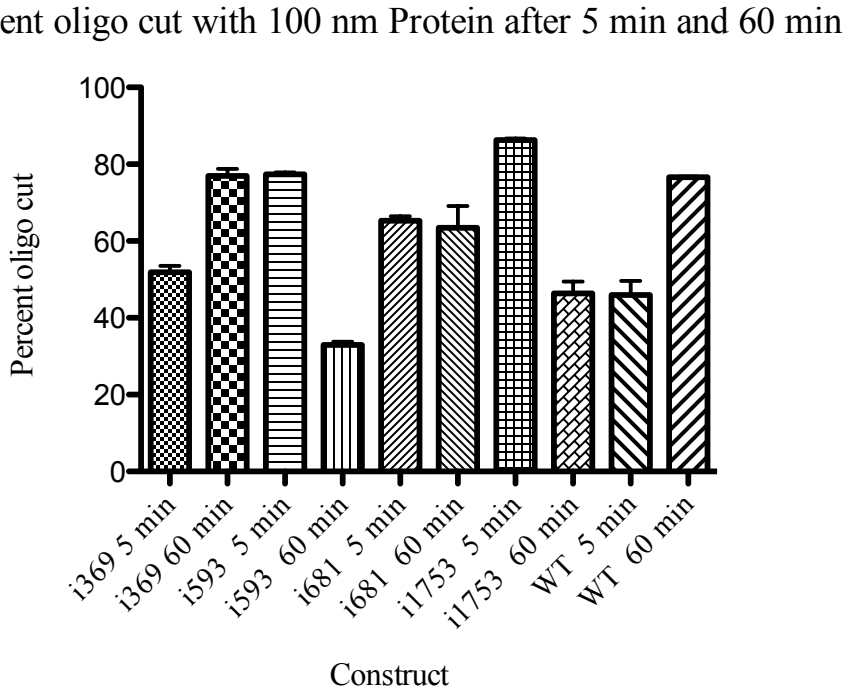

Figure 4.5. Analysis of the percentage of oligo cut of total oligo in the lane from a time course nicking assay with WT TraI and the i31 mutants. Reactions were run for either 5 or 60 minutes. Results indicate all constructs are active.

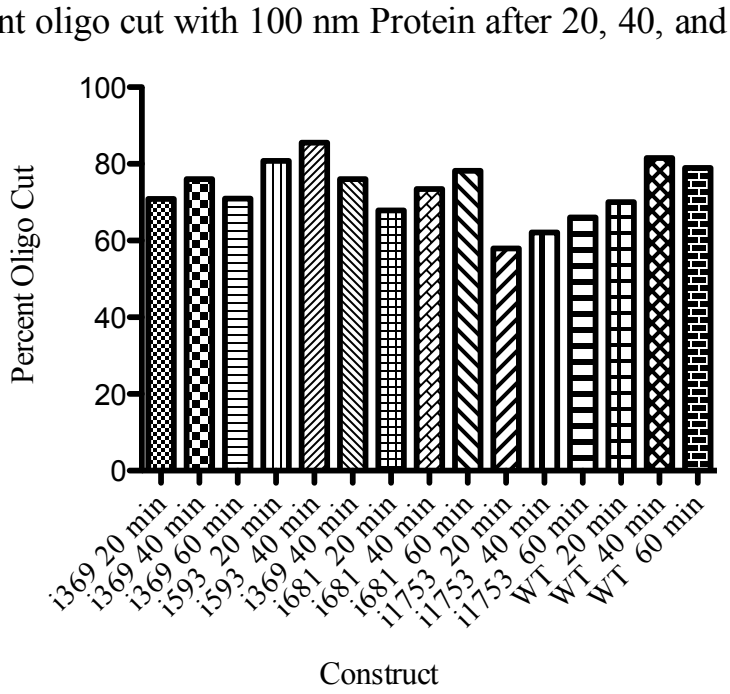

Figure 4.6. Analysis of the percentage of oligo cut of total oligo in the lane from a time course nicking assay with WT TraI and the i31 mutants. Reactions were run for either 20, 40 or 60 minutes. Results indicate all constructs are active.

Addition of TraD Does Not Cause Changes in Nicking Activity

TraD C-terminal domain (CTD, ΔN130) from F plasmid was added to the nicking reaction (see materials and methods) with TraI at varying concentrations to determine if TraD could enhance the nicking reaction. We saw no apparent increase in nicking activity with the addition of TraD to TraI; analyzing the intensity of the bands from the nicking reaction did not show any significant increase in nicking activity when TraD was added (Figure 4.7).

Nicking Assay Discussion

The nicking assay was able to show that all the constructs do have nicking activity, and they are all active at approximately the same levels. There were no large changes in activity seen (Figures 4.5 and 4.6). The assay also proved to be highly variable from gel to gel, and the results only served to underscore the variability in the assay. The assay is not a good measure of the quantitative nicking activity of the constructs, as can be seen in the differences in activity between Figures 4.5 and 4. 6. Unlike the published results from Lang *et al.,* 2011, we did not see any enhancement in the nicking activity of TraI when TraD was added to the reaction. This could be due to differences in the type of assay, as we were using small oligos and Lang *et al.* were using supercoiled *oriT* DNA. We were also using a partial construct of TraD that is not full length, and that could have affected the reaction. To fully assess the effects of TraD on TraI, we would need to run the same assay as in Lang *et al.,* but as

we did not see any changes in our assay we decided not to pursue these experiments any further.

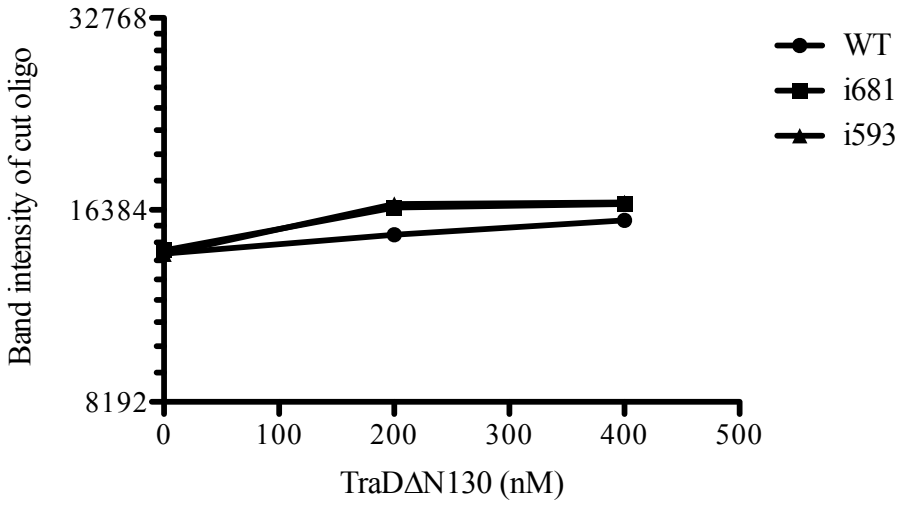

Figure 4.7. Addition of TraDΔN130 to wild type TraI, i593, or i681 in the nicking assay at various concentrations did not change the nicking activity of TraI. TraI and TraDΔN130 were incubated in the nicking reaction for 60 minutes, and the reaction was halted with Proteinase K.

Differences in the Stability of TraI 309-858 Fragments

The changes in mating efficiency seen when TraI-YFP was mutated indicated that altering the stability of TraI is part of the reason for the change in DNA transfer rate in the i31 mutants. In the original paper reporting the i31 mutants, the authors speculated the increase in mating efficiency seen in certain i31 mutants was due to a release from a form of negative regulation (Haft *et al.*, 2006). Previous work in the lab by a former post doc, Lubos Dostal, analyzed some of the i31 mutants and found that the mutants had reduced affinity for ssDNA in their helicase associated binding sites (Dostal and Schildbach, 2010). They also had a reduction in the apparent negative cooperativity of binding. These results, along with other data, indicated the negative cooperativity between the ssDNA-binding domain and the relaxase domain (both of which bind ssDNA) is a major regulatory step in F plasmid transfer (Dostal and Schildbach, 2010). The changes in ssDNA binding partially explain but do not fully explain why there is a change in mating efficiency.

While changes in ssDNA binding may be part of the reason behind the altered phenotype, changes in the protein's stability may be behind the changes in ssDNA binding. Alternatively, changes in ssDNA binding and changes in stability may be working as additive effects to increase mating efficiency. To more directly address the question of the stability of TraI, we conducted stability measurements of TraI. We proposed a model whereby the i31 caused a measurable change in the stability of the protein, which could possibly alter the accessibility of the protein to the pore. The protein more than likely at least partially unfolds as it transits the pore (see TraI-YFP

data) and the stability of the protein may cause a change in mating efficiency and explain the altered DNA transfer seen in the microscopy data.

The transposon insertion inserts 31 amino acids with no obvious structure. Inserting an unstructured peptide into the backbone of TraI could result in changes to the stability of the local environment, or the global environment of the protein. To determine if there is a global change in the stability of the protein, we employed chemical titration measured by circular dichroism to probe the stability of the protein. We used a fragment of TraI in the study of the stability of the protein, as full length TraI could prove problematic in these types of experiments. Full length TraI has intrinsically disordered regions that would not lend themselves well to protein unfolding studies. A previous post doc, Lubos Dostal, had conducted trypsin digests on TraI, and identified the region of 309-858 as a trypsin stable fragment (Dostal and Schildbach, 2010). This region encompasses the i369, i593, and i681 insertion sites. This fragment with the different i31 insertion sites was then cloned into the pET24a vector, and expressed in BL21 cells (see materials and methods).

Wavelength scans of the fragments for wild type, i369, i593, and i681 were carried out. The signal for each construct indicated primarily α-helix secondary structure in each sample, but i593 showed a difference in its wavelength scan compared to the other constructs (Figure 4.8). There is a shift in the minimum of the scan for i593 compared to the minimum at 210 nm for the other constructs, indicating more random coils present in the sample. This could be due to partial unfolding of the protein, or a change in the structure of the protein due to the i31 insertion. After the wavelength scans, titration curves were collected for all constructs (Figures 4.9, 4.10,

4.11, 4.12, 4.13). The $\Delta G^{H_2 0}$ of unfolding values are reported in Table 4.3. There was no statistically significant difference between the ΔG values.

The *m* value represents the dependence of the free energy of unfolding (the ΔG value) on denaturant concentration. The *m* value of a protein correlates with the amount of protein that is surface exposed to solvent as it unfolds (Myers, Pace, and Scholtz, 1995). The calculated *m* values were much smaller than what is reported in the literature for proteins of similar size (Myers, Pace, and Scholtz, 1995). As well as small *m* values, the unfolding curve for i593 has an altered baseline compared with the rest of the constructs (Figure 4.14). This may be due to increased contaminants in the sample, or due to the presence of more random coils in the protein structure. The i593 construct, as detailed in the methods, required an additional column during purification. Even after the additional column, the construct could rapidly degrade from full-length fragment to a degradation product and the sample had to be carefully handled to prevent the degradation.

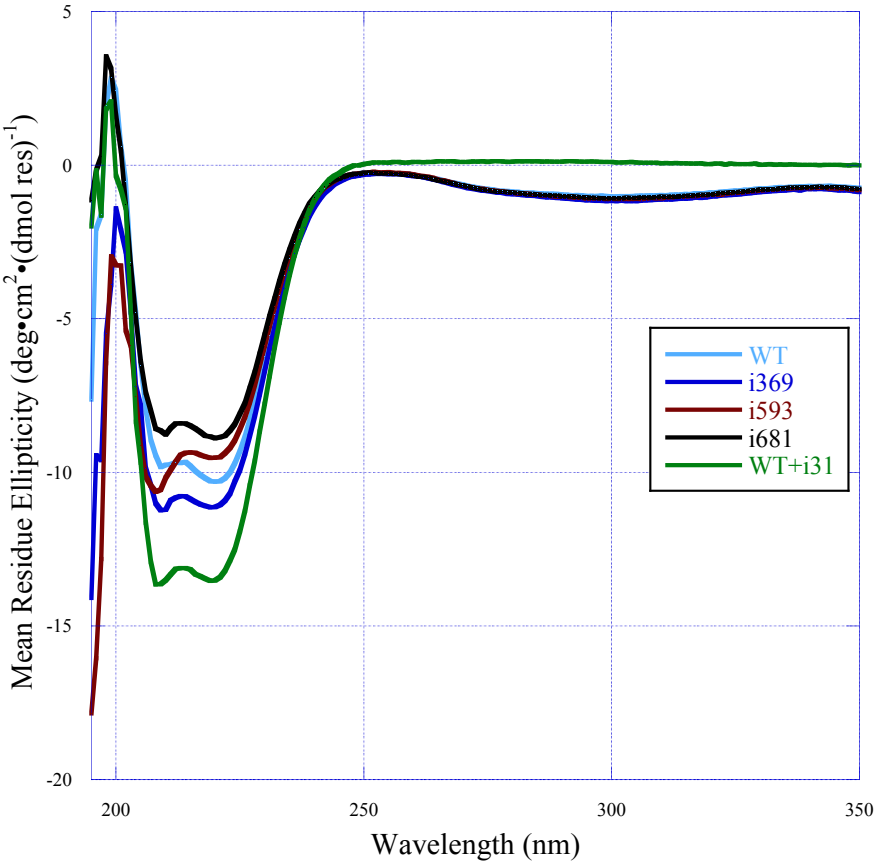

Figure 4.8. Circular dichroism wavelength scans of the 309-858 fragments at 10 µM protein concentration. A shift in the spectrum of i593 can be seen compared to the rest of the fragments. Fragments were scanned at a concentration of 10 µM in buffer containing 20 mM $NaPO_4$ pH 7.4, 0.1 mM EDTA, and 100 mM NaCl.

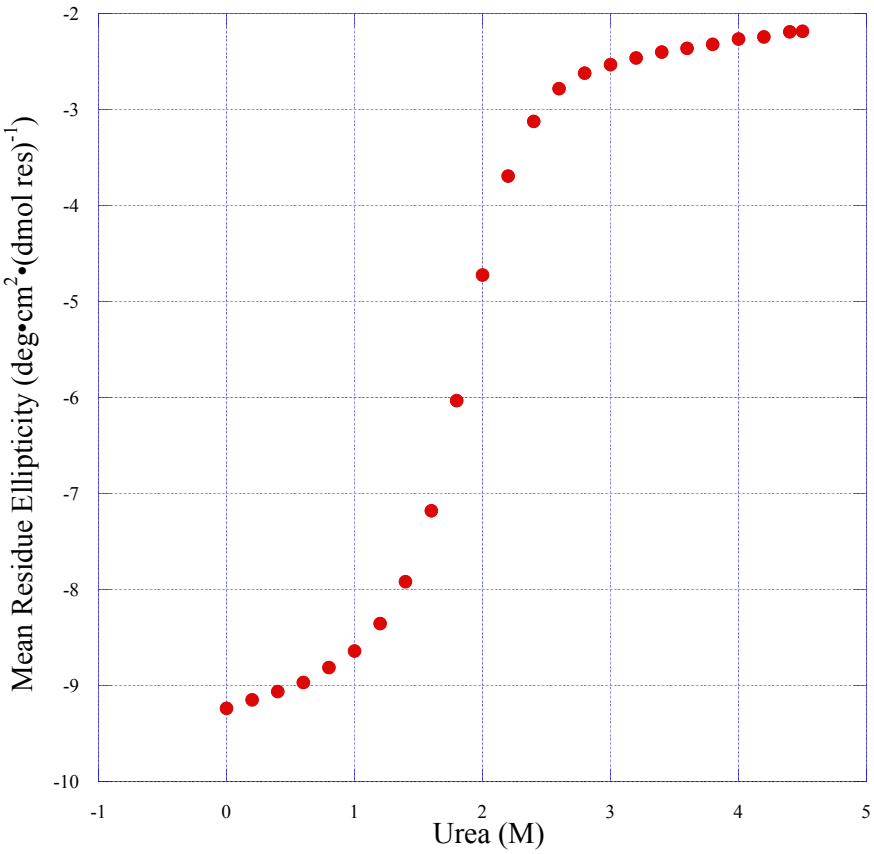

Figure 4.9. Unfolding titration curve for WT TraI 309-858. Plot shown is the average of three separate experiments.

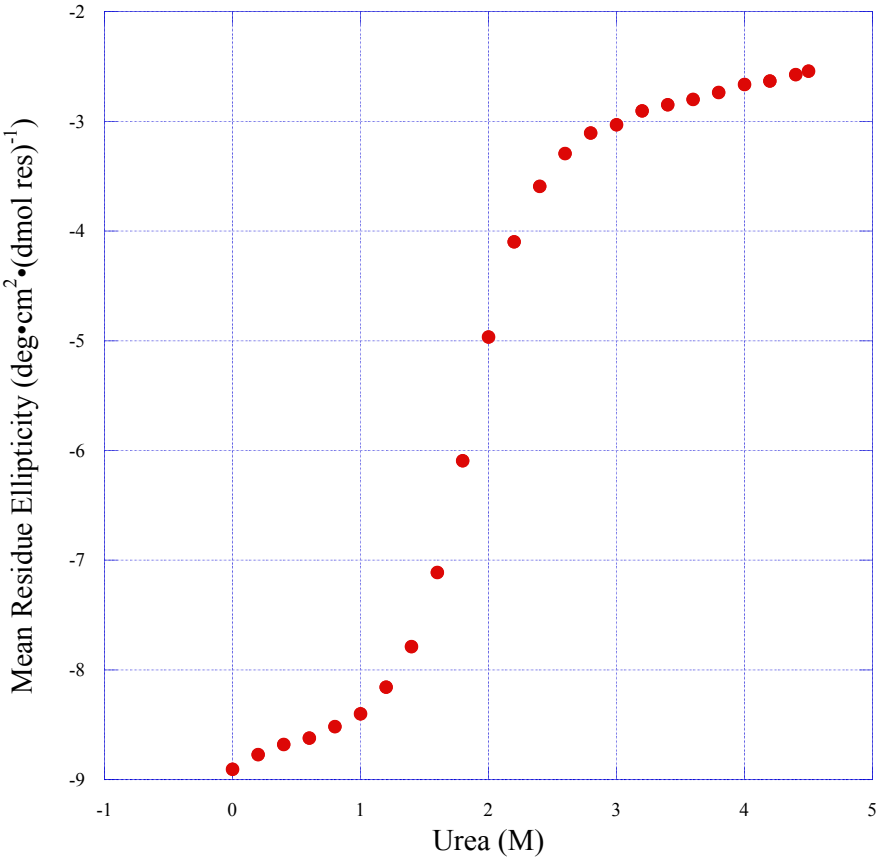

Figure 4.10. Unfolding titration curve for i369 TraI 309-858. Plot shown is the average of three separate experiments.

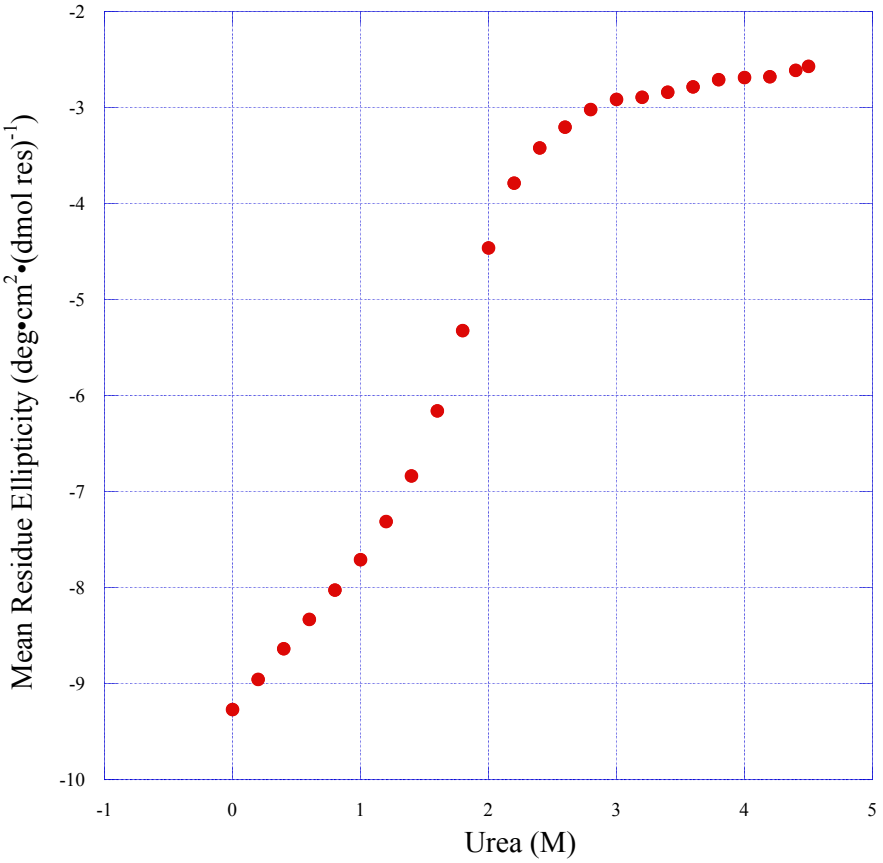

Figure 4.11. Unfolding titration curve for i593 TraI 309-858. Plot shown is the average of three separate experiments.

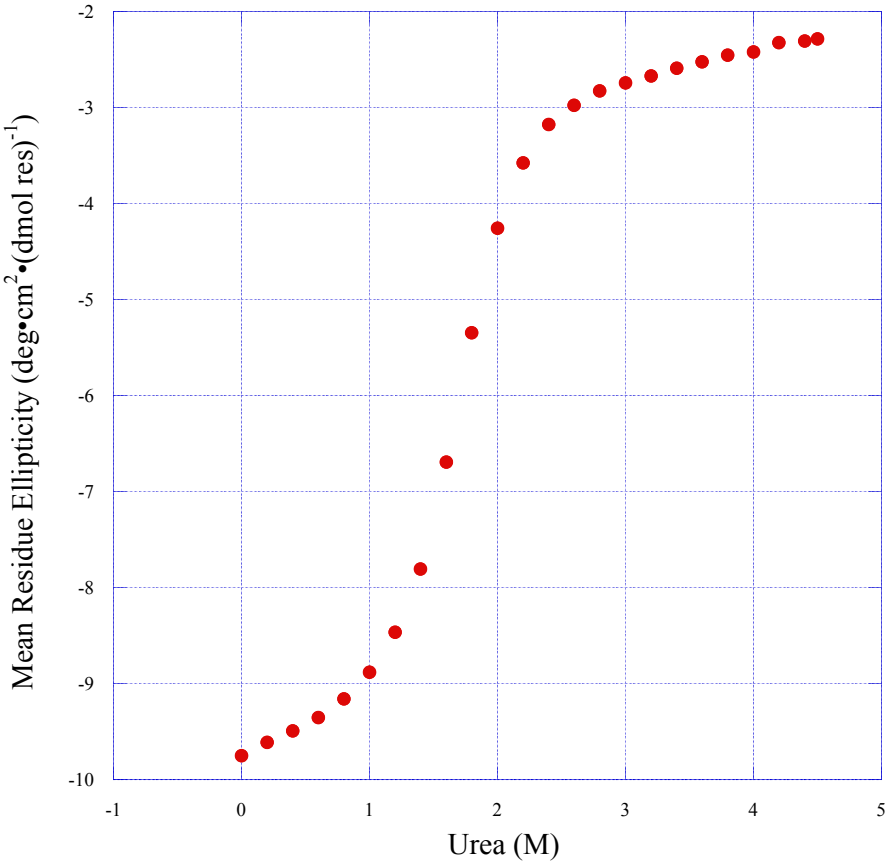

Figure 4.12. Unfolding titration curve for i681 TraI 309-858. Plot shown is the average of three separate experiments.

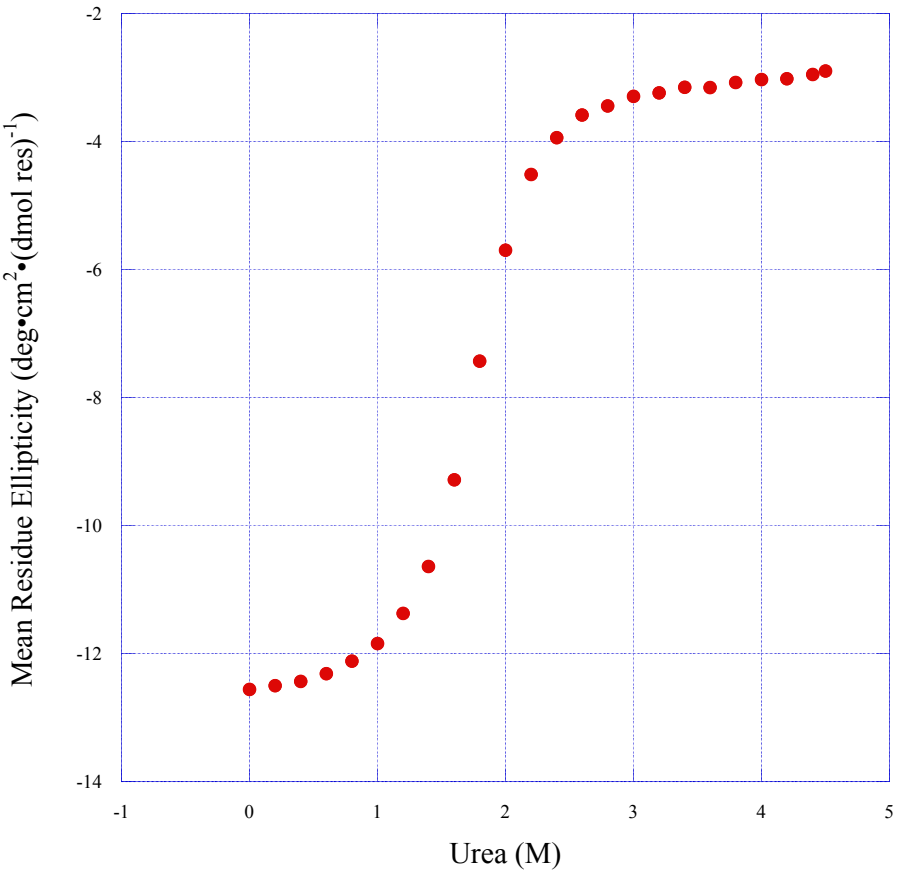

Figure 4.13. Unfolding titration curve for wild type plus i31 TraI 309-858. Plot shown is the average of three separate experiments.

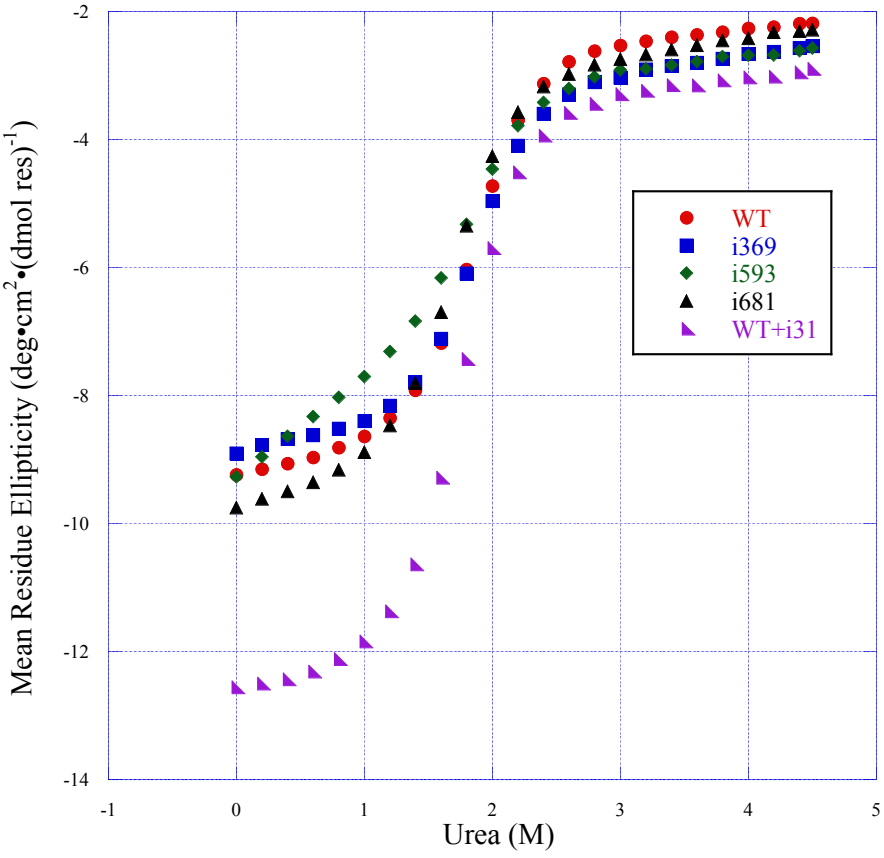

Figure 4.14. Overlay of representative titration curves for all protein fragments.

Plotted lines shown are the average of three separate experiments for each fragment.

Protein	**$\Delta G^{H_2}{}^0$ (kcal/mol)**	***m* value**
WT TraI 309-858	4.87 ± 0.13	2.67 ± 0.04
i369 TraI 309-858	4.84 ± 0.15	2.67 ± 0.05
i593 TraI 309-858	4.83 ± 0.09	2.49 ± 0.01
i681 TraI 309-858	4.6 ± 0.11	2.62 ± 0.02
WT TraI + i31 309-858	4.70 ± 0.05	2.51 ± 0.25

Table 4.3. All of the calculated ΔG values are similar, indicating no change in the chemical unfolding of the various constructs versus WT.

To more clearly define what may be causing the altered baseline for i593, we performed a near UV scan of WT protein to determine if there is a near UV signal peak that could be used for monitoring a titration curve. Near UV CD can give information on the tertiary structure of the protein. By analyzing tertiary structure, we aimed to see if i593 was different from the other constructs in tertiary as well as secondary structure. WT TraI 309-858 was monitored at 100 μM concentration in a 1 cm cuvette, and scanned from 250 nm to 350 nm. The resulting wavelength scan (Figure 4.15) did show a signal peak at 295 nm, but the signal strength was weak. To be able to monitor the titration curve of i593 in the near UV would require a five-fold increase in signal at 295 nm, meaning protein concentration of i593 would need to be quite high and potentially reach saturating concentrations.

To get a more complete picture of the titration unfolding, the midpoint of the unfolding transition was calculated (Cm value, Table 4.4). The data was also plotted as ΔG^{H_20} versus urea concentration using the following equation (2):

$$\Delta G^{\circ}(x) = \Delta G^{H_20} + m(\text{urea concentration})$$

The Cm value for each construct is reported in Table 4.4. There are some differences in the Cm values between the WT construct, i593, i681, and WT+i31. Interestingly there is almost no difference between i369 and WT.

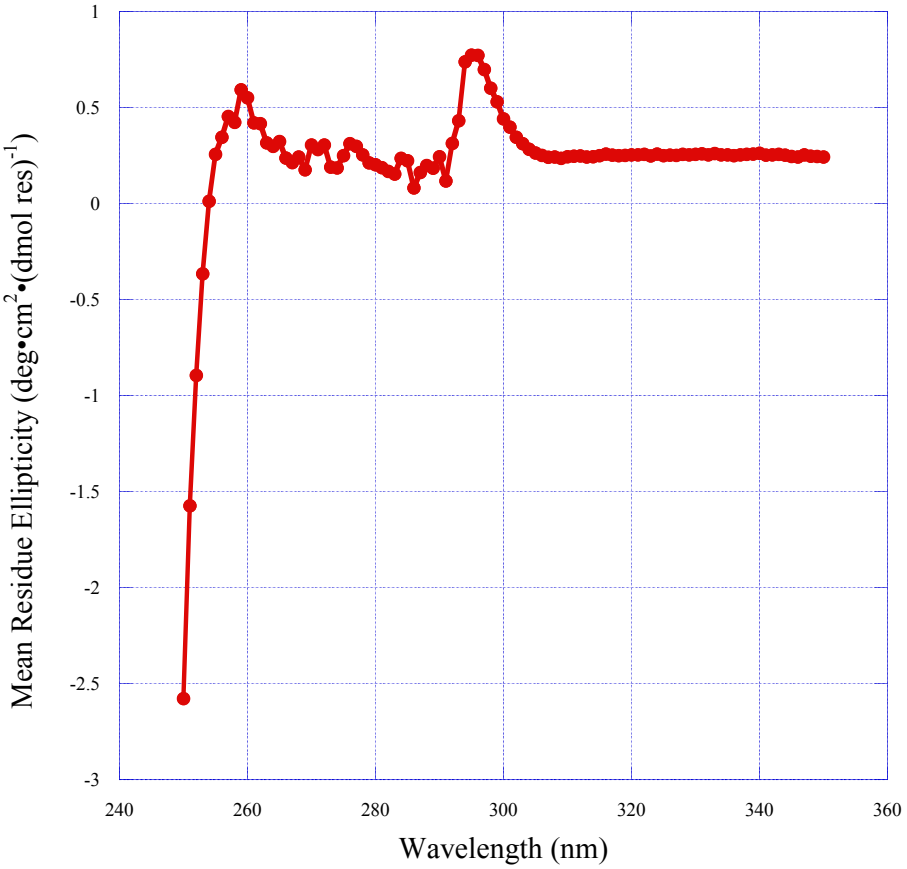

Figure 4.15. The near UV scan of WT protein at 100 μM indicates a distinct signal peak at 295 nm. The peak signal maximum is small and monitoring at 295 nm would not be ideal for chemical titration.

Protein Fragment	Cm Values (M)
i369	1.8127
i593	1.9397
i681	1.7557
WT	1.8239
WT + i31	1.8725

Table 4.4. The calculated midpoint of transition (Cm values). Values were calculated using Eq. 2.

The dependence of $\Delta G^{H_2 0}$ on urea concentration was also plotted. The data for the calculated $\Delta G^{H_2 0}$ versus urea concentration shows there are some differences in the trends for i593, i681, and WT+i31 (Figure 4.16). Interestingly there is almost no difference between i369 and WT. There may be some changes to i593 and i681 that do not occur in i369 due to where the i31 is in the protein. These results, along with the differences in the midpoint of transition, indicate the stability of the i593 and i681 constructs are altered compared to WT.

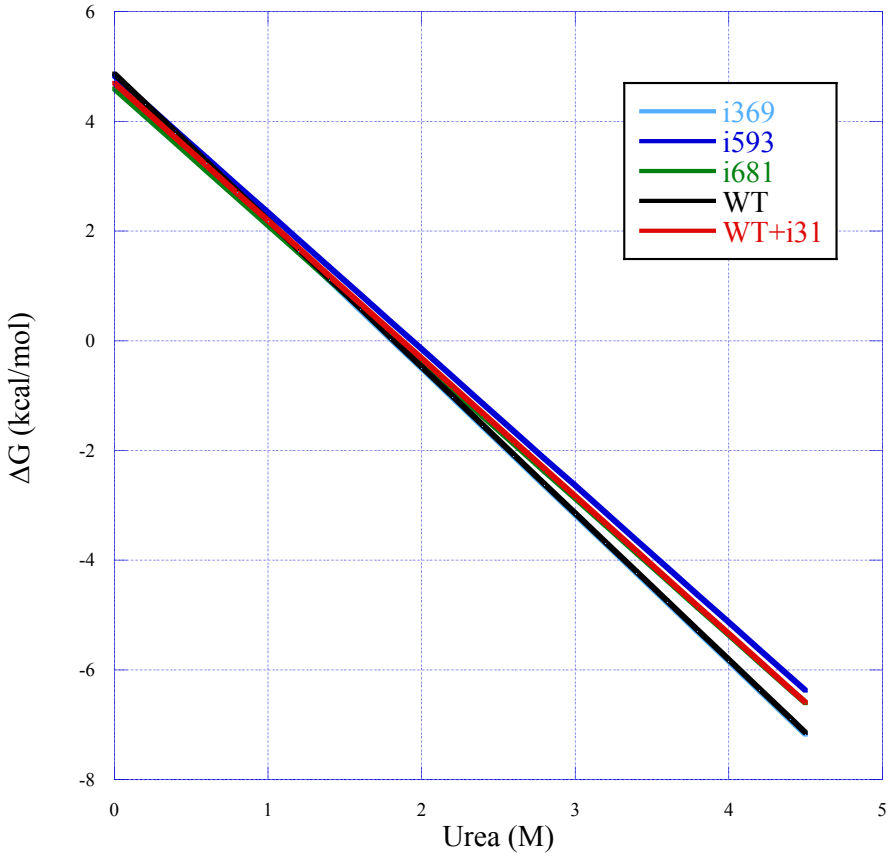

Figure 4.16. Dependence of ΔG on urea molarity. The ΔG^{H_2O} values were calculated from the data in figure 4.15 using equation 2.

The Stability of the TraI Fragments Discussion

Initial analysis of the CD data for the 309-858 constructs did not show any noticeable large changes in ΔG values between the i31 constructs and WT. However, more in-depth analysis indicated there might be some changes in the i593 and i681 constructs that could be contributing to the altered phenotype seen in the microscopy data. The ΔG values for the protein fragments did not show any major differences in the stability of the protein fragments. The changes in stability appear to be small differences, which could possibly account for the changes in mating efficiency.

The protein fragment 309-858 contains 551 residues, and according to published values, should have *m* values in urea much larger than what they are (around 2.5 kcal/mol).A large data set of *m* values for proteins of varying sizes has been published, and can be used as reference for the m values calculated from the i31 unfolding curves. The *m* value for a globular protein (pepsinogen) with 370 residues in urea is 7.8 kcal/mol. A protein with a similar *m* value to the 309-858 fragments is chymotrypsinogen A, which is only 245 residues long (Myers, Pace, and Scholtz, 1995). Small *m* values would be an issue if some of the proteins had a small *m* value and others did not. That scenario would indicate titration unfolding was not capturing some of the unfolding of the proteins. However, the *m* values for all the fragments are small. Although they are not as large as other calculated values for similarly sized proteins, there is no difference between the *m* values, and they do not indicate any issues with the data collection.

We determined the midpoint of the unfolding transition (Cm) to more fully understand the data. The Cm value is calculated by dividing the slope of the line (ΔG)

by the *m* value. The midpoint of transition, the denaturant concentration at which half the protein is unfolded and half is folded, is another indicator of protein stability. As reported in Table 4.4, there are some differences in the Cm values for the different fragments. The value for WT, 1.82 M, is close to the value for i369 at 1.81 M, while the values for the other constructs are changed versus WT. The Cm value for i681 309-858 (1.75 M) is lower than the Cm value for WT, while the Cm value for i593 is not.

The difference in the i593 Cm value could be due to the fragment having an altered baseline compared to the rest of the fragments and an altered wavelength scan. However, if the protein possesses more random coil structure, hypothetically the midpoint of transition should be lower (require less denaturant to unfold). Instead, the value was calculated to be 1.93 M, higher than that of WT. This result, indicating a change in stability, could be due to the *m* value of the protein. The *m* value of this protein is slightly smaller than the *m* values of any of the other fragments. The calculated *m* value of this protein fragment could be altering the Cm in such a way as to make the Cm value for this protein inaccurate.

The Cm value for i681 is lower than that of WT by about 0.6 M. This shift in the midpoint does show there is a change in the stability of the protein. This change in stability could be a part of the effect the i31 insertion has on TraI at this position. The WT+i31 construct midpoint of transition is higher than that of WT, indicating that it is more stable than WT. However, the standard deviation in the calculated *m* value is much higher than that of the rest of the constructs. Like the i593 construct, the *m* value may not be completely accurate, and may not represent the full unfolding

transition of the protein. From the calculated Cm values, we can draw some limited conclusions due to potential issues with the *m* values. For the i681 fragment, more than likely the stability of the fragment is lower compared to WT; it has the lowest ΔG value, and the lowest Cm value. The i369 fragment is close to WT in its ΔG and Cm values, and does not appear to show altered stability. The placement of the i31 in the i369 fragment may not result in altered stability due to the fact that the i31 is in a region of the protein that is disordered and has little structure.

The dependence of ΔG on urea concentration of WT+i31 trends with i593 and i681. Like the Cm values, the equation used to calculate the dependence of ΔG on urea concentration uses the calculated *m* values. The WT+i31 data may not be accurate due to an *m* value with a large standard deviation, and the i593 data may be inaccurate due to unfolding of the protein. These data reinforce the conclusions from the Cm values of the proteins. The i681 fragment is not as stable as the WT fragment, and the i593 fragment possibly has altered stability, but due to other factors, this conclusion is not concrete.

Finally, the concentrations of the protein fragments could have had an effect on the results of some of the unfolding curves. The wild type and i681 constructs purified at much higher concentrations than the rest of the constructs. After the last column, both WT and i681 had concentrations in the hundreds of micromolar range. This was much higher than the rest of the constructs, which purified in the tens of micromolar range (from 20-70 μM approximately). The samples could not be concentrated further, as the sample would have been too small for accurate pipetting. At this low of a concentration, determining an accurate concentration can be difficult.

The baseline of the WT+i31 construct (Figure 4.14) could be different because the concentration used for titration could have been slightly off from 2 μM (the concentration used in titration unfolding curves). Although the concentration could be responsible for the differences in the lower baseline signal, it should not affect the unfolding or the slope of the line. This merely explains the signal differences in the lower baseline.

Alterations to the TSA in Full Length TraI Does Not Effect Mating Efficiency

The change in the i31 mating efficiency data may not be due to changes in protein stability. There is recent evidence published in Redzej *et al.*, 2013 that altering residues in the TSA of TraI can drastically change the translocation of the protein during mating. Residues in the TSA of TraI were mutated to determine if altering the TSA in the presence of the TSB would create a change in mating efficiency. There may be competition between the two domains for access to the pore coupling protein, and altering the binding specificity of one domain might create favorable conditions for faster access for the other domain. To test if altering the TSA changes mating efficiency, we created three different point mutants within the TSA.

The first point mutant, A593V, was reported in Redzej *et al.,* to reduce protein translocation to approximately 10% of wild type levels. We created this mutant in full length TraI, and ran mating assays with the TraI mutant. There was no noticeable change in mating efficiency in the A593V TraI mutant (Figure 4.17). We created a S739N TraI mutant, which reduced protein translocation to 20-30% of WT levels (Redzej *et al.,* 2013). Again, we did not see any change in mating efficiency (Figure

4.17). We also created a D672N mutant, which was not created in the paper, but approximates the published mutations. We created this mutant since most of the mutations published were located around the i593 site. Identifying residues similar to the mutated residues around the i681 site, we chose D672 as it is a charged residue, and changing the charge might produce an effect like the previously identified translocation mutants. The D672N mutant does not show any difference in mating efficiency (Figure 4.17). None of the point mutants we created show any noticeable change in mating efficiency when compared to WT TraI.

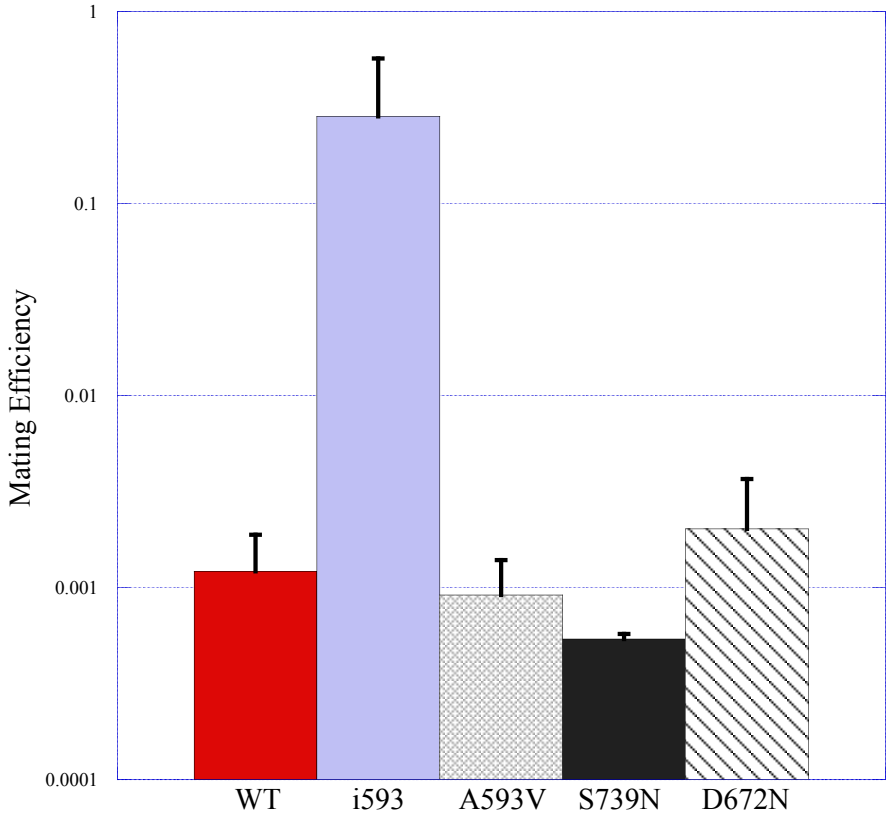

Figure 4.17. Mating efficiencies (transconjugates per donor cell) of wild type TraI point mutants in the TSA region of the protein show no change versus wild type. Values represent the combination of at least three independent experiments for each cell line.

Changes to the TSA of TraI Discussion

There was no change in mating efficiency seen in any of the point mutants that were created in the TSA of TraI. The mutants reported to have an effect on protein translocation were made in a fragment of R1 TraI, 1-992. These were also mutants that affect protein translocation, and the system that is used to measure protein translocation employs a fully functional copy of R1 TraI to ensure mating proceeds and protein can be translocated. In our assay TraI has a fully functional TSB and the small changes in the TSA may not be enough to elicit a change in mating efficiency. R1 and F may also not be completely equivalent, despite only having 2 amino acid differences in the region of the crystal structure (Redzej *et al.,* 2013). There may not be competition between the domains, as posited, in conjunction with a mutation that is quite small in the context of the whole protein. It may be necessary to mutate more residues in the TSA to create an effect similar to the i31. A single point mutation may not be enough of a change in the TSA to cause a change in mating efficiency.

The avenue of investigation into the TSA of TraI playing a role in the i31 phenotype did not show any changes in mating efficiency when the TSA was altered. However, the changes to the TSA of TraI were small compared to inserting 31 amino acids. Amino acid changes that cause mating efficiency to change may need to be more numerous to cause an effect. Possible further investigation could look at different length disruptions. Changing the i31 (i.e. making it shorter) and looking for changes in mating efficiency could be another avenue of investigation into the TSA region of TraI. Using this method, we could see if there is a dosage effect of

insertions, and at what point the insertion is long enough to cause a change in mating efficiency.

CHAPTER 5

OVERALL CONCLUSIONS

The i31 TraI mutants were analyzed by fluorescence microscopy mating and found to have DNA that appeared in recipient cells at earlier time points. Investigating this change, we determined the change seen was not due to factors in the recipient cell line, and we turned our lines of investigation to the donor cell. We used TraI fusion proteins, an activity assay, unfolding measurements, and TraI mutants to assess possible causes of the phenotype seen in the i31 mutants.

Using the TraI-YFP point mutant constructs, we were trying to determine if changing stability of an inserted protein altered mating efficiency. We demonstrated that inserting the same protein with different stabilities changes mating efficiency. These data, while they indicate that altered protein stability can alter mating efficiency, are TraI fusion proteins. These are not measures of the stability of TraI itself or of TraI with the i31 insertion. These data do indicate protein stability is important in mating efficiency and more stable proteins hinder plasmid transfer while less stable proteins do not. These data show there is some degree of unfolding necessary for transfer, and the stability of proteins inserted into TraI can influence transfer.

These data point to stability of TraI as a contributor to the i31 phenotype. It does not appear that the nicking activity contributes to the mating efficiency differences in the i31 mutants. Although the CD data do point to stability as being a potential explanation of part of the change in the mating efficiency of the i31 mutants, the data do not show any major changes in the stability of the protein. We had been

looking for a sizeable measurable change in protein stability of the i31 mutants, but the data do not show any large changes. However, we do see a small trend in the i681 data that indicates it is less stable than WT, and a small change in stability could be part of the cause of the i31 mating efficiency increase. Thirty-one amino acids is not a large insertion (relative to the size of TraI), and the mutation may be causing local changes rather than global changes to stability. The work with the TSA point mutants did not show any changes in mating efficiency when residues in the TSA were altered. These residues had been implicated as being necessary contact points for the TSA to interact with the pore machinery (Redzej *et al.,* 2013). When these contact residues were altered, protein translocation decreased, but with the TSB present, we did not see the same effect.

The trend in the CD data, when correlated with the TraI-YFP point mutant data, makes an argument for protein stability playing a role in the TraI mutants. Although the YFP insertion data are mutations in a protein inserted into TraI, when taken together with the CD data, there are indications that altering protein stability causing changes in mating efficiency. The data also indicate the i31 mutants may have positional effects and one overall model does not explain the effect of the i31 at each site. The microscopy data, in concert with the TraI-YFP and CD data all indicate the effects at i593 and i681 may be due to stability, but the effects of the i31 at i369 is probably due to a different cause. Overall, the data presented here demonstrate the i31 mutants with increased mating efficiencies show an increased rate of DNA transfer, and the increase could be partially explained by changes in the stability of the protein.

REFERENCES

Achtman M, Willetts N, Clark AJ. (1971) Beginning a Genetic Analysis of Conjugational Transfer Determined by the F Factor in *Escherichia coli* by Isolation and Characterization of Transfer-Deficient Mutants. *J. Bact*., **106**, 529-538.

Achtman M, Kennedy N, Skurray R. (1977) Cell-cell interactions in conjugating Escherichia coli: role of traT protein in surface exclusion. *Proc. Natl. Acad. Sci*., **74**, 5104–5108.

Ainavarapu SR, Li L, Badilla CL, Fernandez JM. (2005) Ligand binding modulates the mechanical stability of dihydrofolate reductase. *Biophys. J*., **89**, 3337-3344.

Alvarez-Martinez CE, Christie PJ. (2009) Biological diversity of prokaryotic type IV secretion systems. *Microbiol Mol Biol Rev*., **73**, 775-808.

Anthony KG, Klimke WA, Manchak J, Frost LS. (1999) Comparison of proteins involved in pilus synthesis and mating pair stabilization from the related plasmids F and R100–1: insights into the mechanism of conjugation. *J. Bact.*, **181**, 5149–5159.

Asada K, Sugimoto K, Oka A, Takanami M, Hirota Y. (1982) Structure of replication origin of the Escherichia coli K-12 chromosome: the presence of spacer sequences in the ori region carrying information for autonomous replication. *Nucleic Acids Res*., **10**, 3745-54.

Babic A, Lindner AB, Vulic M, Stewart EJ, Radman M. (2008) Direct visualization of horizontal gene transfer. *Science*, **319**, 1533-1536.

Bolin JT, Filman DJ, Matthews DA, Hamlin RC, Kraut J. (1982) Crystal structures of Escherichia coli and Lactobacillus casei dihydrofolate reductase refined at 1.7 A resolution. I. General features and binding of methotrexate. *J. Biol. Chem.* **257**, 13650–13662.

Boyd EF, Hartl DL.(1997) Recent horizontal transmission of plasmids between natural populations of Escherichia coli and Salmonella enterica. *J Bact*., **179**, 1622–1627.

Bradley DE. (1980) Morphological and serological relationships of conjugative pili. *Plasmid*, **4**, 155-169.

Brendler T, Austin S. (1999) Binding of SeqA protein to DNA requires interaction between two or more complexes bound to separate hemimethylated GATC sequences. *EMBO*, **18**, 2304-2310.

Byrd DR, Matson SW. (1997) Nicking by transesterification: the reaction catalysed by a relaxase. *Mol Microbiol*., **25**, 1011-22.

Cambell JL, Kleckner N. (1990) E. coli oriC and the dnaA gene promoter are sequestered from dam methyltransferase following the passage of the chromosomal replication fork. *Cell,* **62**, 967-979.

Chandran V, Fronzes R, Duquerroy S, Cronin N, Navaza J, Waksman G. (2009) Structure of the outer membrane complex of a type IV secretion system. *Nature*, **462,** 1011–1015.

Cascales E, Christie, PJ. (2004) Definition of a bacterial type IV secretion pathway for a DNA substrate. *Science*, **304**, 1170–1173.

Centers for Disease Control and Prevention. Antibiotic Resistance Threats in the United States, 2013, Atlanta, Georgia, U.S. Department of Health and Human Services, CDC, 2013.

Cheng Y, McNamara DE, Miley MJ, Nash RP, Redinbo MR. (2011) Functional characterization of the multidomain F plasmid TraI relaxase-helicase. *J Biol Chem.*, **286**, 12670-12682.

Christie PJ, Vogel JP. (2000) Bacterial type IV secretion: conjugation systems adapted to deliver effector molecules to host cells. *Trends Microbiol*., **8**, 354–360.

Christie PJ, Atmakuri K, Jabubowski S, Krishnamoorthy V, Cascales E. (2005) Biogenesis, architecture, and function of bacterial Type IV secretion systems. *Ann Rev Microbiol*., **59**, 451-485.

Clark NJ, Raththagala M, Wright NT, Buenger EA, Schildbach JF, Krueger S, Curtis JE. (2014) Structures of TraI in solution. J Mol. Model, 20, 2308.

Clarke M, Maddera L, Harris RL,Silverman PM. (2008) F-pili dynamics by live-cell imaging. *Proc. Natl. Acad. Sci.*, **105**, 17978–17981.

Cody V, Pace J, Rosowsky A. (2008) Structural analysis of a holoenzyme complex of mouse dihydrofolate reductase with NADPH and a ternary complex with the potent and selective inhibitor 2,4-diamino-6-(2'-hydroxydibenz[b,f]azepin-5-yl)methylpteridine. *Acta Crystallogr*., **64**, 977-984.

Cormack BP, Valdivia RH, Falkow 2. (1996) FACS-optimized mutants of the green fluorescent protein (GFP). Gene, 173, 33-38.

Csitovits VC, Dermic D, Zechner EL. (2004) Concomitant reconstitution of TraI-catalyzed DNA transesterase and DNA helicase activity in vitro. *J Biol Chem*, **279**, 45477-45484.

Datta S, Larkin C, Schildbach JF. (2003) Structural insights into single-stranded DNA binding and cleavage by F factor TraI. *Structure*, **11**, 1369-1379.

Di Laurenzio L, Frost LS, Paranchych W. (1992) The TraM protein of the conjugative plasmid F binds to the origin of transfer of the F and ColE1 plasmids. *Mol Microbiol,* **6**, 2951-2959.

Dostál L, Schildbach JF. (2010) Single-stranded DNA binding by F TraI relaxase and helicase domains is coordinately regulated. *J Bact*, **192**, 3620-3628.

Dostál L, Shao S, Schildbach JF. (2011) Tracking F plasmid TraI relaxase processing reactions provides insight into F plasmid transfer. *Nucleic Acids Res*, **39**, 2658-2670.

Edlehoch H (1967) Spectroscopic determination of tryptophan and tyrosine in proteins. *Biochemistry*, **6**, 1948-1954.

Eilers M, Schatz G. (1986) Binding of a specific ligand inhibits import of a purified precursor protein into mitochondria. *Nature*, **322**, 228-232.

Esaki M, Kanamori T, Nishikawa S, Endo T. (1999) Two distinct mechanisms drive protein translocation across the mitochondrial outer membrane in the late step of the cytochrome b(2) import pathway. *Proc Natl Acad Sci*., **96**, 11770-11775.

Filman DJ, Bolin JT, Matthews DA, Kraut J. (1982) Crystal structure of Escherichia coli and Lactobacillus casei dihydrofolate reductase refined at 1.7 A resolution. II. Environment of bound NADPH and implications for catalysis. *J. Biol. Chem.,* **257**, 13650–13662.

Fronzes R, Schafer E, Wang L, Saibil HR, Orlova EV, Waksman G. (2009) Structure of a type IV secretion system core complex. *Science,* **323**, 266–268.

Frost LS, Paranchych W, Willetts N. (1984) DNA sequence of the F traALE region that includes the gene for F pilin. *J. Bact.*, **160**, 395-401.

Frost LS, Paranchych W. (1988) DNA sequence analysis of point mutations in traA, the F pilin gene, reveal two domains involved in F-specific bacteriophage attachment. *Mol Gen Genet.,* **213**, 134-139.

Frost LS, Ippen-Ihler K, Skurray RA. (1994) Analysis of the sequence and gene products of the transfer region of the F sex factor. *Microbiol. Rev.,* **58**, 162-210.

Fu YH, Tsai MM, Luo YN, Deonier RC. (1990) Intrinsic Bends And Integration Host Factor Binding at F Plasmid *oriT*. *J Bact*, **172**, 4603-4609.

Fu YH, Tsai MM, Luo YN, Deonier RC. (1991) Deletion Analysis of the F Plasmid oriT Locus. *J Bact*, **173**, 1012-1020.

Fujikawa N, Kurumizaka H, Nureki O, Tanaka Y, Yamazoe M, Hiraga S, Yokoyama S (2004) Structural and biochemical analyses of hemimethylated DNA binding by the SeqA protein. *Nucleic Acids Res*, **32**, 82-92.

Garcillan-Barcia MP, Francia MV, de la Cruz F. (2009) The diversity of conjugative relaxases and its application in plasmid classification. *FEMS Microbiol Rev*, **33**, 657–687.

Gehde N, Hinrichs C, Montilla I, Charpian S, Lingelbach K, Przyborski JM. (2009) Protein unfolding is an essential requirement for transport across the parasitophorous vacuolar membrane of Plasmodium falciparum. *Mol Microbiol.,* **71**, 613-628.

Greenfield N, Fasman GD. (1969) Computed circular dichroism spectra for the evaluation of protein conformation. *Biochemistry,* **8**, 4108–4116.

Greenfield NJ. (2006) Using circular dichroism spectra to estimate protein secondary structure. *Nat Protoc.,***1**, 2876–2890.

Guarne A, Zhao Q, Ghirlando R, Yang W. (2002) Insights into negative modulation of E. coli replication initiation from the structure of SeqA–hemimethylated DNA complex. *Nat Structure Biol.*, **9**, 839-843.

Guarne A, Zhao Q, Ghirlando R, Austin S, Yang W, Brendler T. (2005) Crystal structure of a SeqA–N filament: implications for DNA replication and chromosome organization, *EMBO J.,* **24**, 1502–1511.

Guogas LM, Kennedy SA, Lee JH, Redinbo MR. (2009) A novel fold in the TraI relaxase-helicase c-terminal domain is essential for conjugative DNA transfer. *J. Mol. Biol*., **386**, 554-568.

Haft RJ, Palacios G, Nguyen T, Mally M, Gachelet EG, Zechner EL, Traxler B. (2006) General mutagenesis of F plasmid TraI reveals its role in conjugative regulation. *J Bact*., **188**, 6346-6353.

Haft RJ, Mittler JE,Traxler B. (2009) Competition favours reduced cost of plasmids to host bacteria. *The ISME Journal*, **3**, 761–769.

Han JS, Kang S, Lee H, Kim HK, Hwang DS. (2003) Sequential binding of SeqA to paired hemi-methylated GATC sequences mediates formation of higher order complexes. *J Biol Chem.,* **278**, 34983-34989.

Harold, F. M. (1986) The Vital Force: A Study of Bioenergetics (Freeman).

Heim R, Cubitt A, Tsien R (1995). Improved green fluorescence. *Nature* **373**, 663–664.

Holzwarth G, Doty P. (1965) The Ultraviolet Circular Dichroism of Polypeptides. *J. Am. Chem. Soc.*, **87**, 218–228.

Huang S, Ratliff KS, Schwartz JM, Spenner JM, Matouschek A. (1999) Mitochondria unfold precursor proteins by unraveling them from their N-termini. *Nat. Struct. Biol*. **6**, 1132-1138.

Hupert-Kocurek K, Kaguni JM (2011). Understanding Protein Function - The Disparity Between Bioinformatics and Molecular Methods, Computational Biology and Applied Bioinformatics, Prof. Heitor Lopes (Ed.), ISBN: 978-953-307-629-4, InTech, DOI: 10.5772/23233.

Jakubowski SJ, Kerr JE, Garza I, Krishnamoorthy V, Bayliss R, Waksman G, Christie PJ. (2009) Agrobacterium VirB10 domain requirements for type IV secretion and T pilus biogenesis. *Mol. Microbiol.*, **71**, 779–794.

Johnson, F.H., Shimomura, O., Saiga, Y., Gershman, L.C., Reynolds, G.T., and Waters, J.R. (1962) Quantum efficiency of Cybridina luminescences, with a note on that of Aequorea. *J. Cell. Comp. Physiol.*, **60**, 85-103.

Ju J, Wong JJ, Edwards RA, Manchak J, Frost LS, Glover JN. (2008) Structural basis of specific TraD-TraM recognition during F plasmid-mediated bacterial conjugation. *Mol Microbiol.*, **70**, 89-99.

Juhas M, Crook DW, Hood DW. (2008) Type IV secretion systems: tools of bacterial horizontal gene transfer and virulence. *Proc Natl Acad Sci*., **102**, 832–837.

Karl W, Bamberger M, Zechner EL. (2001) Transfer Protein TraY of Plasmid R1 Stimulates TraI-Catalyzed oriT Cleavage In vivo. *J Bact*, **183**, 909-914.

Kelly LA, Sternberg MJE. (2009) Protein structure prediction on the web: A case study using the Phyre server. *Nature Protocols*, **4**, 363-371.

Kutrowska BW, Narczyk M, Buszko A, Bzowska A, Clark PL. (2007) Folding and unfolding of a non-fluorescent mutant of green fluorescent protein. *J Phys Condens Matter*., **28**, 285-223.

Lang S, Gruber K, Mihajlovic S, Arnold R, Gruber CJ, Steinlechner S, Jehl MA, Rattei T, Frohlich KU, Zechner EL. (2010) Molecular recognition determinants for type IV secretion of diverse families of conjugative relaxases. *Mol Microbiol,* **78**, 1539-1555.

Lang S, Gruber K, Mihajlovic S, Arnold R, Gruber CJ, Steinlechner S, Jehl MA, Rattei T, Frohlich KU, Zechner EL. (2010). Molecular recognition determinants for type IV secretion of diverse families of conjugative relaxases. *Mol Microbiol*, **78**, 1539-1555.

Lang S, Kirchberger PC, Gruber CJ, Redzej A, Raffi A, Zellnig G, Zangger K, Zechner EL. (2011) An activation domain of plasmid R1 TraI protein delineates stages of gene transfer initiation. *Mol Microbiol.*, **82**, 1071-1085.

Larkin C, Datta S, Nezami A, Dohm JA, Schildbach JF. (2003) Crystallization and preliminary X-ray characterization of the relaxase domain of F factor TraI. *Acta Crystallogr D Biol Chrystallogr*, **59**, 1514-1516.

Larkin C, Datta S, Harley MJ, Anderson BJ, Ebie A, Hargreaves V, Schildbach JF. (2005) Inter- and intramolecular determinants of the specificity of single-stranded DNA binding and cleavage by the F factor relaxase. *Structure*, **13**, 1533-1544.

Larkin C, Haft RJ, Harley MJ, Traxler B, Schildbach JF. (2007) Roles of active site residues and the HUH motif of the F plasmid TraI relaxase. *J Biol Chem.*, **282**, 33707-33713.

Lawley TD, Klimke WA, Gubbins MJ, Frost LS. (2003) F factor conjugation is a true type IV secretion system, *FEMS Microbiol Lett*., **224**, 1-15.

Lawn AM. (1966) Morphological Features of the Pili Associated with Escherichia coli ~12 Carrying R Factors or the F Factor. *J. Gen. Microbial*., **45**, 377-383.

Levy SB (2002) Factors impacting on the problem of antibiotic resistance. *J. Antimicrob. Chemother.*, **49,** 25-30.

Lu J, Frost LS. (2005) Mutations in the C-terminal region of TraM provide evidence for in vivo TraM-TraD interactions during F-plasmid conjugation. *J Bact.*, **187**, 4767-4773.

Lu M, Campbell JL, Boye ES, Kleckner N. (1994) SeqA: A Negative Modulator of Replication Initiation in E. coli. *Cell*, **77**, 413-426.

Lum PL, Rodgers ME, Schildbach JF. (2002) TraY DNA recognition of its two F factor binding sites. *J Mol Biol*., **321**, 563-578.

Majdalani N, Ippen-Ihler K. (1996) Membrane insertion of the F-pilin subunit is Sec independent but requires leader peptidase B and the proton motive force. *J Bact.*, **178**, 3742–3747.

Maneewannakul K, Maneewannakul S, Ippen-Ihler K. (1993) Synthesis of F pilin. J. Bact., 175, 1384-1391.

Manoil C, Bailey J. (2000) A simple screen for permissive sites in proteins: analysis of Escherichia coli lac permease. *J Mol Biol.*, **267**, 250-263.

Manoil C, Traxler B. Insertion of in-frame sequence tags into proteins using transposons. Methods, 20, 55-61.

Melnik TN, Povarnitsyna TV, Glukhov AS, Uversky VN, Melnik BS. (2011) Sequential melting of two hydrophobic clusters within the green fluorescent protein GFP-cycle3. *Biochemistry*, **50,** 7735-7744.

Mihajlovic S, Lang S, Sut MV, Strohmaier H, Gruber CJ, Koraimann G, Cabezón E, Moncalián G, de la Cruz F, Zechner EL. (2009) Plasmid R1 conjugative DNA processing is regulated at the coupling protein interface. *J Bact,* **191**, 6877-6887.

Myers JK, Pace CN, Scholtz JM (1995) Denaturant m values and heat capacity changes: Relation to changes in accessible surface areas of protein unfolding. *Protein Science,* **4**, 2138-2148.

Ninio S, Roy CR. (2007) Effector proteins translocated by Legionella pneumophila: strength in numbers. *Trends Microbiol.*, **15**, 372–380.

Novick RP. (1987) Plasmid Incompatibility. *Microbiol Rev.*, **51**, 381-395.

Oberto J, Rouviere-Yaniv J (1996). Serratia marcescens Contains a Heterodimeric HU Protein Like Escherichia coli and Salmonella typhimurium. *J Bact.*, **178**, 293-297.

Oka A, Sugimoto K, Takanami M, Hirota Y. (1980). Replication origin of the Escherichia coli K-12 chromosome: the size and structure of the minimum DNA segment carrying the information for autonomous replication. *Mol Gen Genet.*, **178**, 9-20.

Okamoto K, Brinker A, Paschen SA, Moarefi I, Hayer-Hartl M, Neupert W, Brunner M. (2002) The protein import motor of mitochondria: a targeted molecular ratchet driving unfolding and translocation. *EMBO J.*, **21**, 3659–3671.

Perez-Jimenez R, Garcia-Manyes S, Ainavarapu SR, Fernandez JM. (2006) Mechanical unfolding pathways of the enhanced yellow fluorescent protein revealed by single molecule force spectroscopy. *J. Biol. Chem*., **281**, 40010-40014.

Phillips G. (2001) Green fluorescent protein--a bright idea for the study of bacterial protein localization. *FEMS Microbiol Lett,* **204**, 9–18.

Prendergast F, Mann K (1978). Chemical and physical properties of aequorin and the green fluorescent protein isolated from Aequorea forskålea. *Biochemistry* **17**, 3448–3453.

Rajagopalan R, Zhang Z, McCourt L, Dwyer M, Benkovic SJ, Hammer GG. (2002) Interaction of dihydrofolate reductase with methotrexate: Ensemble and single-molecule kinetics. *PNAS*, **99**, 13481–13486.

Ranonese H, Haish D, Villareal H, Choi JH, Matson SW. (2007) The F plasmid-encoded TraM protein stimulates relaxosome-mediated cleavage at *oriT* through an interaction with TraI. *Mol Microbiol*, **63**, 1173–1184.

Redzej A, Ilangovan A, Lang S, Gruber CJ, Topf M, Zangger K, Zechner EL, Waksman G. (2013) Structure of a translocation signal domain mediating conjugative transfer by type IV secretion systems. *Mol Microbiol*, **89**, 324-333.

Rice PA, Yang S, Mizuuchi K, Nash HA. (1996) Crystal structure of an IFH-DNA complex: A protein induced U turn. Cell, 87, 1295-1306.

Rivera-Calzada A, Fronzes R, Savva CG, Chandran V, Lian PW, Laeremans T, Pardon E, Steyaert J, Remaut H, Waksman G, Orlova EV. (2013) Structure of a bacterial type IV secretion core complex at subnanometre resolution. *EMBO J.*, **32**, 1195-1204.

Russell DW, Zinder ND. (1987) Hemimethylation prevents DNA replication in E. coli. *Cell*, **50**, 1071-1079.

Schildbach JF, Robinson CR, Sauer RT. (1998) Biophysical Characterization of the TraY Protein of *Escherichia coli* F Factor. *J. Biol. Chem*., **273**, 1329-1333.

Schnell JR, Dyson J, Wright PE. (2004) Structure, dynamics, and catalytic function of Dihydrofolate Reductase. *Annu. Rev. Biophys. Biomol.*, **33**, 119-140.

Shimomura O, Johnson FH, Saiga Y. (1962) Extraction, purification and properties of aequorin, a bioluminescent protein from the luminous hydromedusan, Aequorea. *J Cell Comp Physiol.*, **59**, 223-239.

Silverman PM, Sholl A. (1996) Effect of traY Amber Mutations on F-Plasmid traY Promoter Activity In Vivo. J. Bact., 178, 5787-5789.

Silverman PM, Clarke MB. (2010) New insights into F-pilus structure, dynamics, and function. *Integr. Biol.*, **2**, 25–31.

Skarstad K, Boye E. (1994) The initiator protein DnaA: evolution, properties and function. *Biochim Biophys Acta.*, **1217**, 111-30.

Skarstad K, Lueder G, Lurz R, Speck C, Messer W. (2000) The Escherichia coli SeqA protein binds specifically and co-operatively to two sites in hemimethylated and fully methylated oriC. *Mol Microbiol.*, **36**, 1319-1326.

Smith SL, Patrick P, Stone D, Phillips AW, Burchall JJ. (1979) Porcine liver dihydrofolate reductase. Purification, properties, and amino acid sequence. *J. Biol. Chem.*, **254**, 11475-11484.

Stern JC, Schildbach JF. (2001) DNA recognition by F factor TraI36: highly sequence-specific binding of single-stranded DNA. *Biochemistry*, **40**, 11586-11595.

Street LM, Harley MJ, Stern JC, Larkin C, Williams SL, Miller DL, Dohm JA, Rodgers ME, Schildbach JF. (2003) Subdomain organization and catalytic residues of the F factor TraI relaxase domain. *Biochem et Biophys Acta*., **1646**, 86-99.

Sut MV, Mihajlovic S, Lang S, Gruber CJ, Zechner EL. (2009) Protein and DNA effectors control the TraI conjugative helicase of plasmid R1. *J Bact*, **191**, 6888-6899.

Tsai MM, Fu YH, Deonier RD. (1990) Intrinsic bends and integration host factor binding at F plasmid oriT. *J. Bact*., **172**, 4603-4609.

Tsien R (1998) The green fluorescent protein. *Annu Rev Biochem,* **67**, 509–544.

Velappan N, Sblattero D, Chasteen L, Pavlik P, Bradbury AR. (2007) Plasmid incompatibility: more compatible than previously thought? *Prot Eng, Design & Selection*, **20**, 309-313.

Venyaminov S, Baikalov IA, Shen ZM, Wu CS, Yang JT. (1993) Circular dichroic analysis of denatured proteins: inclusion of denatured proteins in the reference set. *Anal. Biochem.*, **214**, 17–24.

Vergunst AC, Schrammeijer B, Dulk-Ras A, M. T. de Vlamm C, Regensburg-Tuïnk T, Hooykaas PJJ. (2000) VirB/D4-Dependent protein translocation from *Agrobacterium* into plant cells. *Science*, **290**, 979-982.

Vergunst AC, van Lier MCM, Dulk-Ras A, Stüve TAG, Ouwehand A, Hooykaas PJJ. (2005) Positive charge is an important feature of the C-terminal transport signal of the VirB/D4-translocated proteins of *Agrobacterium*. *PNAS*, **102**, 832-837.

Waksman G, Fronzes R (2010) Molecular architecture of bacterial type IV secretion systems. *Trends Biochem Sci*, **35**, 691–698.

Wallace LA, Matthews RC. (2002) Highly divergent dihydrofolate reductases conserve complex folding mechanisms. *J. Mol. Biol.* **315**, 193-211.

Wang YA, Yu X, Silverman PM, Harris RL, Egelman EH. (2009) The structure of F-pili.
J. Mol. Biol., **385**, 22–29.

Wachter RM, Elsliger MA, Kallio K, Hanson GT, Remington SJ. (1998) Structural basis of spectral shifts in the yellow-emission variants of green fluorescent protein. Structure, 6, 1267-1277.

Waksman SA. (147) What is an antibiotic or an antibiotic substance? *Mycologia*, **39**, 565-569.

Willetts NS. (1972) Location of the origin of transfer of the sex factor F. *J Bact*., **112**, 773–778.

Williams SL, Schildbach JF (2007) TraY and Integration Host Factor *oriT* Binding Sites and F conjugal transfer: Sequence Variations but Not Altered Spacing, Are Tolerated. J Bact, **189**, 3813-3823.

Wong JJ, Lu J, Edwards RA, Frost LS, Glover JN. (2011) Structural basis of cooperative DNA recognition by the plasmid conjugation factor, TraM. *Nucleic Acids Res.*, **39**, 6775-6788.

Wright NT, Raththagala M, Hemmis CW, Edwards S, Curtis JE, Krueger S, Schildbach JF. (2012) Solution structure and small angle scattering analysis of TraI (381-569). *Proteins*, **80**, 2250-2261.

CURRICULUM VITAE

Education

PhD in Biology July 2014
Department of Biology, The Johns Hopkins University, Baltimore, MD

Thesis Advisor: Joel F. Schildbach, PhD
Current work: Investigating F plasmid and TraI transfer by fluorescence microscopy and the folded/unfolded state of TraI *in vivo* and *in vitro*

- Graduate level courses: Advanced Molecular Biology, Advanced Cell Biology, Advanced Developmental Biology, Biophysics, Science Writing, Biochemistry Seminar, Physical Chemistry of Biological Macromolecules, Fluorescence Spectroscopy, Ethics in Science, Preparation for University Teaching
- Rotations: Kyle Cunningham, PhD, yeast tiling microarrays to detect mutation
  Craig Townsend, PhD, generation of gene knockouts in *S. argenteolus*
  Andy Hoyt, PhD, 2-hybrid screen for Cse4 binding site on Bub1

Bachelor of Arts, Biochemistry with High Honors May 2007
Smith College, Northampton, MA

Thesis Advisor: Stylianos P. Scordilis, PhD
Thesis title: Knockdown of Hsp25 in C2C12 cells *in vitro* and *in vivo* using RNAi

Teaching Experience

Guest Lecturer, The Johns Hopkins University
- Microbiology, summer 2013
  - Taught two guest lectures
  - Self-designed lectures with input from the professor teaching the course
  - Contributed homework and exam materials

Dean's Teaching Fellow, "The Human Microbiome", The Johns Hopkins University
- Dean's Teaching Fellow 2012-2013
- Taught "The Human Microbiome" a self proposed and designed course, submitted to the Dean's Teaching Fellowship committee, and selected to be taught to upper level undergraduates
- Designed and taught lectures, lead students in class discussion and weekly presentations of primary literature, guided students in writing a primary literature review
- Designed weekly interactive problems, quizzes, and activities

- Created all homework assignments, grading rubrics, and other course materials
- Oversaw administration of the course, administered Blackboard

Teaching Assistant, The Johns Hopkins University
- Phage Hunters, spring 2013, fall 2013
  - Freshmen-only course
  - Answered in-class questions, helped troubleshoot student problems
  - Taught students laboratory techniques
  - Helped with phage genome annotation
  - Prepared solutions and materials for class use
- Graduate Biophysics, 2012
  - Oversaw administration of Blackboard site for course
  - Lead review sessions
  - Created and gave topic review lectures
  - Lead software tutorial
  - Grading of homework and exams
- Biochemistry, 2011
  - Grading and lecture TA for undergraduate biochemistry
  - Helped proctor and grade exams
  - Held recitation section
- Cell Biology Lab, 2009
  - Laboratory TA
  - Lead laboratory section, lead students in lab experiments
  - Graded lab reports and helped grade lecture exams
- Biochemistry Lab, 2008
  - Laboratory TA
  - Lead laboratory section, lead students in lab experiments
  - Graded lab reports and helped grade lecture exams

Tutoring, The Johns Hopkins University
- Graduate Biophysics, 2011
  - Held weekly tutoring sessions
  - Helped students review material, solve problems, exam review

Teaching Assistant, Smith College
- Biochemistry Laboratory Teaching Assistant, 2006
  - Helped laboratory instructor with set-up and preparation for each week's lab
  - Answered student questions, helped resolve experimental issues
  - Cleaned up after each laboratory session

Teaching Workshops and Seminars

Teaching Science Like We Do Science; Integration of Research and Education Workshop. 57th Annual Biophysical Society Meeting, Philadelphia, PA, February 2013.

Department of Biology presents Rebecca Pearlman, Richard Shingles and Katie Tifft, Active Learning Seminar, Johns Hopkins University, Baltimore, MD, February 2013.

Professional development

Johns Hopkins University teaching assistant training, August 2008
AS.360.781, Preparation for University Teaching, spring 2012

Research Experience

Graduate Research Assistant 2007-present
Department of Biology, The Johns Hopkins University
Principle Investigator: Joel F. Schildbach, PhD

- Investigating F plasmid and TraI transfer
- Determining biochemical characteristics of mutant TraI protein
- Carried out live cell fluorescence microscopy, *in vitro* and *in vivo* assays of protein function

Special Studies/Honors Thesis Student 2005-2007
Smith College, Northampton, MA
Principle Investigator: Stylianos P. Scordilis, PhD

- Carried out research on knocking down two specific heat shock proteins *in vivo* (mouse model) and *in vitro* (C2C12 myoblast and myotubes)
- Developed own protocols and procedures for various experiments

Summer Research Student 2002-2007
New England Biolabs, Ipswich, MA

- Summer laboratory research position, worked on a variety of projects
- Carried out research on gene methylation during development in *C. elegans* and *D. melanogaster*
- Helped develop a patented method for large scale purification of small interfering RNAs
- Carried out transfection studies on C2C12 myoblast cells and myotube cells
- Investigated TrxP and DsbC to determine if they are isomerases

Presentations and Posters

Feehery TK, Buss J, Xiao J, and Schildbach JF. Investigating rate of TraI and DNA transfer during bacterial conjugation, *57th Annual Biophysical Society Meeting*, Philadelphia, PA, February 2013.

Feehery TK, Buss J, Xiao J, and Schildbach JF. Investigating F plasmid and TraI transfer by fluorescence microscopy, *Biophysical Society Regional Meeting*, Hershey, PA, November 2011.

Feehery TK, and Schildbach JF. Investigating F plasmid and TraI transfer by fluorescence microscopy, *Johns Hopkins PMB student evening series speaker*, Baltimore, MD, May 2011.

Feehery TK and Schildbach JF. Investigating the folded/unfolded state of TraI *in vivo* and the domains necessary for F plasmid transfer. *Johns Hopkins Cellular, Molecular, and Developmental Biology and Biophysics Retreat*, Cumberland, MD, October 2010.

Feehery TK, Dutton R, Boyd D, Beckwith J, Riggs P, and Berkmen M. Complementation of disulfide bond isomerase activity by a periplasmic reductase, *Boston Bacteriological Meeting*, Boston, MA, July 2007.

Feehery TK, Feehery GR, and Scordilis SP. Knockdown of Hsp25 in C2C12 cells *in vitro* and *in vivo* using RNAi. *Five College Undergraduate Research Symposium,* Amherst, MA, May 2007.

Academic Societies

Dean's Teaching Fellow	2012-2013
Biophysical Society, member	2011, 2013
American Chemical Society, member	2007-2008
Sigma Xi, member	2007-present

Leadership Roles

Chair of the Pioneers in Biology Committee 2009 – 2013
The Johns Hopkins University, Baltimore, MD

- Invited student selected prominent members of the scientific community to give talks, organized their stay

Smith College American Chemical Society Treasurer 2006-2007
Smith College, Northampton, MA

- Helped budget the organization and plan events

Biochemistry Major Student Liaison 2006-2007
Smith College, Northampton, MA
- Helped organize and plan events for the biochemistry major, helped plan 50th anniversary of the program